University of Milano - Bicocca Department of Biotechnology and Biosciences

2010

Alexandre Orsato

Studies on Tumor Drug Targeting

Supported by the Programme Alβan, the European Union Programme of High Level Scholarships for Latin America

Scholarship no. E07D400786BR

Thesis Supervisor

Prof. Francesco Nicotra
Full Professor of Organic Chemistry
University of Milano-Bicocca
Department of Bioscience and Biotechnology
Italy

Thesis Co-Supervisor

Barbara La Ferla Ph.D
Researcher
University of Milano-Bicocca
Department of Bioscience and Biotechnology
Italy

Ph.D. School Coordinator

Prof. Franca Morazzoni
Full Professor of General and Inorganic Chemistry
University of Milano-Bicocca
Department of Material Science
Italy

keywords Drug targeting, Cancer, Gastrin-Releasing Peptide, Peptidomimetics, Computer-based drug design, Synthesis, Akt, Phosphatidylinositol phosphate analogues

abstract Tumor drug targeting is one of the most promising therapeutic strategies in oncology. The aim of this PhD work was the study of the essential features required for the assembly of tumor targeting conjugates.This work was focused on the deveploment of ligands for the GRP receptor that should function as carrier molecules for the targeting of tumor cells overexpressing this receptor. For this purpose, non-peptide GRP mimetics were designed, using a computer-based drug design technique, synthesized and tested. Two analogue compounds based on a bicyclic scaffold exerted an antagonist behaviour on the GRP receptor. Synthetic studies have been performed to optimize their production as well as biological tests to determine their potential as carrier molecules. Apart from the targeting moiety, we also studied the antineoplastic part of tumor targeting conjugates. Akt is a proto-oncogenic kinase that has been associated to cancer development. Therefore, the Akt inhibitory activity of phosphatidylinositol phosphate analogues was exploited. A small library of iminosugar-based phosphatidylinositol phosphate analogues was designed and synthesized. During the biological evaluation, target compounds displayed low to moderate inhibitory activity for Akt, which suggests their feasibility for the development of new and more potent Akt inhibitors.

CONTENTS

ABREVIATIONS

3D	Three-dimensional
Ac	Acetyl
AcOEt	Ethyl acetate
All	Allyl group
AMBA	DO3A-CH_2CO-G-4-aminobenzoyl-Gln-Trp-Ala-Val-Gly-His-Leu-Met-NH_2
BCRP	Breast cancer resistance protein
Bn	Benzyl
BN	Bombesin
Boc	*tert*-butyl carbamate
Bombesin(6-13)	Bombesin fragment from residue 6 to 13
BSTFA	*N*,*O*-bis(trimethylsilyl)trifluoro acetamide
Bu	Butyl group
Bu_2SnO	Dibutyltin oxide
CAN	Cerium Ammonium Nitrate
Cbz	Carboxybenzyl carbamate
CNS	Central nervous system
Cpa	Chlorophenylalanine
CSA	Camphorsulfonic acid
CT	Computer tomography
d	Doublet
DCC	*N*,*N*'-dicyclohexylcarbodiimide
dd	Double doublet
ddd	Double doublet of doublets
des[Met^{14}]	Peptide with $metionine^{14}$ deleted
DIAD	Diisopropyl azodicarboxylate
DIPA	*N,N'*-diisopropylamine
DMAP	Dimethylaminopyridine
DMF	*N*,*N*-Dimethylformamide
DMSO	Dimethyl sulfoxide
DOTA	1,4,7,10-tetraazacyclododecane-1,4,7,10-tetraacetic acid
DPPA	Diphenylphosphoryl azide
DTPA	Diethylene triamine pentaacetic acid
e.g. and i.e.	For example

EDC	1-ethyl-3-(3-dimethylaminopropyl)carbodiimide
EGF	Epidermal growth factor
FGF	Fibroblast growth factor
Glp	Pyroglutamic acid
GRP	Gastrin-Releasing Peptide
GRP10	C-terminal decapeptide fragment of Gastrin-releasing peptide
Hca	Hydrocinnamic acid
IC_{50}	Half maximal inhibitory concentration
IGF	Insulin-like growth factor
IL	Interleukin
IR	Infrared
J	Coupling constant
K_d	Dissociation constant
KDa	Kilodalton
K_i	Dissociation constant for inhibitor binding
LBE	Lowest binding energy
LDL	Low-density lipoprotein
LHRH	Luteinizing hormone-releasing hormone
m	Multiplet
MBE	Mean binding energy
MDR-1	Multidrug resistance protein 1
MeOH	Methanol
min	Minutes
MRP-1	Multidrug resistance associated protein 1
NBS	*N*-bromosuccinimide
Nle	Norleucine
NMR	Nuclear magnetic resonance
NIS	*N*-iodosuccinimide
NOE	Nuclear overhauser effect
PC-3	Human pancreatic carcinoma cell line
PEG	Polyethylene glycol
PIA12	Reference inhibitor of Akt
PIP_2	Phosphatidylinositol diphosphate
PH domain	Pleckstrin homology domain
PKB	Protein kinase B
PPh_3	Triphenylphosphine
ppm	Part per million
Ptx	Paclitaxel
Py	Pyridine
r.t.	Room temperature
s	Singlet
SCLC	Small cell lung cancer

SFB	*N*-succinimidyl-4-fluorobenzoate
SPECT	single photon emission computed tomography
Tac	thiazolidine-4-carboxylic acid
TBAF	Tetra-*N*-butylammonium fluoride
TBAI	Tetra-*N*-butylammonium iodide
TBDPS	*tert*-butyldiphenylsilyl
TEA	Triethylamine
TEMPO	2,2,6,6-Tetramethylpiperidine-1-oxyl
TFA	Trifluoroacetic acid
TGF	Transforming growth factors
THF	Tetrahydrofuran
TLC	Thin-layer chromatography
TMSOTf	Trimethylsilyl trifluoromethanesulfonate
Tpi	2,3,4,9-tetrahydro-1*H*-pyrido[3,4-*b*]indol-3-carboxylic acid
Trt	Trityl
vs	Versus
δ	Chemical Shift
ψ-CH_2NH	Reduced peptide bond

State of the art

"Schur, you remember our 'contract' not to leave me in the lurch when the time had come. Now it is nothing but torture and makes no sense." (Sigmund Freud, after years of suffering from cancer of the jaw, he convinced his personal physician to give him several large doses of morphine for the pain. He fell into a coma and died the next day.)[1]

Cancer is a generic term for a large group of diseases that can affect any part of the body. Other terms used are malignant tumors and neoplasms. One defining feature of cancer is the rapid creation of abnormal cells that grow beyond their usual boundaries, and which can then invade adjoining parts of the body and spread to other organs. This process is referred to as metastasis. Metastases are the major cause of death from cancer.[2]

In the context of cell biology, cancer has a unique importance, and the emphasis given to cancer research has profoundly benefited a much wider area of medical knowledge than that of cancer alone. It is a disease in which individual mutant clones of cells begin by prospering at the expense of their neighbors, but in the end destroy the whole cellular society.[3]

The molecular mechanism of cancer development is a complex multi-step process, which is still subject of intensive research and discussion by the scientific and medical fields.[4] Carcinogenesis (the generation of cancer) is linked with mutagenesis (the production of a change in the DNA sequence), which is a clear correlation for three classes of agents: chemical carcinogens, ionizing radiations and certain viruses. Susceptibility to the disease can also be inherited, as individuals with an inherited genetic defect in the DNA repair mechanisms can accumulate mutations at an elevated rate.[3] In addition to these individual genetic factors, malignant transformation is also strongly influenced by some molecular changes associated with ageing.[4]

The malignant transformation occurs on a time scale of months or years in a population of cells in the body. A single mutation is not enough to convert a typical healthy cell into a cancer cell that proliferates without restraint. Indeed, the genesis of a cancer typically requires that several independent, rare mutational

events occur in the lineage of one cell. Studies revealed that an individual malignant cell generally harbors multiple mutations and that different combinations of mutations are found in different forms of cancers.[3]

Critical mutations involve genes known as proto-oncogenes and tumor suppressor genes. Mutations that activate proto-oncogenes stimulate cells to increase their number when they should not. Mutations that inactivate tumor suppressor genes allow cells to proliferate without inhibition. Both classes of genes code for components of the pathways that regulate the social and proliferative behavior of the cells in the body – in particular , the mechanisms by which signals from a cell's neighbors can impel it to divide, differentiate, or die.[3]

The disease does not usually become apparent until several years after the initial genetic lesion. During this long incubation period, the prospective cancer cells undergo a succession of changes. Cells that descend from the initial mutant clone undergo further mutations that make them proliferate more rapidly. At each stage, one cell acquires an additional mutation that gives it a selective advantage over its neighbors, making it better able to thrive in its harsh environment, with low levels of oxygen, scarce nutrients, and the natural barriers to growth presented by the surrounding normal tissues. Mutations that help cells to increase in number are critical for the development of cancer. These mutations generate either an increased rate of cell division or the resistance to programmed cell death by apoptosis. These special properties include alterations in cell signaling pathways, enabling the cells in a tumor to ignore the signals from their environment that normally keep cell proliferation under tight control. In many cancers, changes that block the normal maturation of cells toward a non-dividing and terminally differentiated state play an important role. The multiple number of mutations needed for tumor development is due to the number of different regulatory systems and barriers that must be disrupted by malignant cancer cell candidates. A powerful contribution to cancer progression is the genetic instability of cancer cells, generated by defective correction and repair of DNA damage and trouble in maintaining chromosome integrity, which increases the probability that cells will experience a mutation that would lead toward malignancy.[3]

During the formation of a neoplasia, dividing cells become no longer confined to their original location, resulting in a slightly disordered tissue. Some lesions may progress to a more serious stage, where most of the original tissue is occupied by undifferentiated dividing cells, which are usually highly variable in cell and nuclear size and shape. At this stage, it is still easy to achieve a complete cure by destroying or removing the abnormal tissue surgically. Without treatment, the abnormal tissue may simply persist and progress no further or may even regress spontaneously; but in at least 30-40% of cases, progression will occur, giving rise to a frank invasive carcinoma – a malignant lesion where cells cross and destroy the tissue boundaries, invade the surrounding tissues, and metastasize via the lymphatic vessels.[3]

Metastasis is the most feared and least understood aspect of cancer. To metastasize, a cancer cell must detach from the primary tumor, invade local tissues and vessels, survive and proliferate in an alien environment to generate new colonies at distant sites. Metastatic cells need a whole range of aberrant properties - in other words, new skills - to overcome several barriers and regulatory checkpoints during this process. Indeed, just one in a thousand, perhaps one in a million malignant cells manage to complete this sequence of events. Surgical cure becomes progressively more difficult as the invasive growth spreads, as well as localized irradiation. For this reason, early detection of cancer development enhances the chances to eradicate the disease.[3]

Although rare events are required in the development of cancer cells, the incidence of the disease is becoming progressively higher in the present days. This fact is supported by the observation that carcinogenic environmental factors have been linked to 75% of human cancers. Such factors are limited to societies that are affected by modern lifestyle issues such as tobacco use and pollution resulting from industrialization. Consequently, every year millions of people learn for the first time that they have cancer.[5]

Cancer is one of the main causes of death worldwide. It is the second leading cause of death in developed countries and the third in developing countries. The disease accounted for an estimate 7.6 million deaths (around 12% worldwide) in 2008, with 1.7 million in Europe (around 19% of deaths).[6] Deaths

from cancer worldwide are projected to continue rising, with an estimated 12 million deaths in 2030. The main types of cancer leading to overall mortality are: lung, stomach, colorectal, liver and breast.[2]

In addition to the human toll of cancer, the financial cost of cancer is substantial. The direct costs include payments and resources used for treatment, as well as the costs of care and rehabilitation related to the illness. Data limitations do not allow estimating the worldwide economic costs of cancer. However, the costs of cancer are staggering.[7]

1.1. Tumor Drug Targeting

Clinical cancer chemotherapy in the 20th century has been dominated by the development of cytotoxic drugs, initiated by the accidental discovery of the anticancer properties of nitrogen mustard and the folic acid analog aminopterin in the 1940's.[8] For more than five decades, chemotherapy has been the main modality for systemic treatment of advanced or metastatic cancers.[9] With the advances in the comprehension of cancer mechanisms, several cytotoxic compounds with high potential to become antitumor drugs have been discovered over the last decades. However, their success in turning into new cancer therapeutics has been hampered by their lack of selectivity for tumor cells. Most of the currently available cancer chemotherapeutic agents target DNA or the enzymes involved in DNA replication so that they can exploit the enhanced proliferative rate of cancer cells. Thus, these chemotherapeutic agents (and ionizing radiations, which also target mainly DNA) do not have any selective destructive effect against cancer cells. They destroy all rapidly dividing cells, including normal dividing cells in vital tissues such as lympho-hematopoetic tissues, gonads, hair follicles, and the lining epithelium of the gastrointestinal tract and mouth. The high toxicity of these drugs make them a threat for healthy cells. Their low chemotherapeutic index leads to severe generalized toxic effects when used at dosages necessary to kill tumor cells.[10] Undesirable side effects can be so devastating to result in the death of the patient.

Therefore, enhancement of the selectivity of cytotoxic drugs for tumor cells is a matter of extreme importance in oncology. The ultimate goal of cancer therapy is to develop agents that will selectively destroy cancer cells, sparing the normal tissues of the patient. One hundred years ago, after detecting the specificity of antigen-antibody interactions, Paul Ehrlich created the concept of a “magic-bullet” for cancer therapy, consisting of a molecule selective for a targeted cancer cell that should be linked to a highly toxic group. This concept became the basis of tumor drug targeting. The expectation has been that the cytotoxicity of these conjugates will be focused onto tumor cells, sparing normal tissues. Quantitatively more drug can thus be selectively delivered to the tumor site, to allow a higher drug concentration in the target cells and avoid systemic toxicity.[10] In general, the aim of tumor drug targeting is to increase the efficacy and reduce the toxicity of drugs. The use of a targeting system attached to the drug could help considerably to manipulate its body distribution and cellular disposition. This genuine idea made a major impact on medicine and chemistry, but remained essentially unexplored for many decades.[11]

Tumor targeted therapies need to take advantage of some properties of cancer cells that distinguishes them from normal cells. The first approach to target cytotoxic compounds directly to the cancer cells exploited tumor-associated antigens present on their surface.[3] More than 25 years ago, monoclonal antibodies against these antigens became very popular as potential “magic bullets” to be used in cancer. However, this fascinating and simple principle turned out to be much more difficult to transpose into reality than expected, mainly because of the excessive molecular mass (~150KDa) of antibodies. It was only in the past few years that adequate drugs based on antibody or antibody fragments have become commercially available for diagnosis and therapy of cancer, in particular of hematological neoplasias.[12] A large number of tumor-associated antigens have been discovered in the last decades, paving the way for the development of the immunotherapy of tumors.[10] The approach was used for the construction of monoclonal antibodies-toxin conjugates called immunotoxins and other chimeric toxins.[9] However, the efficacy of cancer immunotherapy with antibodies remains limited not only by their large size, which compromises its infiltration into the entire

tumor mass, but also by their relatively nonspecific binding to the reticuloendothelial system. This later property is particularly problematic if the antibody is used as a vehicle to deliver radionuclides, cytotoxic drugs, or toxins to the tumor site, resulting in high toxicity to bone marrow, liver and spleen.[13]

Apart from antibodies, a number of other carriers with varying degrees of tumor specificity have been investigated for drug targeting to tumors. The selectivity of most of these carriers is based on specific recognition of cell-surface associated receptors that are found overexpressed and abundant on cancer cells. This group of carriers includes lectins, growth factors (epidermal growth factor [EGF], transforming growth factors [TGF], insulin-like growth factor [IGF], fibroblast growth factor [FGF], and transferring), cytokines (IL-2, IL-4, IL-6), hormones, low-density lipoproteins (LDL) and folic acid. Hormones that have been successfully used for drug targeting include melonotropin, insulin, thyrotropin, luteinizing hormone-releasing hormone (LHRH), somatostatin and bombesin/gastrin-releasing peptide. Effective tumor inhibition by cytotoxic agent-linked hormones, cytokines, and transferrin have been demonstrated in human tumor xenografted models especially when adequate numbers of high-affinity receptors are available on tumor cells. Peptide-hormone receptors have also been successfully targeted by small peptide derivatives of the receptor-specific hormone and their analogs.[10]

1.2. Peptide Receptors as Tumor Targets

An innovative and fascinating application is the use of small peptides to deliver cytotoxic drugs to tumors. One of the main reasons for the increasing interest for peptides and peptide receptors in cancer is the possibility of receptor targeting, because the peptide receptors are often overexpressed in many primary human cancers, in comparison to their expression in normal tissue adjacent to the neoplasm and/or in its normal tissue of origin. Thus, these receptors can be used as binding sites for the selective delivery of cytotoxic drugs or radionuclides to the cancer cells.[12]

This field of investigation, which appears to be a small niche in the very large oncology field, has gained increased interest in the past decade. The

targeting of overexpressed peptide receptors in tumors by small peptides has become a very strong focus of interest for nuclear medicine. The international authority on nuclear medicine, Dr. Henry Wagner, at the 100-year anniversary of nuclear medicine, named the peptide approach in nuclear oncology as one of the most promising fields for the present decade. Gastroenterologists and endocrinologists are also attracted by the concept of peptide receptor targeting.[12]

Regulatory peptides represent a group of different families of molecules known to act on multiple targets in the human body at extremely low concentrations. Targets of these peptides are not only the brain and the gastrointestinal tract, but also the endocrine system, the kidneys, the lungs, and the immune, vascular, and peripheral nervous systems. Therefore, regulatory peptides control and modulate the function of almost all key organs and metabolic processes. Their action is mediated through specific membrane-bound receptors, almost all of which belong to the group of G-protein coupled receptors. They can influence many intracellular effector systems, playing an important role in cell proliferation, or in apoptosis, which contributes to the current interest for peptides in cancer research. These peptides play prominent roles in not only normal conditions but also pathological processes. They may be factors involved in inflammation, but may also play a receptor-mediated role in cancer and cancer progression.[12] In summary, studies on peptide receptor-based drug targeting have the potential to bring benefits not only to oncology, but also to other fields covered by the influence of these receptors.

Peptides, peptidomimetics, or small molecule peptide analogs are considered an attractive alternative to antibodies in cell surface targeting for cancer therapy, imaging and diagnostics. This is due to their small molecular mass, excellent tissue permeability, lack of antigenicity, chemical stability, ease to synthesize and modify chemically (to optimize their binding affinity and metabolic stability), flexibility in chemical conjugation (can be readily conjugated to radionuclides, cytotoxic drugs or toxins), and for their high affinity for receptor binding. All of these attributes promote penetration into tissue and more effective targeting. However, as physiological compounds, their long-term administration can produce side effects due to the normal actions of the peptides. Nevertheless,

it can be negligible in the therapeutic doses that are used, especially if compared to the side effects generated by current chemotherapeutic drugs.[12,14]

It is well established that many common malignant tumors overexpress peptide receptors, allowing enhanced uptake of peptide ligands which are selective for these receptors. Targeted cytotoxic peptide conjugates are hybrid molecules, composed of a peptide carrier (the ligand in figure 1), which binds with high-affinity to receptors on tumor cells, and a cytotoxic (antineoplastic) moiety.[15] After binding, this procedure takes advantage of one important characteristic of many G protein-coupled receptors, namely that they can internalize into the cell together with their ligand, after receptor-ligand interaction at the cell membrane (receptor-mediated endocytosis). Therefore, the internalized conjugate is hydrolyzed inside the cell to release the cytotoxic moiety, and may be able to selectively destroy the targeted cancer cell (Figure 1).[12]

Figure 1: representation of the cellular mechanism of tumor drug targeting. The concept takes advantage on the overexpression of peptide receptors in the membrane of tumor cells. After high-affinity binding between the peptide-carrier and its receptor, the cytotoxic conjugate is internalized. It is then hydrolyzed to release the cytotoxic drug inside the tumor cell, which triggers the apoptosis of the tumor cell.

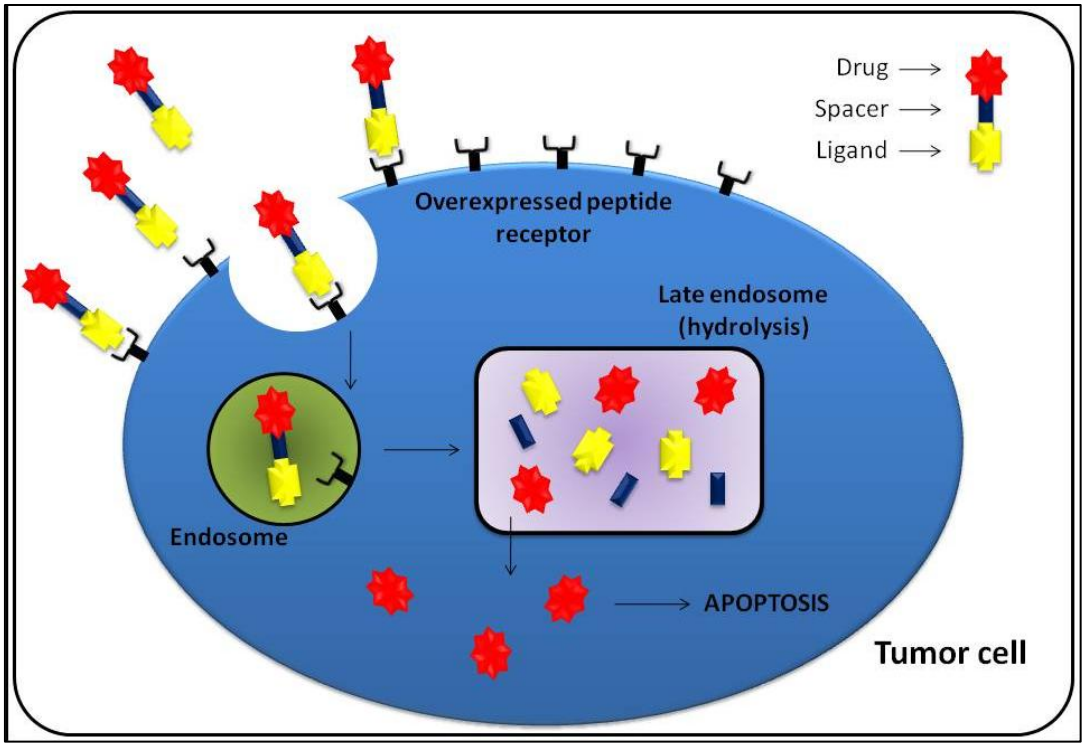

Apart from therapeutic applications, molecular imaging techniques are now indispensable tools in modern diagnostics, because they are highly specific and can provide biological information at the molecular level in living systems. They have enabled visualization of some of the specific molecular events that play key roles in disease processes, and they have enabled earlier diagnosis, as well as monitoring of therapeutic responses. From a practical standpoint, synthetic peptides have attracted much attention as molecular imaging probes for small molecules and macromolecules.[14]

The first hormonally targeted chemotherapeutic agents developed for the treatment of prostate and breast cancer used estrogenic steroid molecules as carriers for various alkylating agents, in order to enhance selectivity and cytotoxicity on estrogen receptor-positive cancer cells. These conjugates were used clinically in patients, but objective responsive rates were low. Therefore, the use of other hormonal carriers that could increase the efficacy of chemotherapeutic agents appeared to be worthy of extensive exploration.[9] This fact points out peptide hormone receptor as potential candidates for this purpose. After a sequence of unsuccessful attempts and average results in early studies, a conjugate containing DNA intercalator anthracyclins daunomycin linked to the *N*-terminal residue of β-melanocyte-stimulating hormone was reported to kill melanoma cells *in vitro*.[16]

In early studies, rare occurrence of positive results from *in vivo* targeting of cancer cells with natural peptide hormones can be explained by their low metabolic stability. The structure of natural peptides makes them extremely sensitive to peptidases. They are rapidly broken down due to cleavage of peptide bonds by several types of peptidases present in most tissues. The enzymatic destruction can be reduced by molecular modifications, such as the substitution of D-amino acids by L-amino acids or unnatural amino acids.[12,15] Thus, metabolically stable analogs must be developed as a prerequisite for successful clinical applications, in particular for long-term treatments.

A very good example is the development of the somatostatin analog octreotide (Figure 2). The oncological potential of somatostatin has been appreciated for more than 30 years, but its half-life is very short, so that its

therapeutic use is impractical. Compared with natural somatostatin, octreotide has a much prolonged half-life in plasma and tissue and a longer action. Octreotide lacks key enzyme cleavage sites and is more stable than native somatostatin (half-life: 90-110 min vs <3 min). The development of octreotide and some derivatives has only been possible through a long and considerable effort of development. Not surprisingly, the production of further somatostatin analogs with more selective and prolonged activities was addressed by several research groups.[9,12,14]

About 20 years ago, a radiolabeled conjugate of ocreotide (Figure 2) appeared as an alternative to radiolabeled antibodies and natural peptides. Indium-111 labelled DTPA-octreotide (Octreoscan) led to a major breakthrough in this field. On the basis of the discovery that most human neoroendocrine tumors express a high density of somatostatin receptors, it became a method for localizing these tumors and their metastasis by *in vivo* scintigraphy. The tumors, after radioligand binding to their receptors and internalization of the ligand-receptor complex, could thus be identified as hot spots on γ-camera scans. Currently ^{111}In-OctreoScan is considered the best standard for investigations of targeted radiolabeled peptides for the effective targeting of somatostatin receptors overexpressed in neuroendocrine tumors.[17] This is the first US Food and Drug Administration approved diagnostic radiopeptide for scintigraphy of patients with neuroendocrine tumors.[15] However, due to its moderate binding affinity to somatostatin receptor subtype-2 and because DTPA is not a suitable chelator for many other nuclides, the next generation of somatostatin analogs has been introduced.[14] This fact inspired the development of several radiolabeled analogs that show great promise for diagnosis and therapy of somatostatin receptor-expressing tumors *in vivo*. Most of them are under clinical investigation.[15]

In addition, a variety of promising new targets and drug targeting candidates are under active development, and other key players are likely to be available in the clinic in the near future.[14]

Figure 2: structure of human somatostatin (A) and related analogs, octreotide (B) and radiolabeled Octreoscan (C)

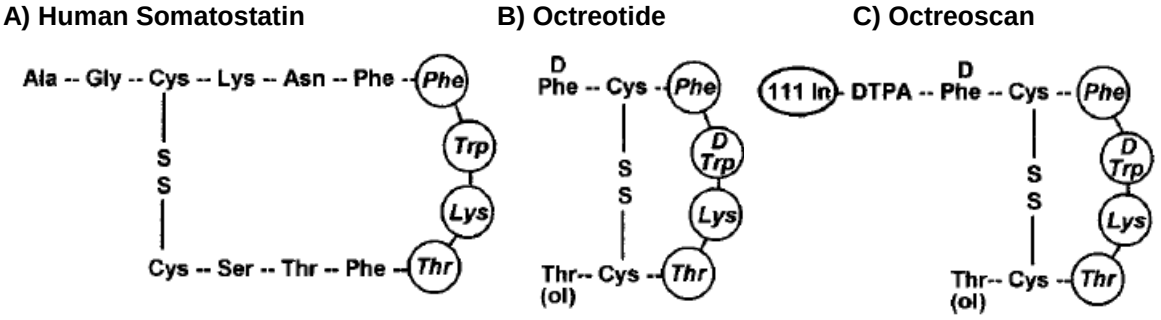

Although the clinical use of somatostatin has been refined during the past decade, it remained limited to tumor categories that express somatostatin receptors in sufficiently large quantities, i.e., mainly neuroendocrine tumors. Therefore, it has been of increasing interest to investigate whether receptors for other regulatory peptides are overexpressed in more common human cancers (i.e., in lung, prostate, colon, or pancreatic carcinomas) to apply a strategy similar to that used with somatostatin.[12]

For many of the other peptides, only limited advances have been made to develop peptide analogs having an improved stability in the order of hours. The information provided by molecular biology over the structure-activity relationship of regulatory peptides and their receptors is a great advantage that can be used in the design, synthesis and development of novel peptide analogs that may become useful for clinical applications.[12,13] For this purpose, remarkable efforts have been made to screen or design membrane receptor ligands.[9,12,15,18]

Many naturally occurring peptides exhibit extremely high affinities (nano- or subnanomolar range) for cell-surface receptors. The successful development of new receptor-binding peptide analogs is thus dependent on the molecular modifications of a given natural peptide, while preserving the original binding affinity for the target receptors. Conjugation of cytotoxic compounds to analogs of hormonal peptides, such as LHRH and bombesin/Gastrin-Releasing Peptide (BN/GRP), have been developed for targeting certain tumors that overexpress receptors for those peptides, and therefore are more selective for killing cancer cells. In addition to somatostatin receptor scintigraphy, bombesin/GRP receptors have recently shown great promise for tumor targeting. This potential is attributed

primarily to the overexpression of these receptors in human cancers including prostate, breast and small cell lung cancer. Several radiolabeled BN/GRP analogs have shown potential for *in vivo* visualization of BN/GRP receptor-expressing tumors.[15]

The research group of Nobel laureate Andrew V. Schally and Attila Nagy synthesized a large number of cytotoxic analogs of hypothalamic peptides, after years of intensive work. These consisted of diverse hormonal analogs, mostly of luteinizing hormone-releasing hormone (LHRH), conjugated to a variety of chemotherapeutic agents. The high specificity of peptide receptors was utilized in an attempt to deliver these agents to the tumor cells where they might exert their cytotoxic effects. This has been an extremely active area of their research. The findings that LHRH receptors were found in a large number of tumor cell lines provided support for the development of a new class of targeted antitumor agents. Substitution of some amino acids in the LHRH structure generated analogs with high affinity to the receptors for LHRH. Further studies on their conjugation to diverse cytotoxic agents using different linkers resulted in the development of two active LHRH analogs, containing cytotoxic doxorubicin and its more potent derivative 2-pyrrolino-doxorubicin, named AN-152 and AN-207 (Figure 3).[9]

Figure 3: structures of Schally's cytotoxic LHRH analogs AN-152 and AN-207.[9]

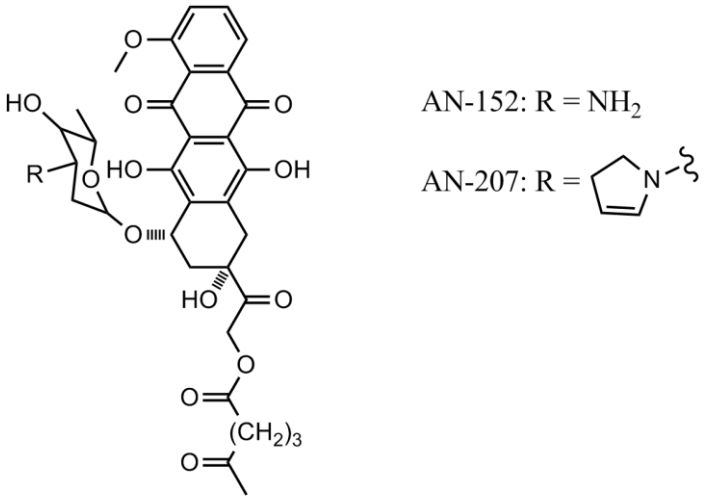

These cytotoxic conjugates showed high-affinity binding to membranes of human breast cancer specimens and cell lines displaying IC_{50} values in nanomolar concentration range, and less toxic than equimolar doses of the cytotoxic agent alone.[19] The same result was obtained by testing cytotoxic conjugates based also on analogs of bombesin/GRP (AN-215) and somatostatin (AN-238) in tumors that express the corresponding receptors. All four targeted cytotoxic conjugates effectively inhibited the growth of human ovarian and endometrial tumors (positive for the respective peptide receptor) xenografted in mice, and caused a powerful inhibition of mouse mammary cancer growth.[20] A complete regression of human breast cancer xenografted in mice was observed for the treatment with AN-207. This conjugate produced also the regression of rat prostate carcinoma and human prostate cancer xenografted in mice, an effect that was not observed by the injection of the doxorubicin cytotoxic moiety alone. Because of the presence of LHRH receptors on a high percentage of ovarian, breast and prostate cancers, targeted therapy based on cytotoxic analogs of these peptides should be more efficacious and less toxic than the currently used systemic chemotherapeutic regimens and might be indicated for primary therapy of patients with the respective cancers in advanced stage.[9] AN-152 is currently submitted to a multi-center Phase II clinical trial conducted in 15 centers in Europe. Preliminary positive results for LHRH-expressing ovarian and endometrial cancers have been disclosed and will be officially present soon (source: Æterna Zentaris Inc.).[21]

1.3. Bombesin/Gastrin-Releasing Peptide Receptors

Bombesin is a tetradecapeptide that was first isolated from the skin of the amphibian *Bombina bombina*.[22] Subsequently, gastrin-releasing peptide (GRP) was discovered as the mammalian counterpart of bombesin.[23] GRP is a 27-amino acid peptide that shares the same C-terminal decapeptide with bombesin, except by one amino acid (Table 1), which accounts for an essentially identical physiologic action for both peptides.

Table 1: amino acid sequence of bombesin and the C-terminal decapeptide of GRP

Peptide	**Amino acid sequence** (bombesin numbering) 1 2 3 4 5 6 7 8 9 10 11 12 13 14
Bombesin	pGlu-Gln-Arg-Leu-Gly-Asn-Gln-Trp-Ala-Val-Gly-His-Leu-Met-NH_2
GRP	Gly-Asn-His-Trp-Ala-Val-Gly-His-Leu-Met-NH_2

Gastrin-Releasing Peptide and bombesin have been associated to an important role in cancer development as Cuttitta and coworkers reported that they function as autocrine growth factors in human small cell lung cancer, and likely for other tumors.[24] This finding stimulated several laboratories to synthesize antagonists of the GRP receptor for hormonal treatment of these malignancies.

Mammalian receptors for bombesin-like peptides are divided in three different subclasses: 1) BB_1, known as the neuromedin-B-preferring receptor (neuromedin-B is a natural bombesin-like peptide); 2) BB_2, known as the GRP-preferring receptor (the only that preferentially binds GRP with high affinity); 3) BRS-3, bombesin receptor subtype 3, considered an orphan receptor because it binds only with low affinity the naturally occurring bombesin-like peptides. In order to simplify the nomenclature used in this thesis, the BB_2 subclass, associated to cancer development and subject of the present work, will be called simply by its traditionally used name: GRP receptor.[25,26]

GRP receptors are guanine nucleotide binding protein (G-protein)-coupled receptors, have seven transmembrane domains, and activate phospholipase C to increase intracellular concentrations of inositol phosphates, calcium and diacyl glycerol.[27]

As a membrane receptor, the first requirement to consider the GRP receptor as a potential drug target in oncology is to be overexpressed by tumor cells, a feature that can differentiate them from healthy cells. Indeed, GRP receptors were found in high density in a wide range of human tumors. This is one of the reasons why bombesin/GRP receptors attracted our attention, as they have shown great promise for tumor targeting.[15]

Nowadays, lung cancer is the most commonly diagnosed malignancy. The GRP receptor was found overexpressed in 85% of patients with lung cancer (small-cell lung cancer and non small-cell lung cancer).[28] In another study, the receptor was massively found in 30 of 30 invasive prostatic carcinomas and in 26 of 26 cases of prostatic intraepithelial neoplasias. Prostate cancer is the second most common in man (following lung cancer). Conversely, GRP receptors are absent in normal prostate.[29] The massive GRP receptor expression in prostate tissues that are in the process of malignant transformation or that are completely neoplastically transformed suggests that GRP receptors may be markers for early molecular events in prostate carcinogenesis and useful in differentiating prostate hyperplasia from prostate neoplasia.[12] Breast cancer, the most common in women, was also reported to overexpress the same receptor: one study reported two thirds of neoplastic mammary epithelial cells,[30] whereas another study observed overexpression in 72% of breast cancer cells.[31] The lymph node metastases originated from primary breast cancers were all positive for the GRP receptor. The strong GRP receptor expression in these carcinomas suggests that these tumors may be a consequential target for GRP and bombesin analogs.[12] These receptors have also been found in high quantity in ovarian and uterine cancers, head and neck squamous cell carcinomas, various CNS/neural tumors, neuroblastomas, colon, pancreatic and gastric cancer, gastrointestinal carcinoid tumors and renal cell cancers.[25,26,32,33] It was observed also that GRP exerted a mitogenic role in most of the malignancies cited above.[26] These findings suggest GRP receptors on breast cancer as a potential target for the therapy with cytotoxic bombesin/GRP analogs.

In a mechanism that is typical for G-protein coupled receptors (GPCR), the GRP receptor internalizes by endocytosis after binding to agonists. This phenomenon was observed by Grady and co-workers by confocal microscopy using GRP labeled with a fluorescent probe, cyanine 3.18, as shown in figure 4. During the timescale of 60 min, fluorescent GRP was confined to the plasma membrane (0 min, A), internalized into superficial vesicles (5 min, B), which merged to form larger vesicles near the nucleus (from 10 to 60 min, C-D).[34]

Figure 4: internalization of fluorescent-labeled GRP in cells expressing the GRP receptor. Cells were incubated with 100 nM peptide for 60 min at 4°C, washed and incubated at 37°C. Then, cells were observed at 0 (A), 5 (B), 10 (C) and 60 (D) min. Scale bar = 10 μm

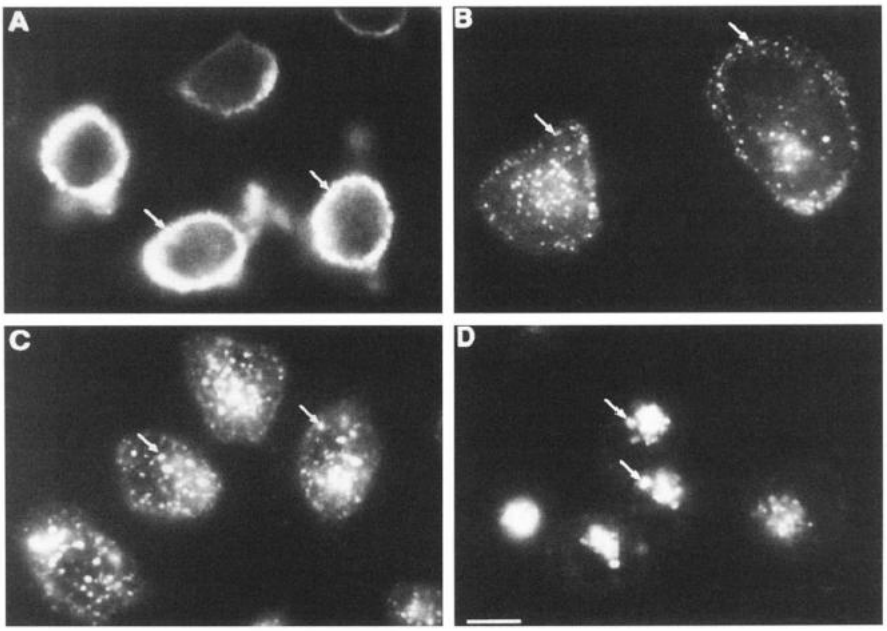

Taking into account all the data regarding the GRP receptor overexpression in a large spectrum of human cancers, and reminding that as a GPCR it internalizes after ligand-binding, it is clear that the GRP receptor is considered one of the most promising targets for anticancer targeted therapy.

The use of natural GRP and bombesin as peptide carriers for tumor targeting is however a very limited strategy, because of the low metabolic stability of these peptides, as already mentioned. For example, like other naturally occurring peptides, bombesin has a very short circulation half-life (<2 min). Consequently, in the last decades various bombesin/GRP analogs based on their key amino acid sequence, the C-terminal decapeptide and its fragments, were screened and developed as GRP receptor-selective ligands, mostly by incorporating radioisotopes at the N-terminus of the peptide.[14]

1.4. Bombesin/GRP analogs – antagonists, agonists and tumor targeting conjugates

Useful guidance for designing GRP receptor ligands for tumor targeting with high binding affinities was provided through insights gained from earlier studies on developing receptor antagonists for antiproliferative therapy.[12] Researchers considered that by blocking the bindings of GRP to its receptor, these antagonists could block the physiological effects of this peptide and inhibit the growth of tumor cells that respond to the growth-promoting action of GRP. Thus, these antagonists could have a powerful application as potential anticancer compounds.[15]

The C-terminal 7–14 amino acid sequence (Gln/His^{7}-Trp^{8}-Ala^{9}-Val^{10}-Gly^{11}-His^{12}-Leu^{13}-Met^{14}-NH_2), of bombesin/GRP is known to be critical for receptor binding affinity and biological activity.[35] With only rare exceptions, GRP analogs produced to date are essentially peptides and pseudopeptides based on this sequence. They have been produced from the variation of the amino acid sequence by replacing natural amino acids with D-amino acids and unnatural amino acids, also by using reduced peptide bonds (CH_2NH_2 instead of CONH), and deletion of the C-terminal residue ([desMet^{14}]GRP analogs), with various chemical groups replacing this last amino acid (such as amides, esters and hydrazides).[25]

Two research groups gave useful contributions in the search for efficient GRP analogs. During years of intensive research on the structure/activity relationships of bombesin/GRP derivatives, the group of Jensen produced GRP receptor antagonists that were able to inhibit the growth of tumor cells.[36] The same was described later by Schally's group working with GRP receptor antagonists developed after several efforts.[37,38] Their observations were essential to bring the GRP receptor to the light of tumor drug targeting.

Studies on GRP antagonists provided useful structure/activity relationship information for the design of GRP receptor ligands. Early bombesin structure-function studies demonstrated that Trp^{8} and His^{12} in the C-terminus were essential for biologic activity.[39,40] Substitution of His^{12} by D-amino acids result in analogs with antagonist activity, however with less affinity and low selectivity for the GRP

receptor.[25] It was demonstrated also that desirable elimination of the last residue, the readily oxidized Met[14], and replacement by Leu ([Leu[14]]bombesin) results in retention of 33% of the biological potency and binding affinity compared to bombesin, proving that methionine, and consequently its side-chain, was not essential for the biological activity.[41] This approach was used later on by several research groups.

In a pioneer work, the group of Jensen replaced each peptide bond CONH group in the C-terminal octapeptide of [Leu[14]]bombesin by a CH_2NH group. Among the six peptides produced by this procedure, the analog that had the peptide bond between Leu[13] and Leu[14] replaced, [Leu[13]-ψ-CH_2NH-Leu[14]]bombesin, exerted potent and specific receptor antagonist activity compared to previously reported GRP receptor antagonists. This was the first analog described with an affinity < 0.1 μM. The results were used by the authors to suggest a possible β-sheet receptor-binding conformation for bombesin, according to putative hydrogen-bonding points (Figure 5).[41]

Figure 5: putative receptor-binding conformation for C-terminal octapeptide [Leu[14]]bombesin suggested by Coy and coworkers.[41]

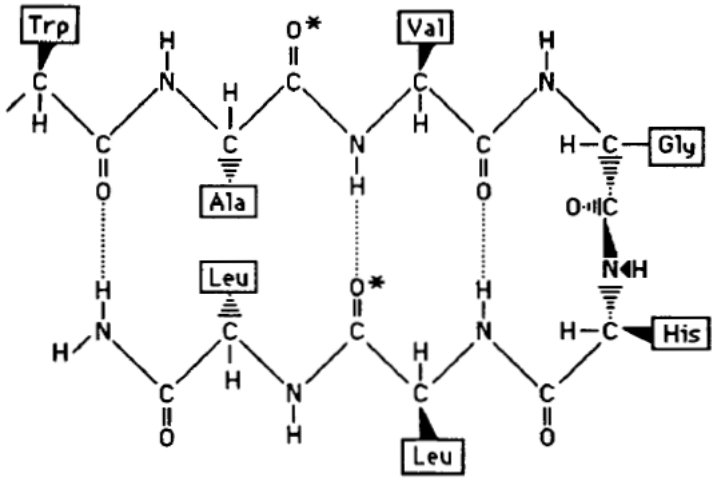

Controversially, the reduction of the peptide bond between Val[10] and Gly[11] resulted in an derivative that retained 30% of agonist activity relative to the parent peptide. This reduction brakes an important hydrogen-bond that would maintain the suggested conformation and consequently, result in loss of potency, which is

not explained by the authors.[41] Later, Coy and coworkers produced conformationally restrained analogs of the C-terminal of bombesin with two cysteine residues in positions 6 and 14 linked via a disulfide bridge. The cyclization of the C-terminal of bombesin could mimic the β-sheet receptor-binding conformation suggested by the authors. However, the cyclized bombesin analog displayed a 1000 times weaker binding affinity for the receptor, which did not help to support the proposed β-sheet conformation.[42]

The group of Jensen synthesized and examined the effect of C-terminal modifications of des[Met^{14}]bombesin(6-13) analogs, where des[Met^{14}] means the elimination of the C-terminal methionine residue and bombesin(6-13) means that the analogs are based on the C-terminal sequence from residues Asn^{6} to Leu^{13}. The formation of an amide function in the C-terminal of these analogs provided a variety of potent antagonists and partial agonists according to the alkyl group that substitutes the amide function.[43] Similarly, Mokotoff and coworkers found that amide derivatives in the C-terminal of des[Met^{14}]bombesin/GRP analogs were promising peptide modifications for imparting antagonism.[44]

Subsequent studies in the class of analogs with reduced peptide bonds described the substitution of the natural amino acids by D-amino acids as D-Phe and unnatural aminoacids like chlorophenylalanine (Cpa). This approach produced the potent GRP receptor antagonist [D-Phe^{6}, Leu^{13}-ψ-CH_2NH-Cpa^{14}]bombesin(6-14).[36] Following the same approach Leban and coworkers described a potent class of antagonists characterized by a D-Pro-ψ-CH_2NH-Phe-NH_2 C-terminus. This class is represented by the highly potent analog (3-phenylpropanoyl)-His,Trp,Ala,Val,D-Ala,His,D-Pro-ψ-CH_2NH-Phe-NH_2, that accounts for a very high binding affinity (K_i 0.001 nM) and selectivity.[45] This antagonist was reported to inhibit the growth of small cell lung cancer and other GRP receptor physiological responses.[25]

Later, the Jensen group developed two highly potent ligands, [D-Phe^{6},β-Ala^{11},Phe^{13}, Nle^{14}]bombesin(6–14) and the analog amenable to radiolabelling [D-Tyr^{6},β-Ala^{11},Phe^{13}, Nle^{14}]bombesin(6–14), which shown to be bound by all GRP receptor subtypes with high affinity (1-8 nM).[46,47] The first compound was identified as a high affinity agonist of the GRP receptor, providing the useful observation that

the presence of the D-Phe^6 residue instead of Asn^6 maintains the biologic activity of GRP, with a slightly lower potency. Darker and coworkers described that deletion of this N-terminal D-Phe^6 residue and cyclization of the resultant N-terminal Gln^7 to a pyroglutamic acid (Glp) resulted in a high increase in functional potency and selectivity.[47] This effect could be linked to the presence of His in that position for GRP, therefore the pyroglutamic ring could make this analog more "GRP-like" (Figure 6). Removal of the Glp^7 residue afforded a strong drop in the agonist potency. Then the authors performed an alanine scan, in which each residue was replaced by alanine. Substitution of Glp^7 and Phe^{13} resulted in analogs with reduced potencies.[47] The result suggests that the presence of a hydrophobic residue in position 13 is required for agonist activity. This conclusion is supported by a previous study of Guard and coworkers that described the importance of Leu^{13} for binding affinity of bombesin to the GRP receptor. They also observed the critical importance of Trp^8 by an alanine scan.[48]

On the other hand the analog [D-Tyr^6,β-Ala^{11},Phe^{13}, Nle^{14}]bombesin(6–14), iodinated at the D-Tyr^6 residue, yielded a useful radioligand able to distinguish the various bombesin receptor subtypes on the basis of the rank order of their affinity for GRP, neuromedin B, [D-Tyr^6,β-Ala^{11},Phe^{13},Nle^{14}]bombesin(6–14), or bombesin. Using this approach, they could specifically detect receptor subtype expression in human pancreatic islets.[49]

Recently, the group of Jensen synthesized His^{12} substituted [D-Tyr^6,β-Ala^{11},Phe^{13}, Nle^{14}]bombesin(6–14) analogs in an attempt to identify possible GRP receptor-selective ligands. This strategy however does not seem useful for making GRP analogs, as it did not yield any GRP receptor-selective agonists, which accounted to the findings that His^{12} is essential for biologic activity. Also, N-methylation of the residues did not result in selective analogs.[50]

Figure 6: comparison between the structures of GRP and its analog [Glp^{7},β-Ala^{11},Phe^{13}, Nle^{14}]bombesin(6–14)

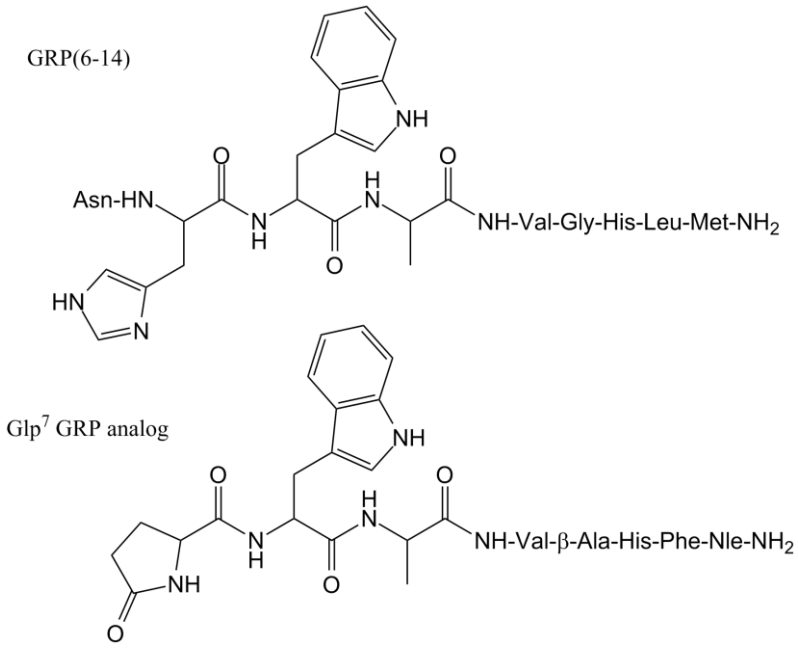

During the past decade, the group of the Nobel laureate Andrew V. Schally performed many efforts in the development of bombesin/GRP analogs. Most of them were on the search for more potent C-terminal [Leu^{13}-ψ-CH$_2$NH-Leu^{14}] analogs and its derivatives. During this long survey they obtained analog RC-3095 [D-Tpi^{6}, Leu^{13}-ψ-CH$_2$NH-Leu^{14}]bombesin(6-14), where Tpi means 2,3,4,9-tetrahydro-1*H*-pyrido[3,4-*b*]indol-3-carboxylic acid. RC-3095 was reported to strongly inhibit several experimental cancers *in vitro* and *in vivo*. RC-3095 and related analogs block the binding of bombesin/GRP to the receptors on Swiss 3T3 cells (overexpressing GRP receptor) and various human cancers.[9] Subsequent modification of the C- and N-terminal amino acids led to new and more powerful antagonists, such as RC-3940-II [Hca^{6}, Leu^{13}-ψ-CH$_2$NH-Tac]bombesin(6-14) which has an increased affinity (sub-nanomolar) to the receptors and higher antitumor activity (Hca = hydrocinnamic acid, Tac = thiazolidine-4-carboxylic acid).[51,52] In a recent phase I clinical trial, RC-3095 was administered to 25 patients with different advanced malignancies. No side effects occurred, but there were no tumor responses.[53] The tumor inhibitory mechanism of bombesin/GRP antagonists is a much more complex than a simple competitive action on the receptor, and is incompletely understood. Therefore, the inhibition of the GRP

receptor is not a guarantee of tumor inhibition. The authors then assumed that cytotoxic bombesin conjugates using these bombesin/GRP analogs would be more potent than the straight bombesin/GRP antagonists and that they could produce a complete tumor regression and not merely a palliative stabilization.[9]

Thus, Schally and coworkers used the chemistry developed for the preparation of the highly active cytotoxic LHRH hybrids described previously, containing doxorubicin and its 2-pyrrolino derivative, for the synthesis of cytotoxic conjugates containing their bombesin/GRP analogs. The cytotoxic radicals were linked to the amino terminal of a series of [X^{13}-ψ-CH_2NH-X^{14}]bombesin(6/7-14) analogs (X represents the variable amino acids involved in the study). The resulting conjugates showed high binding affinities to GRP receptors on Swiss 3T3 cells, comparable with those of their respective carriers.

The conjugate AN-215 (Figure 7), in which [Leu^{13}-ψ-CH_2NH-Leu^{14}]bombesin(7-14) (RC-3094) is covalently attached to 2-pyrrolino-doxorubicin, showed the highest binding affinity to receptors for bombesin/GRP (K_D<1 nM). AN-215 and its corresponding cytotoxic radical exerted similar inhibitory effects on the *in vitro* growth of many cancer cell lines that have receptors for bombesin/GRP. Preliminary *in vivo* experiments on pancreatic cancers in hamsters indicated that cytotoxic bombesin analog AN-215 had significant antitumor activity and lower toxicity than the unconjugated cytotoxic radical. They evaluated whether bombesin receptors could be used for targeting cytotoxic bombesin analogs to experimental small-cell lung cancer *in vivo*. The growth of SCLC tumors was significantly inhibited by AN-215 as compared with the control groups, while equimolar doses of the unconjugated cytotoxic radical were toxic and produced only a minor tumor inhibition. This supports the concept that cytotoxic bombesin analog AN-215 was preferentially targeted to SCLC tumors. The effectiveness of targeted cytotoxic AN-215 was also described in experimental models of gastric, colon, ovarian, endometrial, breast and prostatic cancer.[9,54] A low or no induction of multidrug resistance proteins MDR-1, MRP-1 and BCRP occurred after treatment with AN-215.[55] In summary, these results demonstrate that cytotoxic conjugates consisting of bombesin/GRP analogs could be used for targeted therapy of tumors that

express GRP receptors.[9,54] AN-215 is currently under pre-clinical investigation as property of Æterna Zentaris Inc.

Figure 7: structure of the cytotoxic conjugate AN-215

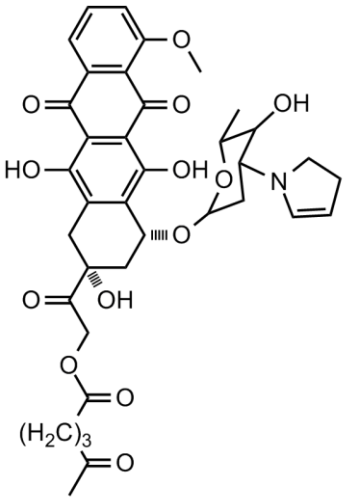

Gln-Trp-Ala-Val-Gly-His-Leu-ψ-(CH_2NH)-Leu-NH_2

Several research groups have been using the GRP receptor for tumor targeting. The biologically active C-terminal fragment of GRP and analogs based on the same amino acid sequence have been used as targeting vectors for radionuclides for experimental therapy and diagnostic applications.[15] In the same manner, conjugates with cytotoxic compounds are used for their potential antitumor activity. Moody and colleagues developed a tumor drug targeting conjugate by linking camptothecin to the peptide [D-Tyr^6,β-Ala^{11},Phe^{13}, Nle^{14}]bombesin(6–14) using a N-methyl-ethylenediamine linker (Figure 8). This conjugate is a potent full agonist and inhibited the growth of GRP receptor-overexpressing cells *in vitro* and *in vivo*. The antitumor effect is exerted by receptor-mediated cytotoxicity, where the conjugate functions as a pro-drug. Using fluorescent imaging, the conjugate was found to co-localize with GRP receptors initially and later to be internalized in cytoplasmic compartments. The authors detected that 25% of internalized conjugate was metabolized to release free camptothecin.[56,57]

The same was observed for the conjugate of a shortened bombesin agonist with the cytotoxic anticancer drug paclitaxel (Ptx), Ptx-PEG-bombesin(7–13),

which has a PEG spacer connecting the carrier and the cytotoxic moieties. This conjugate (IC_{50} 14 nM) was more than twice as potent as paclitaxel (IC_{50} 35 nM). The results demonstrate that the receptor-mediated tumor-targeting by the bombesin analog enhanced the drug delivery into the cancer cells. Moreover, the binding affinity of the complex was retained as compared with the unconjugated peptide.[58,59]

Figure 8: camptothecin-[D-Tyr^{6},β-Ala^{11},Phe^{13}, Nle^{14}]bombesin(6–14) conjugate structure

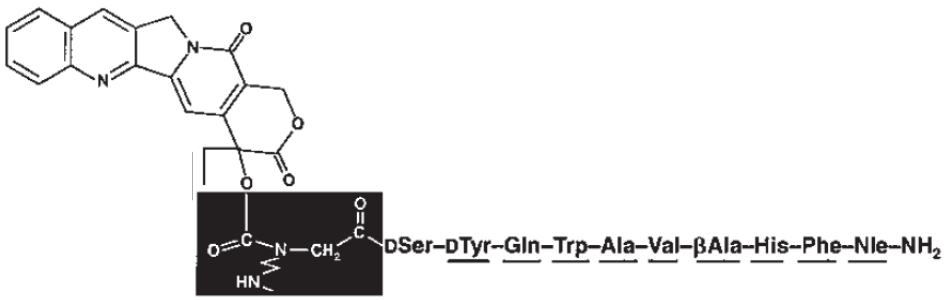

Apart from cytotoxic targeted peptides, considerable interest has been devoted to radiolabeled analogs of bombesin/GRP. Recent studies with somatostatin radiolabeled analogs showed promising results for advanced neuroendocrine tumors that overexpress somatostatin receptors, and they have entered phase 3 studies.[15,25] The finding that GRP receptors are more widely overexpressed than somatostatin receptors prompted researchers to produce a huge number of GRP-like peptides labeled with various radionuclides (^{111}In, ^{68}Ga, ^{177}Lu, ^{64}Cu, ^{86}Yt, ^{18}F, ^{99m}Tc and ^{188}Re). These targeting agents have been proposed for both tumor imaging and therapy.[25,26,32,33] Examples of radiolabeled GRP analogs are so many that just the most representative members of this group will be mentioned here.

One of the most potent radiolabeled agonists described in the literature is ^{177}Lu AMBA (^{177}Lu-labeled DO3A-CH_2CO-G-4-aminobenzoyl-Gln-Trp-Ala-Val-Gly-His-Leu-Met-NH_2), which has high affinity (K_d 1 nM) for the GRP receptor. Lantry and colleagues described that one or two doses of ^{177}Lu-AMBA significantly prolonged the life span of PC-3 (pancreatic tumor cell line) tumor-bearing mice

and decreased PC-3 tumor growth rate over controls. Also, it has low retention of radioactivity in the kidneys and demonstrates a very favorable risk-benefit profile. ^{177}Lu-AMBA is in phase I clinical trials.[60]

In a comparative study between five promising radiolabeled bombesin analogs, including the prospective radiopharmaceutical [^{111}In] AMBA, [^{99m}Tc] Demobesin-1 demonstrated to be the best, showing superior *in vivo* stability, highest tumor uptake and retention while pancreatic and renal clearance were faster.[61] This conjugate is formed by [D-Phe^{6},Leu-NHEt^{13},desMet^{14}]bombesin(6-14) and an open chain tetraamine chelator for stable ^{99m}Tc binding, connected by a benzylaminodiglycolic acid linker (Figure 9). It demonstrated a very high affinity for the GRP receptor, good plasma stability (more than 1h), exhibiting high GRP receptor-mediated uptake with high and prolonged localization at the tumor site.[62] A very similar radiolabeled conjugate, ^{111}In-Bomproamide, was generated with the same amino acid sequence of Demobesin-1, with a propyl group attached to C-terminal Leu^{14}-NH_2. DOTA was used as chelator with an aminohexanoyl linker. ^{111}In-Bomproamide displayed also similar binding affinity, and rapid (15 min) and high uptake in human PC-3 prostate cancer tumors xenografted in mice, as observed by SPECT/CT imaging (Figure 10).[63]

Figure 9: structures of [^{99m}Tc] Demobesin-1 and ^{111}In-Bomproamide

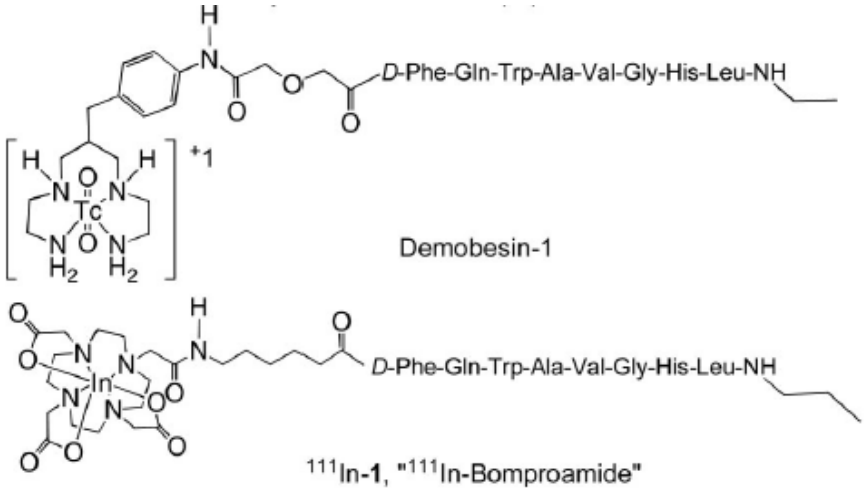

Figure 10: (a) MicroSPECT/CT image of PC-3 xenografts in a mouse after 1h of ^{111}In-Bomproamide administration. (b) Skin CT image.

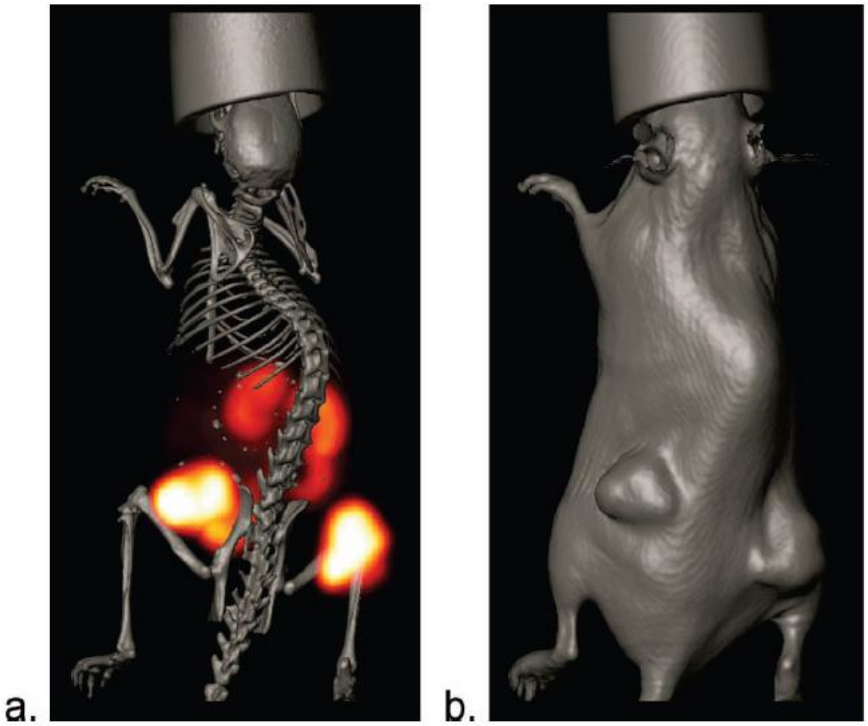

The prospective radiopharmaceutical ^{99m}Tc-RP527, a tripeptide chelator coupled to bombesin(7-14) via a Gly-5-aminovaleric acid linker, was successful in imaging breast cancer and metastases in patients. The administration of ^{99m}Tc-RP527 results in specific tumor localization in humans and exhibit good imaging characteristics with a good tumor/background ratio that may be further enhanced by single photon-emission tomography.[64,65]

In addition, several other radiolabeled GRP analogs are currently under development, among them: the positron emission tomography probe ^{69}Ga-BZH-3 (DOTA-PEG$_2$-[D-Tyr^6,β-Ala^{11},Phe^{13}, Nle^{14}]bombesin(6–14)) for gastrointestinal stromal tumor imaging in humans;[66] the newly designed ligand DOTA-PESIN with high potential with regard to SPECT imaging with $^{68/67}$Ga and targeted radionuclide therapy with ^{177}Lu;[67] and both suitable prostate cancer radiotracers ^{18}F-SFB-[Lys^3]bombesin and ^{18}F-SFB-aminocaproic acid-bombesin(7-14).[68] These findings indicate that radiolabeled bombesin/GRP analogs may be a means for *in vivo*

localization of cancers in humans and potentially of receptor-mediated radiotherapy.

In an *in vivo* study, using both agonist and antagonist radiolabeled DTPA-bombesin analogs with high affinity for the GRP receptor, Breeman and coworkers described that the ^{111}In-labeled agonist showed much higher specific uptake in GRP receptor-positive tissues and in tumor compared to the antagonist. Despite similar affinity for the receptor, the radiolabeled agonist was internalized by GRP receptor-expressing cell lines, but not the antagonist.[69,70] These results are supported by the previous work of Mantey and co-workers, which demonstrated that a radiolabeled agonist, but not the antagonist with identical receptor affinity, was able to internalize in the cell system.[71] Internalization of targeted therapeutic bombesin/GRP analogs by tumor cells may be essential for application in cancer therapy of GRP receptor-expressing lesions, but not for their imaging.

All the aforementioned bombesin/GRP-based radioactive and cytotoxic conjugates consist of peptides and pseudopeptides. Despite their advantages, the difficulty with peptides is often their short metabolic half-life, because of their rapid proteolysis in plasma by endogenous peptidases and proteases, which results in a short time to exert their full potency. To illustrate that, in another study, two bombesin/GRP analogs were prepared with the idea of targeting GRP receptors for radiotherapy. DTPA-γ-aminobutyric acid-[D-Tyr^6-β-Ala^{11}-Thi^{13}-Nle^{14}-NH_2] bombesin(6–14) (BZH1) and DOTA-γ-aminobutyric acid-[D-Tyr^6-β-Ala^{11}-Thi^{13}-Nle^{14}-NH_2] bombesin(6–14) (BZH2) were radiolabeled with diagnostic ^{111}In and BZH2 was also labeled with therapeutic ^{177}Lu and ^{90}Y radiometals. ^{111}In-BZH1 and particularly ^{90}Y-BZH2 analogs were shown to have high affinity to human GRP receptors with binding affinities in the nanomolar range. However, in human serum the metabolic cleavage was found between the β-Ala^{11} and His^{12} residues with an approximate half-life of 2 h.[72] This observation indicates the need for GRP analogs with more favorable pharmacokinetics, that could be achieved with non-peptide analogs.

The unique non-peptide GRP analog found in the literature was described by Ashwood and coworkers, named PD176252 (Figure 11).[73] It is a competitive antagonist at the GRP receptor and displayed a very high affinity for the receptor.

However, it demonstrated low selectivity for this receptor subtype, exhibiting nanomolar affinity for both the neuromedin B-preferring receptor (K_i 0.15 nM) and GRP-preferring receptor (K_i 1 nM). This aspect is probably due to the structural flexibility of the scaffold, which allows conformational freedom for the pharmacophores to adopt diverse orientations. It is worth to emphasize that PD176252 has an indole group pharmacophore, which corresponds to the side chain of Trp. The presence of an indole group for the high affinity binding of PD176252 reinforces the importance of Trp^8 in bombesin/GRP.

Figure 11: structure of the GRP non-peptide analog PD176252[73]

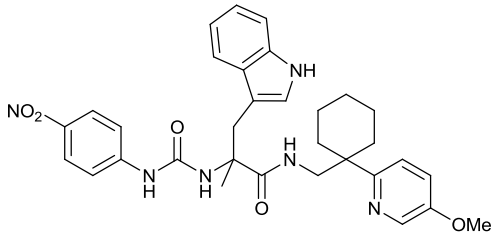

In addition, there is still a lack of bombesin/GRP receptor agonists, which are more appreciated for receptor targeting of cytotoxic drugs, considering that for drug delivery the conjugate must be internalized. This lack of receptor agonists lead us to choose the bombesin/GRP receptor for tumor targeting.

Taking into account all the information presented above, we decided to produce GRP analogs with structural features that could overcome the typical drawbacks described for the current GRP analogs. These features include a non-peptide structure to avoid the degradation by peptidases, and a rigid scaffold to lock the orientation of the pharmacophores in order to enhance the selectivity for the GRP receptor. The GRP receptor ligands generated in this work could be used in the future as targeting vectors for the specific delivery of cytotoxic compounds to tumor cells.

The development of small molecule non-peptide GRP analogs is extremely rare in the literature concerning GRP receptor ligands, mainly because of the lack of structural information on the receptor binding site. However, with the help of

computer-assisted drug design it should be possible to develop additional small non-peptide ligands with high affinity and specificity for the GRP receptor.

1.5. Computer-aided design of peptidomimetics

A fact that makes more challenging the design of non-peptide GRP mimetics is that the three-dimensional structure of the GRP receptor is not available, which is the case for many membrane-bound receptors. This fact brings a critical consequence: the design of GRP receptor ligands must be based on the structure of its natural ligand, GRP.

We proposed the design of non-peptide GRP mimetics inspired by the brilliant work of Hirschmann, Nicolau and co-workers on the design and synthesis of non-peptidal somatostatin peptidomimetics.[74] In 1990, they described the use of the ubiquitous D-glucose as a non-peptide scaffolding in the design of a somatostatin mimetic (Figure 12). This mimetic represented the first use of a sugar scaffold to mimic a β-turn.

Figure 12: Somatostatin and its glucose-based peptidomimetic[75]

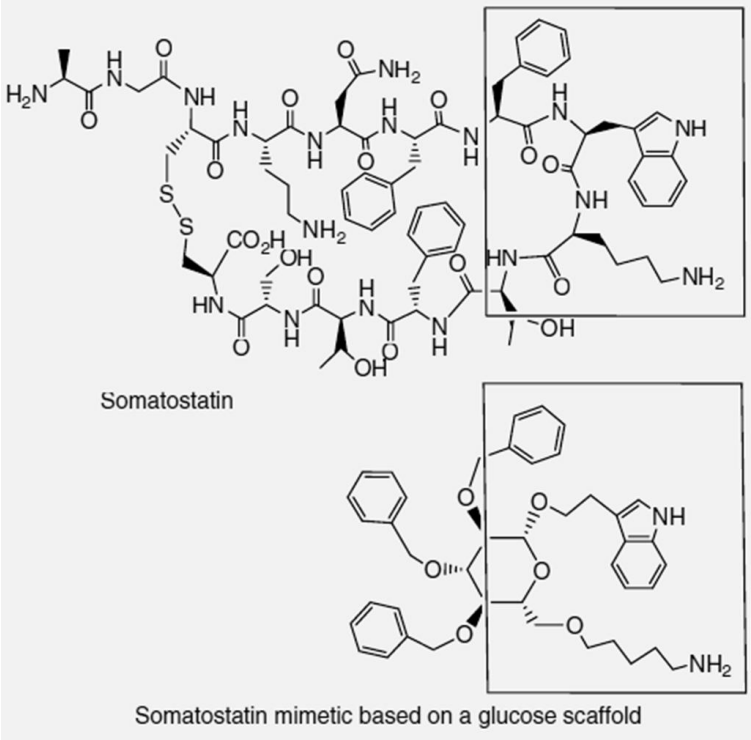

The maintenance of the agonistic activity, by replacement of the peptide backbone by the sugar scaffold, was considered a strong evidence that the peptide backbone is not required for receptor binding or signal transduction.[76] Molecular modeling of the peptidomimetic generated a minimized structure that was superimposed on the solution structure of the highly active hexapeptide L-363,301. A high quality overlapping was observed between the pharmacophores of the pyranosidic peptidomimetic and the peptide, as demonstrated by the interatomic distances within the structures (Figure 13).[75] The authors suggest the possibility that agonists and antagonists of other G-protein coupled receptors can be found by the strategy described.[74]

Figure 13: overlap of the minimized structure of peptidomimetic glycoside with the bioactive conformation of somatostatin analog L-363,301[75]

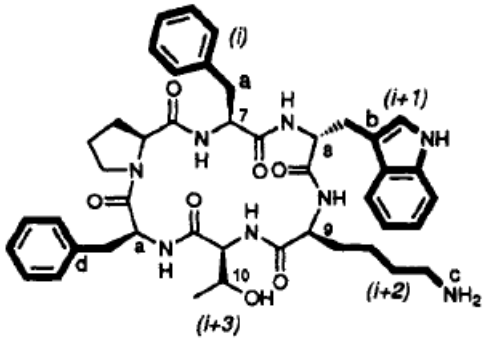

Cyclic hexapeptide L-363,301 (3)

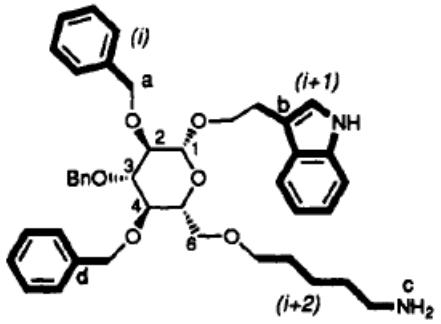

Non-peptide mimetic **4a**, derived from β-D-glucose

Distances between labelled atoms (Å)						
	a-b	a-c	a-d	b-c	b-d	c-d
L-363,301 (3)	7.1	11.3	9.2	7.3	9.2	14.1
Peptidomimetic 4a	5.6	10.6	8.0	6.6	10.3	13.5

The search for compounds that describe the same bioactivity of a reference ligand, but with different molecular frameworks, is known as “scaffold hopping”.[77,78] According to this concept, isofunctional molecules can be produced based on different chemical scaffolds, a common procedure during early drug discovery and development. In our case, scaffold hopping can be applied to move from a natural ligand to a more drug-like agent, maintaining the affinity for the receptor. In many virtual screening studies the identification of potential scaffold hopps has been grounded on molecular similarity, stating that similar structures should exhibit a similar function or property. However, an appropriate level of abstraction from the atomistic molecular representation is required to consider different chemotypes as functionally similar.[79]

Applied to the design of peptidomimetics, this approach requires the availability of a 3D pharmacophore template, which is obtained from the natural peptide and shows the arrangement of the side-chain functional groups.[80] Small peptidomimetic molecules can be designed by connecting these pharmacophores onto a rigid organic scaffold in a way that positions these elements in a similar relative orientation to that in the 3D pharmacophore template from the bioactive peptide.[81] The efficacy of a scaffold can be evaluated by measuring the distances between the pharmacophores connected to the new scaffold, and comparing them with those measured in the template, as exemplified by the work of Hirschmann (Figure 13).[75]

In order to generate a 3D pharmacophore template that displays a reliable representation of the natural peptide, it is important to predict the bioactive conformation of the peptide.[81] The 27 amino acid GRP, as expected, has a high structural flexibility. The binding to its receptor is supposed to be performed in concomitant folding into a specific conformation. Several studies have been performed regarding the conformation of GRP and bombesin. Many of them studied the structure of bombesin and GRP in aqueous solution, however these peptides did not show any ordered secondary structure, describing a random coil conformation.[82-86] This fact is not favourable for the generation of a reliable pharmacophore template for the bioactive conformation of GRP. Theoretical calculations indicated that GRP has a large hydrophobic surface and small

hydrophilic surface. Accordingly, the binding site of the GRP receptor could consist of large hydrophobic surface.[86] Consequently, the conformation of GRP in solution probably should not be related to the active conformation of the peptide.

The experimental determination of GRP's conformation in complex with its receptor would be the key for solving this problem. However, crystallization of integral membrane proteins is extremely difficult and no structure for the GRP receptor has been determined experimentally.[87]

Following the discovery of preferred conformations, orientations and accumulations of flexible regulatory peptides (including bombesin[88]) on the surface of artificial lipid bilayer membranes, a new concept emerged, named membrane-compartments concept. It proposes that the cell membrane exerts conformational constraints on hormone peptides that enable the peptide to find its receptor on the target cell, and to enter and fit the binding site with great ease.[89] Along the last two decades, many experimental studies provided strong support to this concept, and to the assumption that the membrane-induced conformation is critically related to the bioactive conformation.[90] Therefore, the cell membrane would induce conformations and orientations that are required by the receptors.[89] A considerable number of research groups suggested that this is the case of bombesin and GRP.

Already in 1986, Cavatorta and co-workers reported a helical structure for bombesin in membrane mimetic media (lysolecithin micelles and phospholipid vesicles).[91] One year later, Erne and Schwyzer detected by IR spectroscopy that the C-terminus of bombesin was shown to adopt an α-helical conformation in contact with flat phospholipid bilayer membranes.[88] Later on, Cavatorta and co-workers observed that GRP interacts with lipids and assume a lipid specific configuration not observed in buffer.[83] An interesting work by Malikayil and co-workers reported the formation of a helix formed by three connected turns in the potent GRP receptor agonist [Glp^6,Phe^{13},Leu^{14}-NH_2]bombesin(6-14) in phospholipid micelles.[92] Working on the C-terminal decapeptide of GRP, Polverini and colleagues obtained by circular dichroism and computational methods the same strongly stabilized α-helix conformation reported from the beginning, [93] which was also observed by Condamine and co-workers in a full agonist

nonapeptide analog (JMV635), reflecting their similar biological activities.[84] More recently, the α-helical conformation was reported in NMR studies with bombesin and the membrane mimetic trifluoroethanol,[85] and in molecular dynamics simulations of the C-terminal decapeptide of GRP in phospholipid bilayers.[87] A common feature for some of these studies was the orientation of the peptide, perpendicular to the lipid surface with the bioactive C-terminus inserted into the hydrophobic membrane whereas the N-terminus, less hydrophobic, is oriented outwards.

Two of these works demonstrated to be very useful for the generation of a 3D pharmacophore template of GRP:

1) In the most recent work, Prakash and co-workers[87] used molecular dynamics simulations to investigate the behaviour of the C-terminal decapeptide of GRP (GRP10), responsible for full biological activity, in explicit membrane environment (dimyristoyl phosphatidylcholine). The simulated structures demonstrated an α-helical conformation, described by the six C-terminal residues (Figure 14). The values of the backbone dihedral angles φ and ψ were described, which are very important parameters for the reproduction of the respective peptide model.

Figure 14: (**A**) GRP10 and phospholipid complex after minimization, peptide is shown in ribbon representation. (**B**) GRP10 saved at the end of 8 ns simulation.[87]

A) **B)**

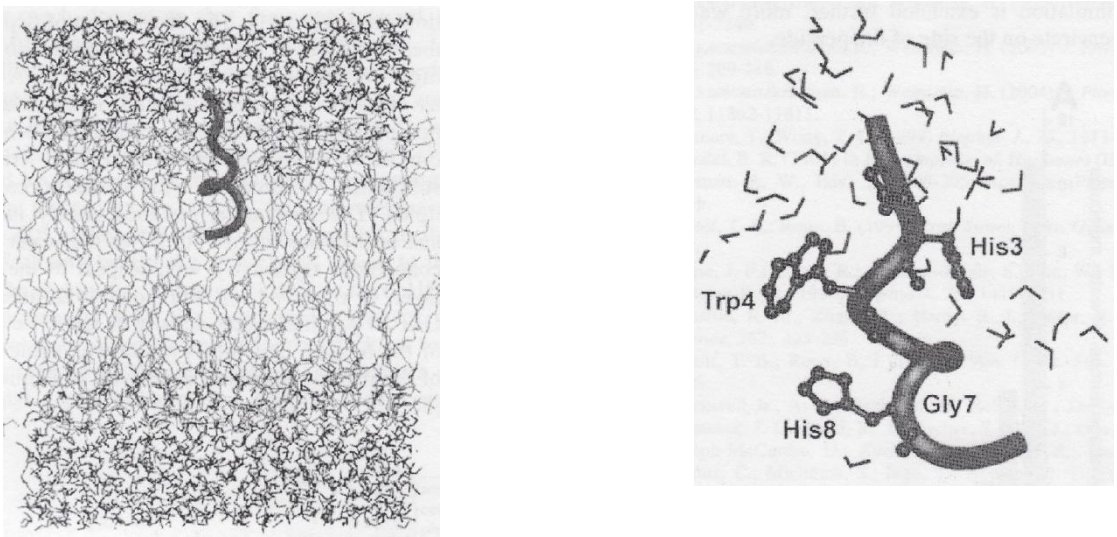

2) The study of Malikayil and co-workers reported the conformation of a potent GRP receptor agonist in membrane mimetic dodecylphosphocholine micelles.[92] All protons of the peptide [Glp^6,Phe^{13},Leu^{14}-NH_2]bombesin(6-14), in the membrane mimetic medium, were assigned by two-dimensional NMR spectroscopy. Interproton distances were derived from nuclear Overhauser enhancement spectra. The conformation of the peptide was achieved by distance-restrained molecular dynamics simulations using the interproton distances as constraints. The peptide assumed a relatively rigid backbone conformation describing a helix formed by the linear arrangement of three connected β-turns (Figure 15). This helical conformation is consistent with the proposed structure of GRP10. There was an excellent agreement between the calculated structures and the experimental data. The authors also report the dihedral angles of the modelled conformation, which are essential for the molecular modelling of the 3D pharmacophore template of this peptide.

Figure 15: positional-average backbone conformation of the GRP receptor agonist[92]

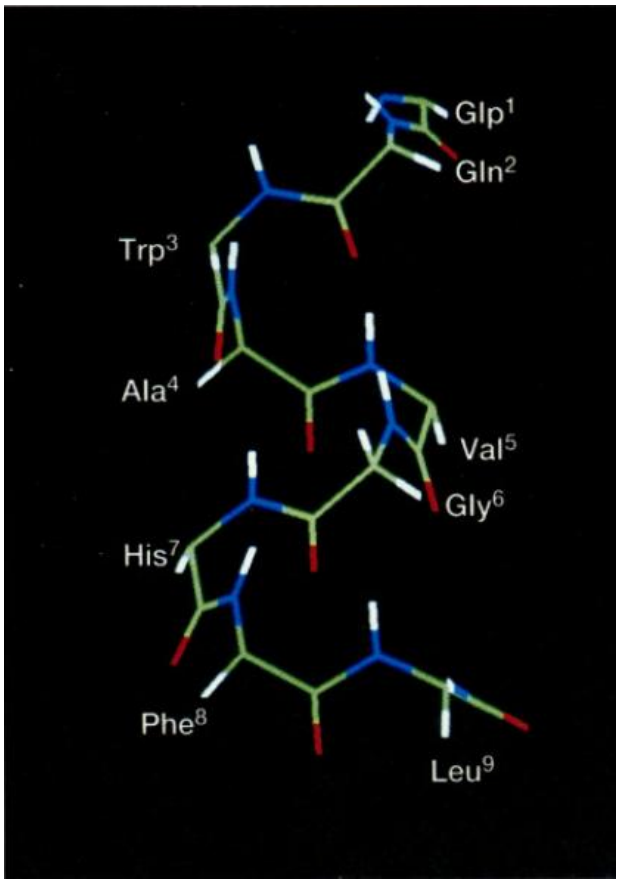

Taking into account all the information presented above, and in order to obtain non-peptide GRP analogs as potential carrier molecules for tumor drug targeting, one of the goals of this thesis is represented by the design of structures that mimic the supposed bioactive conformation of GRP, achieved using a computer-assisted ligand-based drug design. For this purpose, as described in the following section, we performed two critical procedures: the preparation of a 3D pharmacophore template based on the models of Prakash[87] and Malikayil;[92] and the search for a rigid scaffold that connected the pharmacophores in the right orientation, maintaining the molecular similarity with GRP and hopefully, also the functional similarity.

1.6. Akt kinase inhibitors as potential anticancer drugs

Looking back to the tumor targeting conjugate, we turned our attention to the study of drugs that can be targeted to cancer cells. For tumor therapeutic purposes, the drug must inhibit the proliferation of the cancer cells, which is usually achieved by the use of cytotoxic or antiproliferative drugs.

Phosphorilation is a key event in many proliferative cellular processes and the over activation of kinases and phosphatases that control such processes is found in many pathological events such as tumor growth and progression. For this reason there has been an increasing interest in the study of kinase selective inhibitors.[94]

Akt (or Protein Kinase B, PKB) is a proto-oncogenic serine/treonine kinase involved in the PI3K/Akt transduction pathway (Figure 16). Its activation has been detected in many types of human cancers[95-100] and promotes the subsequent activation of proliferative pathways and inhibition of apoptotic pathways, resulting in cellular growth and survival *in vitro*, and tumor formation *in vivo*. Thus, because of the functions associated to Akt, selective inhibitors of such enzymes would represent interesting lead compounds for the development of new anticancer drugs.

Figure 16: the activation of Akt promotes the activation of cell survival pathways and inhibition of apoptotic pathways.

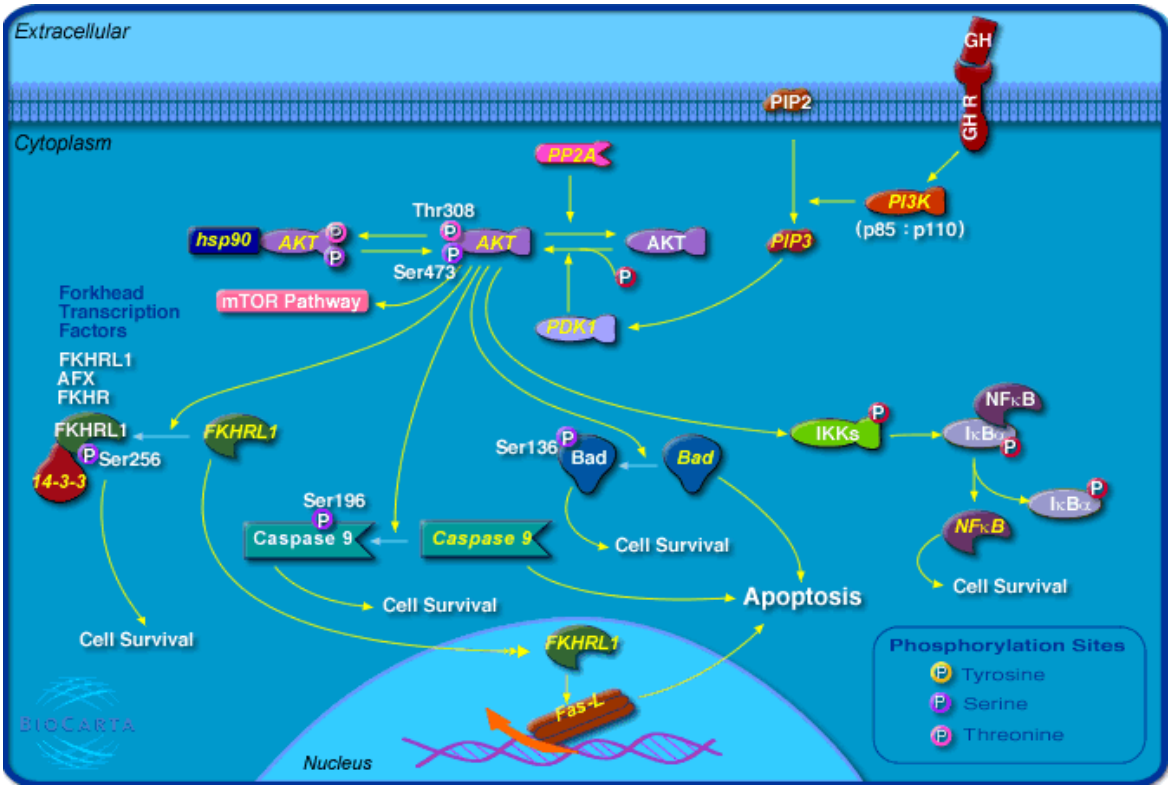

Akt activation[101-108] is caused by the binding of phosphatidylinositol phosphorilated in position 3 and 4 of the inositol ring [PI(3,4)P_2 or PIP_2] (Figure 17) with a specific protein domain, the so called pleckstrin homology domain (PH). Recently[100,109,110] few phosphatidylinositol ether lipid analogues with good inhibitory activity (IC_{50} 3-30μm) and in some cases with good selectivity towards Akt have been synthesized. Among them, a carbonate derivative PIA12[100,111] (Figure 17) showed very good inhibitor properties (5.0 ± 1.9 μM) of Akt, even if less potent than the corresponding phosphate, but much more selective so that this compound is used as the selective inhibitor of choice. According to modelling studies,[111] the axial hydroxymethyl group in position 3 of the inositol ring has a strong hydrogen bonding interaction with the Arg^{25} residue of Akt PH domain that seems to be important for the selectivity, and the corresponding compounds with equatorial hydroxymethyl group showed a 6-fold reduction in Akt inhibition activity.

Figure 17: structures of the natural ligand of Akt [PI(3,4)P_2] and the carbonate-based reference inhibitor of Akt PIA12

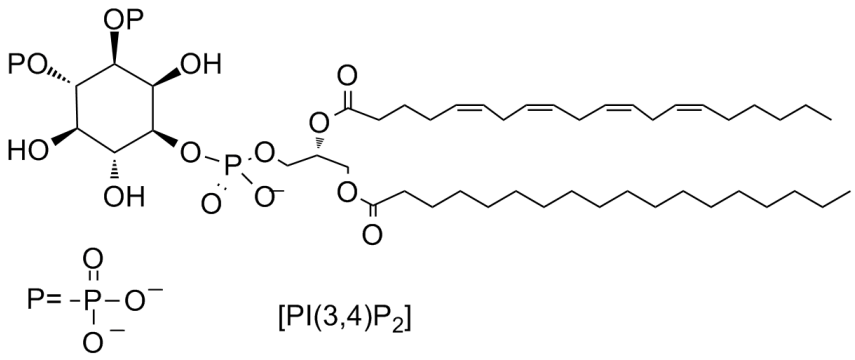

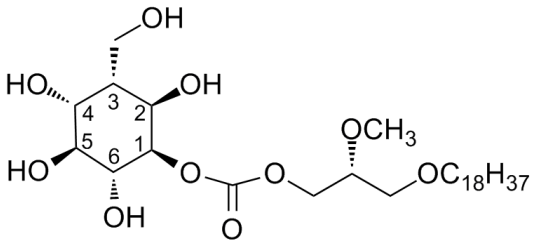

Reference inhibitor PIA12

Previous X-ray crystallographic investigations showed that the inositol-(1,3,4,5)tetrakisphosphate (IP4) in the phosphoinositide-binding site of the PH domain of Akt, which has been shown also to correctly represent the orientation of PIP_2 and PIP_3 in the binding pocket,[100] is positioned with the 2-hydroxyl group oriented inside the binding cleft. Moreover, a network of hydrogen bonds in the binding pocket involves the three phosphate groups linked to the equatorial 1-, 3- and 4-hydroxyl groups of the inositol ring, as well as the axial hydroxyl group in position 2.[112] These molecular features of the phosphoinositide-binding site of the PH domain of Akt have been already exploited, in previous studies, to design and test Akt inhibitiors.[100,111,112] Our analysis of the X-ray structure of the PH domain of Akt reveals also that, close to the polar pocket discussed above, a hydrophobic cleft including residues Ile^{74}, Val^{83}, Ile^{84} is present, suggesting that this hydrophobic cleft might be potentially exploited to design novel Akt inhibitors.

In light of the previous considerations and with the aim of generating a new class of inhibitors targeting the phosphoinositide-binding site of the Akt PH domain, we have initially built and tested, using docking calculations, a small

library of iminosugar-based phosphatidylinositol analogues. The library was designed including some features of the inhibitor PIA12 and also some modifications, considered potential for bioactivity. From the results of the docking experiments, the most appropriate compounds were selected and synthesized from a common close precursor. These target compounds were tested for the inhibition of Akt *in vitro*, in order to preliminary evaluate their biological activity.

Objectives

"Bodies which possessed a particular affinity for a certain organ... as a carrier by which to bring therapeutically active groups to the organ in question"

Paul Ehrlich (1898)

The main goal of this work is to study the essential features to target cytotoxicity to cancer cells. Molecules developed for this purpose must satisfy two important requirements: selectivity for cancer cells and cytotoxic or antiproliferative activity. The best results have been achieved by the conjugation of molecules that fulfil the first requirement with molecules that satisfy the second one, generating tumor drug targeting conjugates. In other words, tumor targeting conjugates are composed by a targeting moiety with high affinity for tumor-associated proteins, linked to a drug that is carried to the tumor site to exert its antineoplastic activity. The idea is represented in the following illustration, where the targeting moiety is the yellow part that binds to the cancer cell receptor to deliver the therapeutic drug, represented by the red entity:

In light of this concept, and in order to provide useful information for the assembly of tumor targeting conjugates, we proposed the study of both the targeting moiety and the antineoplastic drug. Our efforts on the study of the targeting moiety were directed to the production of GRP receptor ligands, based on the potential of this receptor for targeting. On the other hand, the study of antineoplastic drugs was dedicated to the discovery of inhibitors of the proto-oncogenic Akt kinase.

2.1. Design and synthesis of ligands for the GRP receptor

This part of the work is dedicated to the computer-aided *de novo* design of potential ligands for the GRP receptor. The idea is to use the structure of GRP, the natural ligand of the receptor, to design new small molecules that could be able to bind to the receptor with high affinity. In order to overcome the metabolic instability of peptide analogs of bombesin/GRP, we decided to use a synthetic scaffold instead of the peptide backbone, that could afford the same chemical features of the peptide necessary for biological activity. The matter of selectivity is also approached by the choice of rigid scaffolds that could mimic the putative receptor-binding conformation of GRP. Structural and functional similarity were focused

2.2. Design and synthesis of iminosugar-based Akt inhibitors

The antineoplastic potential of Akt inhibitors is exploited in this part of the work. In particular, the use of analogues of phosphatidylinositol phosphates, which bind with high affinity to the PH domain of Akt. The structural similarity observed between phosphatidylinositols, inositides and iminosugar derivatives prompted us to design and produce a small library of iminosugar-based inositol analogues, in the search for a potential new class of Akt inhibitors.

Results and Discussion

3.1. 3D pharmacophore template

The first step for the design of non-peptide GRP peptidomimetics was the generation of a 3D pharmacophore template, which was based on the structures presented above for the C-terminal decapeptide of GRP[87] (GRP10) and the potent agonist [Glp[6],Phe[13],Leu[14]-NH_2]bombesin(6-14).[92] As a group of organic chemists with a short experience of computational chemistry, we decided to use Chem3D, a simple program with an easy-to-handle interface. This program makes use of the MM2 force field,[113] the same that was used by Hirschmann and colleagues in the design of somatostatin peptidomimetics.[75]

In order to reliably reproduce the conformation obtained for both peptides, the use of the dihedral angles published by the respective authors was critical (Table 2). Each structure was inserted in the interface of the program, and then the dihedral angles φ and ψ were informed as constraints before the energy minimization (for details: Experimental Procedures). The minimized structures for both the C-terminal decapeptide of GRP[87] and the potent agonist [Glp[6],Phe[13],Leu[14]-NH_2]bombesin(6-14)[92] are presented in Figure 18.

From the minimized structures it is possible to observe that both peptides describe a helical conformation, in accordance to the reference papers. The studies along the last decades on peptide analogues of GRP provided wide information on the importance of some amino acids, and therefore their side-chains, on the bioactivity for the GRP receptor. The numbering presented here corresponds to the amino acid numbers of bombesin. As already discussed in the introductory part of this thesis, Trp[8] and His[12] are the most important amino acids for both bombesin and GRP. The presence of His[7] or a similar hydrophobic group in the same position or in the neighborhood is also considered of great importance, as much as the presence of hydrophobic amino acids in position 13, as the natural Leu[13].

Table 2: Dihedral angles φ and ψ obtained from the studies of Prakash[87] and Malikayl.[92]

Residue	Φ	Ψ
C-terminal GRP10[87]		
Asn[18]		n. a.
Gln[19]	-95	-80
His[20]	-98	118
Trp[21]	-99	-35
Ala[22]	-56	-60
Val[23]	-70	-33
Gly[24]	-68	-18
His[25]	-72	-28
Leu[26]	-95	-62
Met[27]	-101	-100
Agonist[92]		
Glp[6]		-50
Gln[7]	-97	-60
Trp[8]	-62	-52
Ala[9]	-62	-34
Val[10]	-70	-51
Gly[11]	-67	-41
His[12]	-73	-44
Phe[13]	-93	-42
Leu[14]	-101	n. a.

n. a. = not available in the reference paper

The side-chains that represent these requirements are shown in yellow in figure 18. These are: the indole group of Trp^{8} (Trp^{21} for GRP) and the imidazole group for His^{12} (His^{25} for GRP) for both peptides; the imidazole group of His^{20} for GRP, corresponding to the Glp^{6} for the agonist; and the isobutyl group of Leu^{26} for GRP; which is related to Phe^{13} in the agonist. All these side-chains fit the requirements observed from the past studies on the bioactivity of GRP, bombesin and their analogs. Considering that these groups are the structural features that are necessary to ensure the optimal interactions with the GRP receptor and are responsible for the bioactivity, they can be defined as the pharmacophores of both peptides. The evaluation of the structures presented in figure 18 allowed us to detect a convenient similarity between the pharmacophores of both peptides, regarding the orientation of these groups. Equivalent pharmacophores, for example the indole groups, displayed very similar orientation when the peptide backbones were positioned in the same manner. The fact that both peptides have a similar amino acid sequence and exert the same biological activity suggests that their side chains should be presented to the GRP receptor in a similar fashion. The structural similarity between both peptides observed in figure 18 seems to be an appropriate illustration of this claim.

Once the reproduction of the modelled structures of GRP10 and the GRP receptor agonist was ready, the following step was the generation of the 3D pharmacophore template. In order to superimpose the peptides, four pharmacophore pairs were identified by selecting equivalent pharmacophores in each peptide: indole in both peptides, C-terminal imidazole also for both, N-terminal imidazole in GRP10 coupled to pyrrolidone in the agonist, and isobutyl in GRP10 coupled to phenyl in the agonist. These pharmacophore pairs were superimposed and from the resulting overlay the peptide backbones and less important side chains were deleted. This procedure afforded the 3D pharmacophore template of both peptides shown in figure 19, which is the set of chemical features required for the design of GRP mimetics.

Figure 18: Minimized structures of the C-terminal decapeptide of GRP and the agonist [Glp^{6},Phe^{13},Leu^{14}-NH_2]bombesin(6-14) obtained from the reference papers.[87,92]

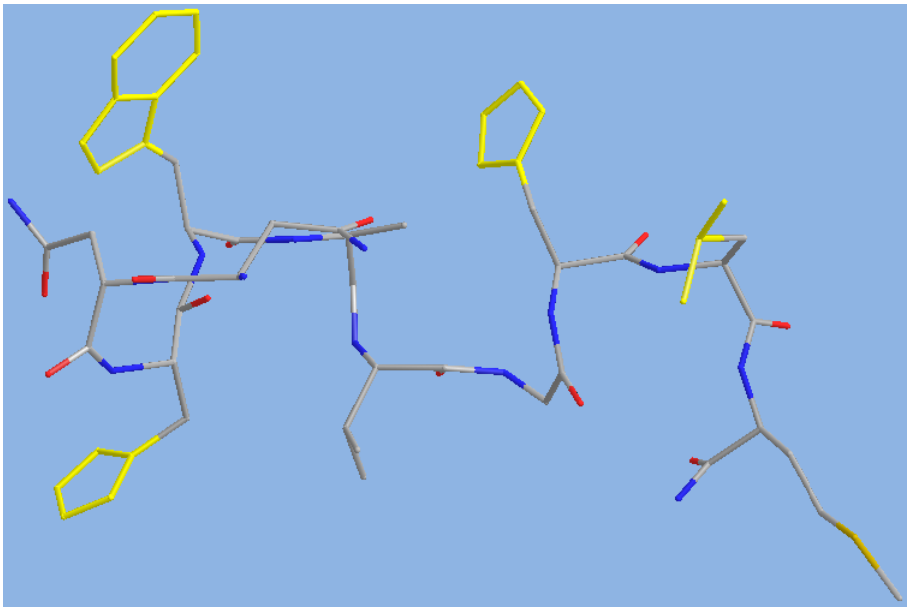

C-terminal decapeptide of GRP

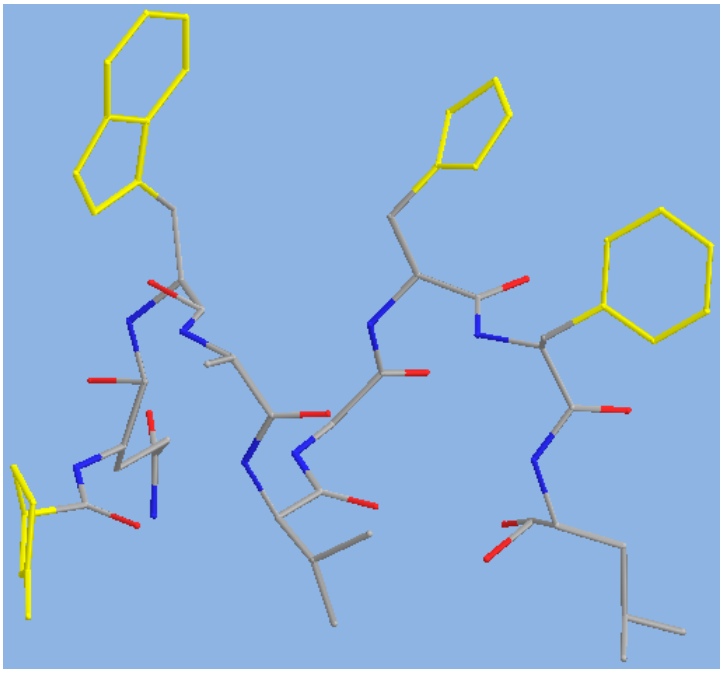

GRP receptor agonist

Figure 19: 3D pharmacophore template obtained from the selection of the critical pharmacophores present in GRP10 and the GRP receptor agonist

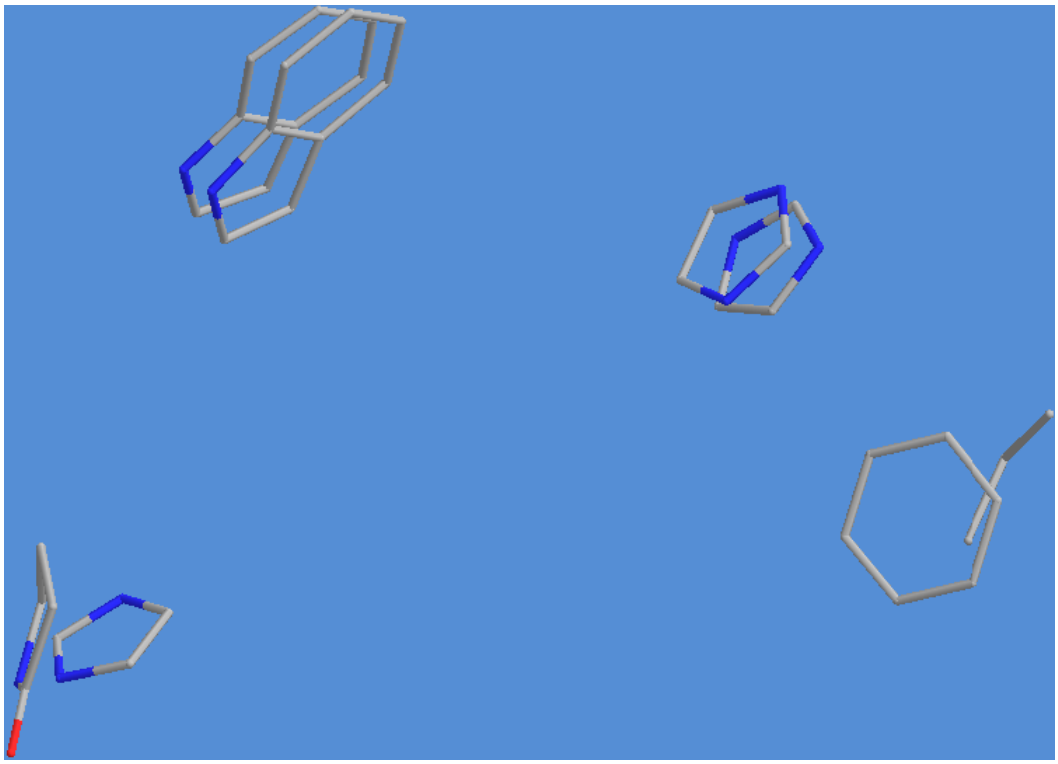

3.2. Scaffold hopping

The design of GRP mimetics started from the evaluation of prospective structures for scaffold hopping. According to the principle of scaffold hopping the empty space between the pharmacophores can be occupied by a convenient scaffold that connects all the groups.[78] The shape of the scaffold attached to the pharmacophores is a critical property, as it must conserve the chemical features of the 3D pharmacophore template. In the search for appropriate scaffolds we decided to explore the broad structural diversity of carbohydrates. One benefit of carbohydrate-based scaffolds lies in the ability to produce rigid, unique products with well-defined, 3D orientation of selected substituents. These are essential requirements for the generation of peptidomimetics. Sugars and their derivatives are able to mimic most of the peptide secondary structures, from turns to helices. This is possible due to the number of stereocontrolled functionalized positions in

their structure, which generates a good control of the relative orientation of substituents attached to sugars.[114]

Considering the distance between the pharmacophores in the template, we observed that monosaccharides were too small to directly connect all of them. To do so, monosaccharides would require the use of long linkers, that would compromise the rigid orientation expected for peptidomimetics. Therefore, sugar derivatives seemed to be a better choice, and we pointed towards bicyclic structures, more rigid than monosaccharides. We selected a number of sugar-derived bi- and tricyclic structures (Figure 21), and tested their ability to fit into the 3D pharmacophore template.

The pharmacophores were attached to the scaffolds in the following manner: the C-terminal imidazole bound to the O-3 of the sugar, indole bound to the O-4, imidazole (from GRP10) or pyrrolidone (from the agonist) bound to O-6, and the phenyl group bound to the second cycle through an appropriate linker according to the scaffold (Figure 20). Between imidazole in GRP and the pyrrolidone ring in the agonist we chose the second for a simple reason, it is synthetically more tractable.

Figure 20: Representation of the fashion for attachment of the pharmacophores to the scaffolds, a generic scaffold with variable second cycle is presented

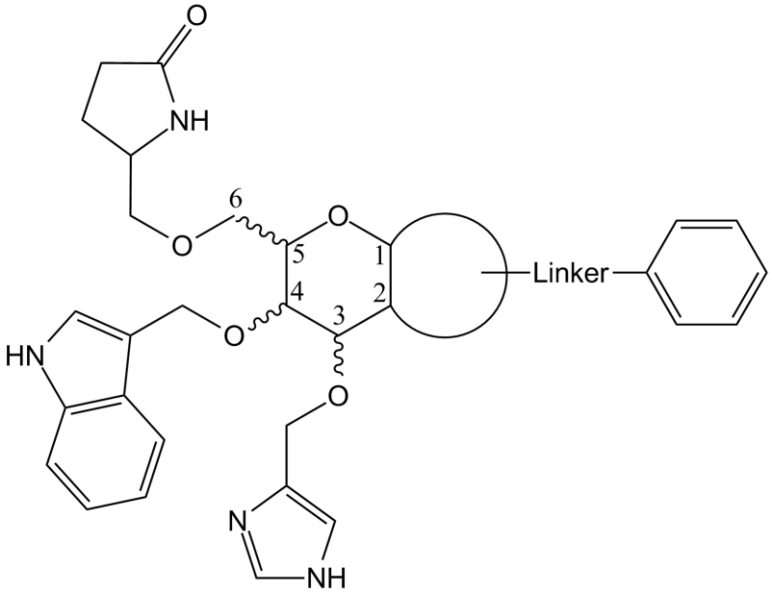

Figure 21: Sugar-based scaffolds selected and tested for their ability to fit the 3D template

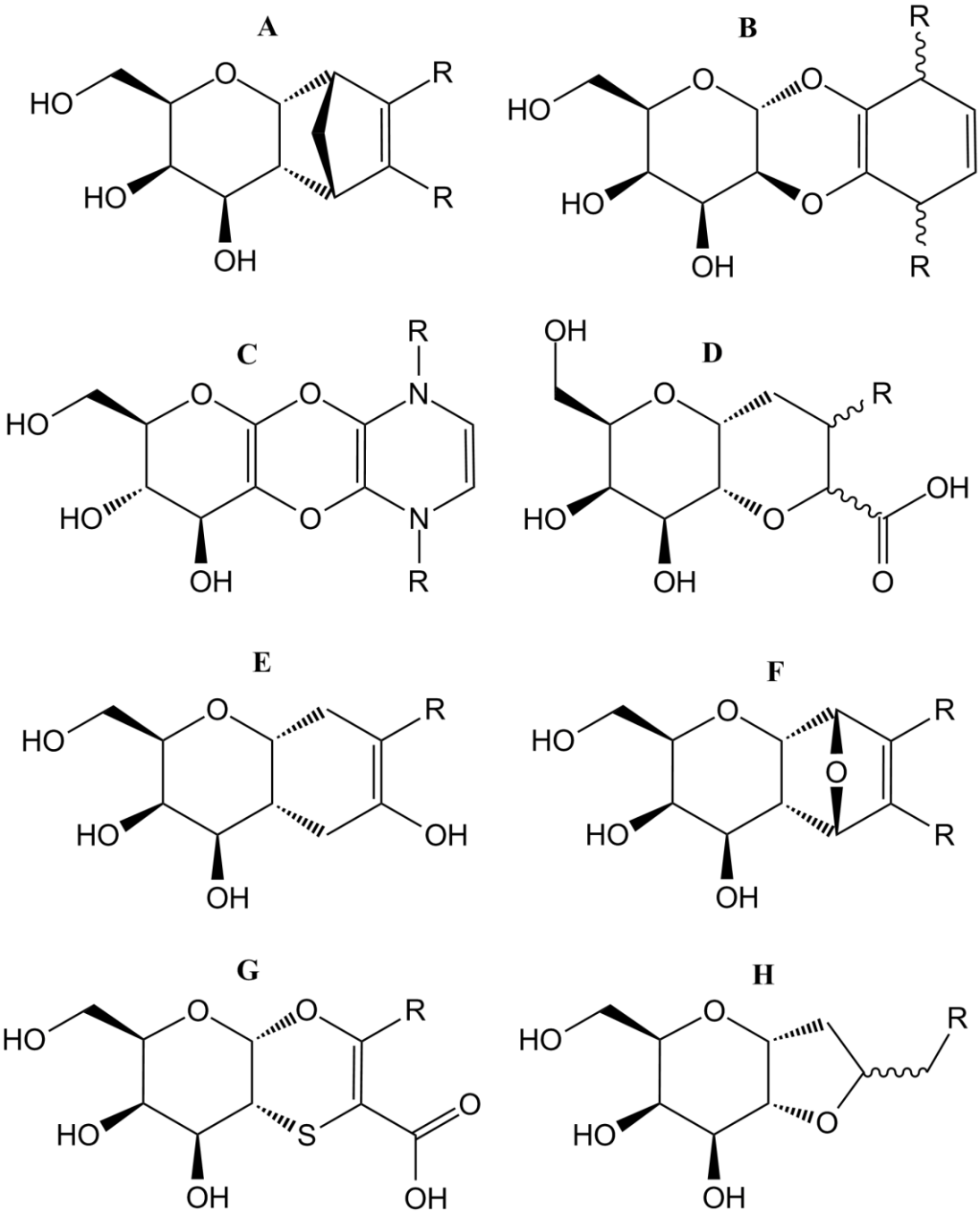

As soon as we started to try the scaffolds into the 3D pharmacophore template, we observed that the structures derived from D-glucose, such as scaffold C, could not fit the requirements for orientation of groups in the space. This is explained by the stereocenter in position 4, which keeps the indole group in an

equatorial position in relation to the ring, compromising the overlay with the template. Therefore, glucosidic scaffolds were rejected. On the other hand, the galactosidic scaffolds displayed good overlay with the template, as the same stereocenter is inverted, and keeps the indole group in an axial position, which superimposes it better in relation to the 3D template illustrated in figure 19.

A good scaffold has not only to conserve the chemical features of the 3D pharmacophore template, but it must be synthetically accessible in high yield. Several of the scaffolds put in doubt the feasibility of their chemistry, then scaffolds A to F were rejected. Under this point of view scaffolds G and H seemed to be very attractive. In addition, as C-glycosides, they are stabilized against chemical and enzymatic hydrolysis. The synthesis of scaffold H was already performed in our research group, while the synthesis of scaffold G (Figure 22)[115] seemed to be sensibly more complicate.

Figure 22: synthesis of scaffold G via Diels-Alder reaction[115]

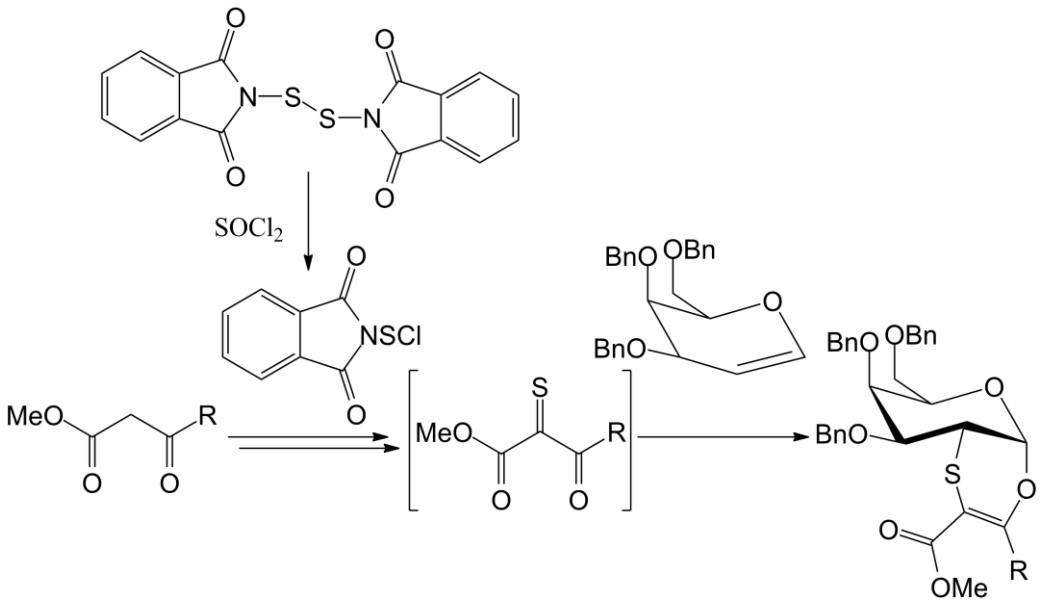

Presenting a high quality overlay with the 3D template (Figure 23), scaffold H was considered the best structure for scaffold hopping. Its potential as a synthetic accessible structure prompted us to design the synthesis of GRP peptidomimetics based on this scaffold.

Figure 23: Prospective GRP mimetic containing scaffold H (**1a**) and its superimposition over the 3D pharmacophore template

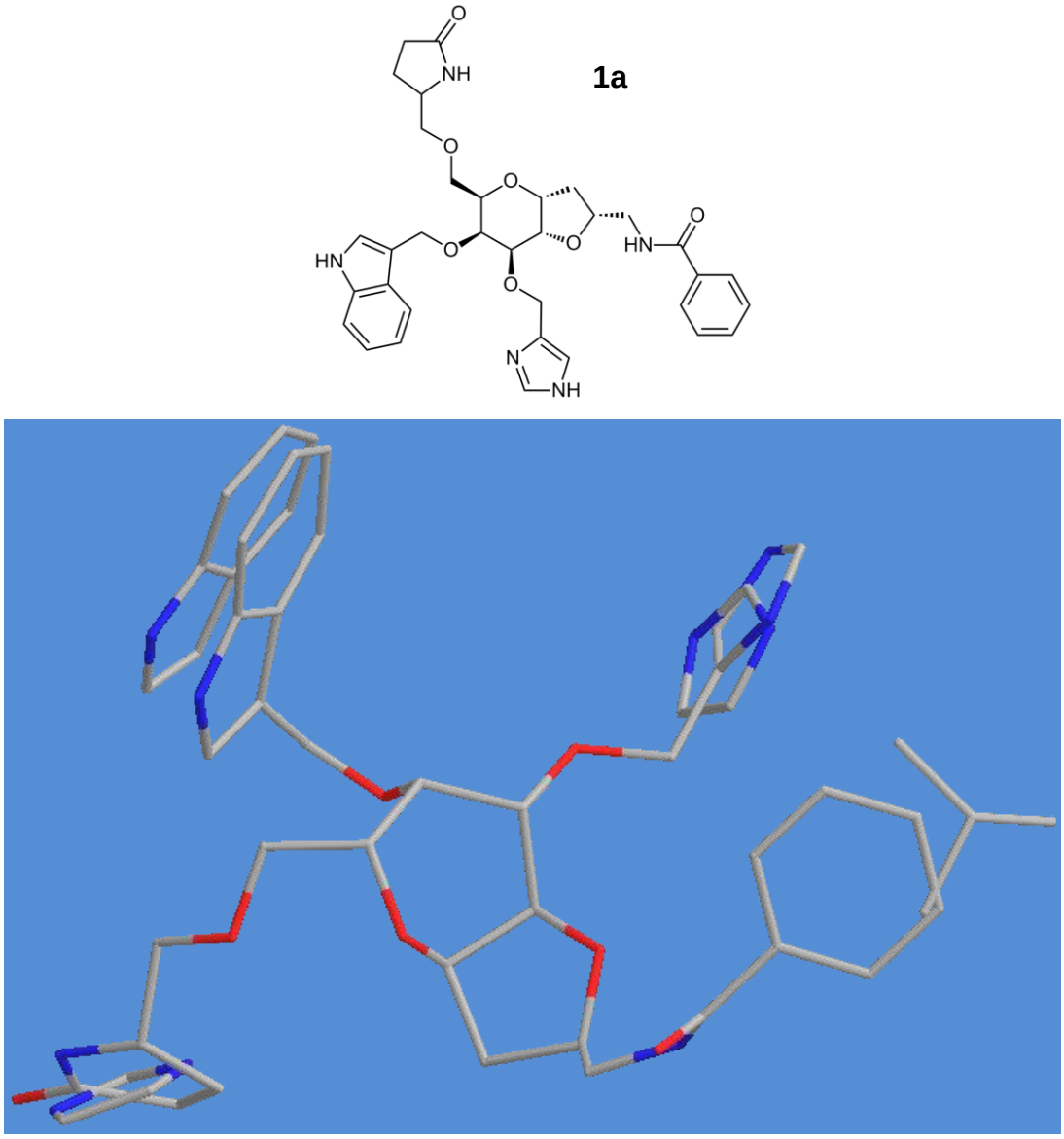

In order to measure the quality of the overlay between the structure containing scaffold H and the 3D pharmacophore template, we used the distances between pharmacophores as descriptors. The arrangement of the four key groups in the 3D template described a distorted tetrahedron. Each distance was measured from the center of one pharmacophore to the center of the adjacent pharmacophore, affording each side of the tetrahedron. This procedure was performed for both GRP10 (Figure 24) and the potential GRP mimetic (Figure 25).

Figure 24: Distances between adjacent pharmacophores* in GRP10 (in Å)

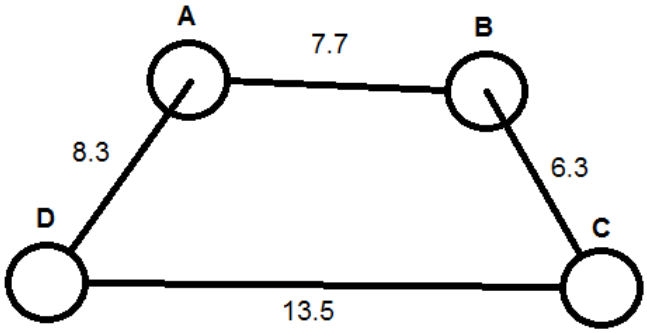

* A = indole (Trp^{21}), B = imidazole (His^{25}), C = isobutyl (Leu^{26}), D = imidazole (His^{20})

Figure 25: Distances between adjacent pharmacophores* in our GRP mimetic (in Å)

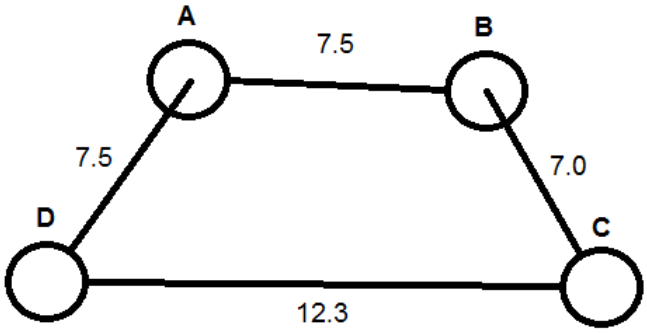

* A = indole, B = imidazole, C = phenyl, D = pyrrolidone

Comparing the distances observed for GRP10 to the related distances in our prospective GRP mimetic, a clear similarity is observed. For example in GRP10, the distance between the indole group of Trp^{21} and the imidazole group of His^{25} (7.7 Å), with three residues in between, was just 0.2 longer than the same distance in our analog compound (7.5 Å). Therefore, according to these descriptors, the structure containing the bicyclic scaffold H complies with the requirements of the 3D pharmacophore template. These results indicated that the scaffold hopping of GRP was satisfactory and complete. The next step started by designing the synthesis of the GRP mimetic.

3.3. Synthesis of GRP mimetics

Once we designed the structure of the prospective GRP mimetic (Figure 23), our study focused the synthetic methods for its preparation. This study can be divided in two parts: the synthesis of the scaffold and the attachment of the pharmacophores at the appropriate sites around the scaffold.

3.3.1. Synthesis of the scaffold

The scaffold is the starting material for the attachment of the bioactive substituents, therefore as already mentioned, its synthesis must be easy, fast and high-yielding. All these rules are fulfilled by the synthesis of scaffold H, published by our group in 2006.[116] Little modifications on the reagents were performed from the published method, but the reactions remained the same (Figure 26).

Figure 26: Synthetic method for the preparation of scaffold H (**5**)[116]

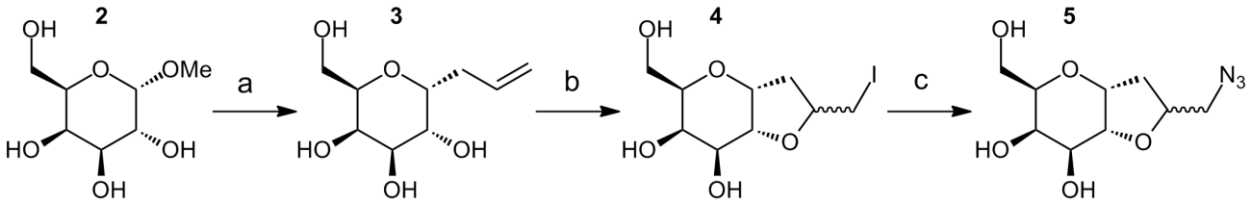

Reagents and conditions: a) i. BTSFA, CH_3CN, reflux, 1h; ii. $AllSiMe_3$, TMSOTf, 0°C – r.t., 18h, 85%; b) NIS, DMF, 1.5h, 91%; c) NaN_3, DMF, 100°C, 18h, 85%.

The synthetic method presented above allowed us to prepare the scaffold in a multi-gram scale with high purity, without the need for protective groups. It comprises three high-yielding steps: Sakurai reaction after silylation with BTSFA to afford *C*-allyl galactoside **2**, followed by iodocyclization and azide displacement of the resulting iodide to afford compound **5** (Figure 26). The procedure afforded an inseparable 7:3 mixture of isomers, being the major isomer the one used in the design of target compound **1a**. The overall yield (over three steps) was 54%.

3.3.2. Design and synthesis of the building blocks

In order to proceed with the attachment of the pharmacophores, it was important to define the building blocks responsible for the attachment and the order of attachment of these different groups. Indole and imidazole represent the most important side chains of GRP, which belong to Trp^{21} and His^{25} respectively. Therefore, we decided to incorporate them to the scaffold exactly as they are found in the peptide, namely linked to the backbone by a methylene group (CH_2). For these reason, the building blocks designed for the attachment of the indole group and the imidazole group are the following alkyl halides, respectively: 3-(bromomethyl)-1-(*tert*-butoxycarbonyl)indole (**6**) and 4-(chloromethyl)-1-trityl-imidazole (**7**) (Figure 28). These alkyl halides seemed to be good reactants for *O*-alkylation of the appropriate hydroxyls in the scaffold. The resultant ethers are chemically and metabolic stable functional groups.

The pyrrolidone group, which is a pharmacophore of the GRP agonist and found in the peptide as a pyroglutamic acid, is bound to the *N*-terminus through an amide linkage. In order to reproduce the situation found in the peptide we believed that the ester formed between pyroglutamic acid (**8**) and OH-6 in the scaffold could be a good surrogate of the amide linkage. Despite the original linker in the designed molecule (**1a**) was an ether, the use of the ester linker did not change the overlay between the prospective GRP mimetic and the 3D template. The measures between the pharmacophores remained in the same value. From this point, the target compound with all four pharmacophores became compound **1b** (Figure 27).

Figure 27: Structure of target compound **1b**, containing ester linked pyroglutamic acid

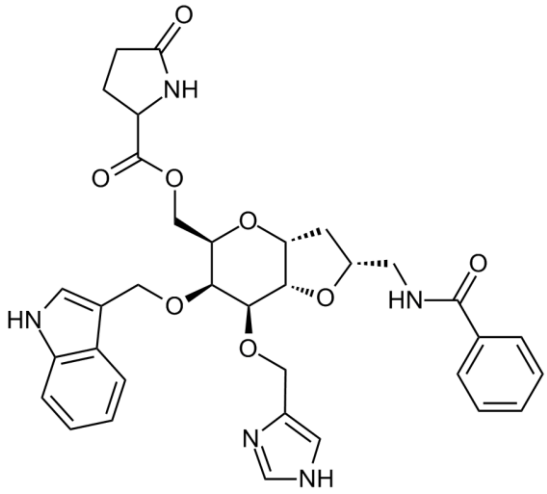

During the synthesis of the target compound (**1b**), the azide of compound **5** must be reduced to allow the derivatization of the resulting amine. The last building block to be defined was responsible for the attachment of a phenyl group to this primary amine. The use of benzyl halides could result in overalkylation of the amine, therefore, we preferred benzoyl chloride (**9**) as a convenient building block to attach this pharmacophore. The resulting benzamide is a very stable functional group, both metabolic and chemically.

Figure 28: Building blocks designed for the orthogonal attachment of the pharmacophores to the scaffold (**5**)

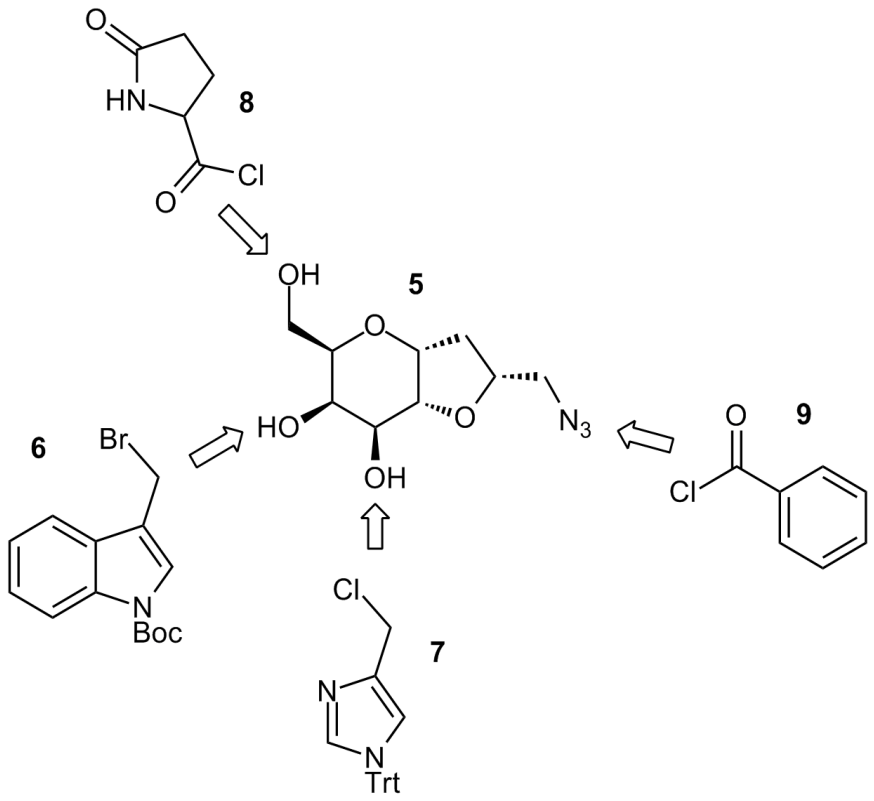

Then, we proceeded we the synthesis of the building blocks, which is presented in the Figure 29.

The synthesis of building block **6** was performed following the procedure of Schollkopf and coworkers,[117] starting by the Boc-protection of the nitrogen of indole-3-carbaldehyde, reduction of the carbonyl to a primary alcohol and a Mitsunobu reaction to substitute the hydroxyl by a bromide. The overall yield was 65% (3 steps).

Building block **7** was synthesized by protecting chemoselectively the secondary amine of 4-(methylhydroxy)-imidazole with a trityl group. The primary alcohol was then displaced by chloride. The yield over two steps was 96%.

Figure 29: Synthesis of the building blocks **6**, **7** and **8**

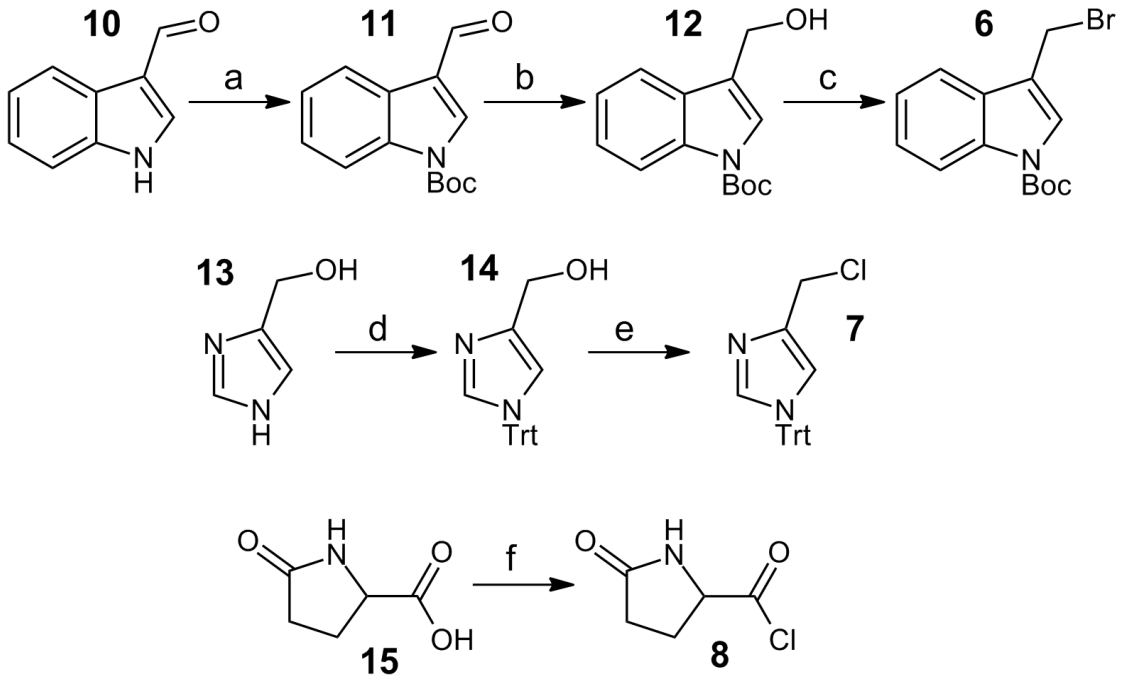

Reagents and conditions: a) $(Boc)_2O$, KOH 1M, THF/H_2O 7:3, 15h, 90%; b) $NaBH_4$, ethanol, 6h, 90%; c) PPh_3, Br_2, CCl_4, 3 days, 80%; d) TrtCl, TEA, DMF, 15h, quantitative; e) $SOCl_2$, DMF, 30 min, 96%; f) $(COCl)_2$, CH_2Cl_2, reflux, 2h.

Building block **8** can be produced by the reaction of pyroglutamic acid with oxalyl chloride[118] to afford the acyl chloride **8**. Compound **15** can also be used as a building block for direct esterification of the OH-6 in the scaffold, with DMAP and DCC.[119] Benzoyl chloride, corresponding to building block **9**, is commercially available, therefore it was purchased.

3.3.3. Attachment of the pharmacophores to the scaffold

In order to explore the bioactivity of the different pharmacophores around the scaffold, not only the final compound would be tested for its biological activity on cells overexpressing the GRP receptor, but also compounds with less pharmacophores. In this way, during the synthesis, compounds with two (**16**) and

three (**17**) bioactive groups were derivatized and used as final compounds for this purpose (Figure 30).

Figure 30: Structures of the target compounds containing two (**16**) and three (**17**) pharmacophores, designated to the biological tests

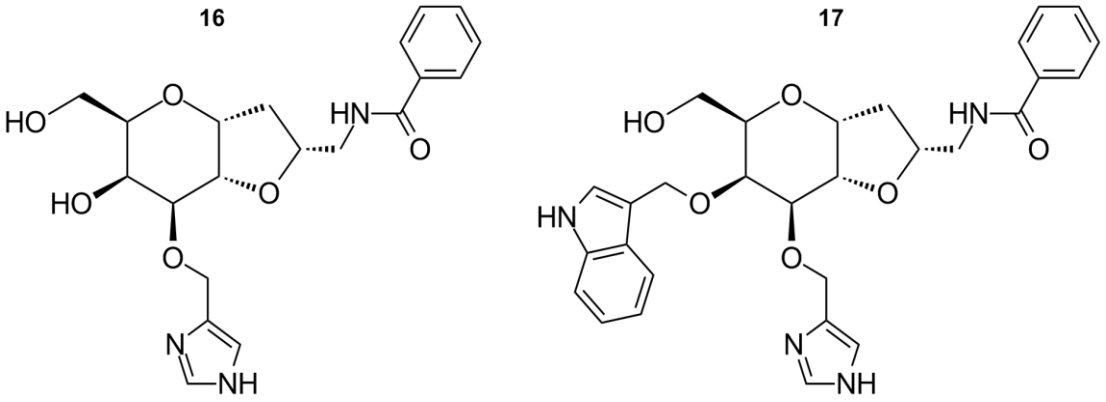

The order of attachment of the building blocks to the scaffold is a critical procedure for optimal synthesis of the target compound. The choice of orthogonal protecting groups depends on this order. First, they must be compatible with the reactions responsible for the attachment, and second, their removal must preserve the protecting groups of the bioactive heterocycles. Therefore, they cannot be acid-labile as trityl and Boc groups that protect the pharmacophores.

Observing the three OH groups in the galactosidic scaffold, and using our knowledge on galactose protecting groups, we decided to protect both OH-4 and OH-6 with a benzylidene group (Figure 31). This procedure makes OH-3 ready for derivatization with **7**, as the fourth functional group, the azide, is stable under the conditions for the attachment of the building blocks. After the regioselective protection of **5** with benzylaldehyde dimethyl acetal, surprisingly, the enantiomers of position 2' (Figure 31) could be separated by flash chromatography, to give 66% of the major isomer **18**.

Figure 31: Benzylidene protection of **5** allowed the separation of the mixture of R and S enantiomers

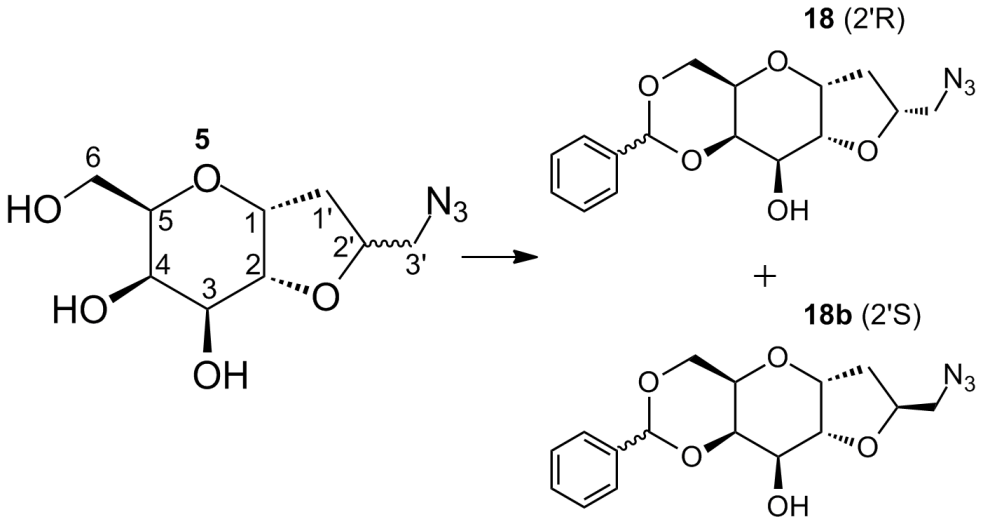

Reagents and conditions: benzaldehyde dimethyl acetal, CSA, DMF, 70°C, *in vacuo*, 1h, 66% (major isomer).

Before the attachment of building block **7**, we preferred to reduce the azide and derivatize the resulting amine with **9**. As a precaution, instead of reducing the azide at the end of the synthesis, when the heterocyclic rings would be present, we preferred to perform the reduction with H_2/Pd Lindlar during the first steps, giving compound **19**. No sign of benzylidene deprotection was detected. The primary amine was then reacted with **9** to generate the amide **20** in high yield, which contains the first pharmacophore.

The next step consisted in the attachment of the second building block (**7**) by *O*-alkylation. Substitution of OH-3 afforded compound **21** with a disappointing low yield. Attempts to optimize the reaction yield by raising the equivalents of alkylating agent and NaH did not produce better results. Indeed, forcing reaction conditions resulted also in the *N*-alkylation at the benzamide function.

Figure 32: Synthesis of **16**, the first target compound used in the biological tests for GRP receptor activity

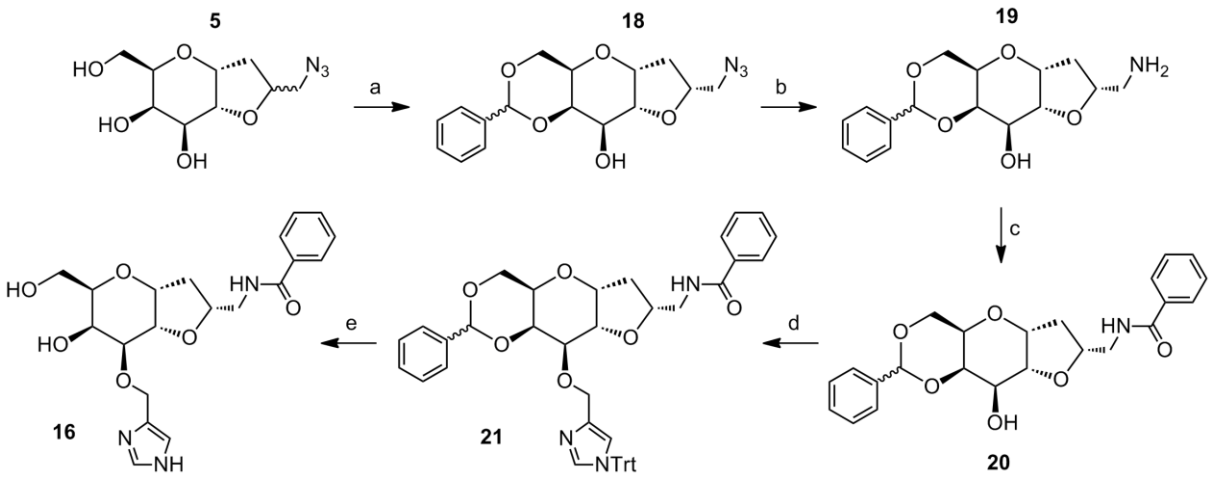

Reagents and conditions: a) benzaldehyde dimethylacetal, CSA, DMF, 70°C, *in vacuo*, 1h, 66% (major isomer); b) Lindlar catalyst/C, H_2, AcOEt, overnight, quantitative; c) benzoyl chloride, TEA, methanol, 0.5h, 90%; d) **7**, NaH 60%, DMF, 60°C, 20h, 23%; or **22**, NaH 60%, DMF, 20h, 23%; e) TFA/CH_2Cl_2 1:4, 1h, 66%.

Looking for better yields in the alkylation step of compound **20**, we decided to change the imidazole building block. Instead of the alkyl chloride, a more reactive alkyl bromide **22** was engaged for this purpose. The synthesis of the new building block is presented in Figure 33.

Figure 33: Synthesis of the imidazole building block **22** containing bromide

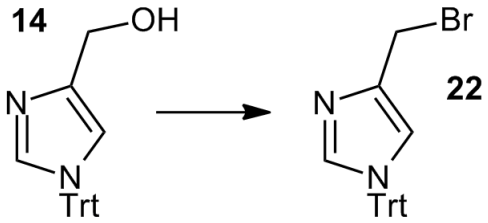

Reagents and conditions: PPh_3, NBS, CH_2Cl_2, 1.5h, 40%.

Building block **22** demonstrated to be very unstable, thus, after work-up it was directly used for alkylation without further characterization. Alkylation of

compound **20** with building block **22** afforded product **21** in low but workable yield, exactly as the reaction with building block **7**. No enhancement was obtained from this change. We carried on the synthesis by deprotecting compound **21** with trifluoroacetic acid, affording the first target compound **16**. This compound has an important pharmacophore, the imidazole group representing His^{25} of GRP. For this reason we found useful to investigate the biological activity of product **16**, which will be discussed in the next topic.

A small amount of **16** was used in the biological tests, whereas the bulk of **16** was used in the synthesis of the second target compound **17**. At this point, we decided to attach the most important bioactive substituent, the indole group. The influence of this additional pharmacophore in the biological activity could be evaluated by comparison to the bioactivity of compound **16**, which is structurally very similar but lacks the indole group.

Before the reaction with building block **6**, protection of OH-6 and also *N*-protection of the imidazole ring were required. Simultaneous protection of both functional groups by a common protective group seemed interesting. For this purpose, the trityl group was selected as the appropriate protecting group. The primary alcohol and the heterocyclic amine of **16** were protected, while OH-4 remained free, to afford compound **23** (Figure 34). Attachment of the third pharmacophore was performed by reacting **23** with building block **6**, which produced compound **24**. Similarly as the attachment of the imidazole building block, this reaction resulted in low yield. Attempts to optimize the results by raising the equivalents of alkylating agent and NaH did not enhance reaction yield, resulting also in the *N*-alkylation at the benzamide function. The availability of a workable quantity of compound **24** prompted us to proceed with the total deprotection of **24**. The procedure was performed in a solvent-free mild reaction, using silica saturated with HCl, heating and vacuum. The conversion was complete as followed by TLC, but unfortunately, work-up and purification by flash chromatography recovered less than 50% of the product **17**, which was quite enough for biological tests.

Figure 34: Synthesis of compound **17**

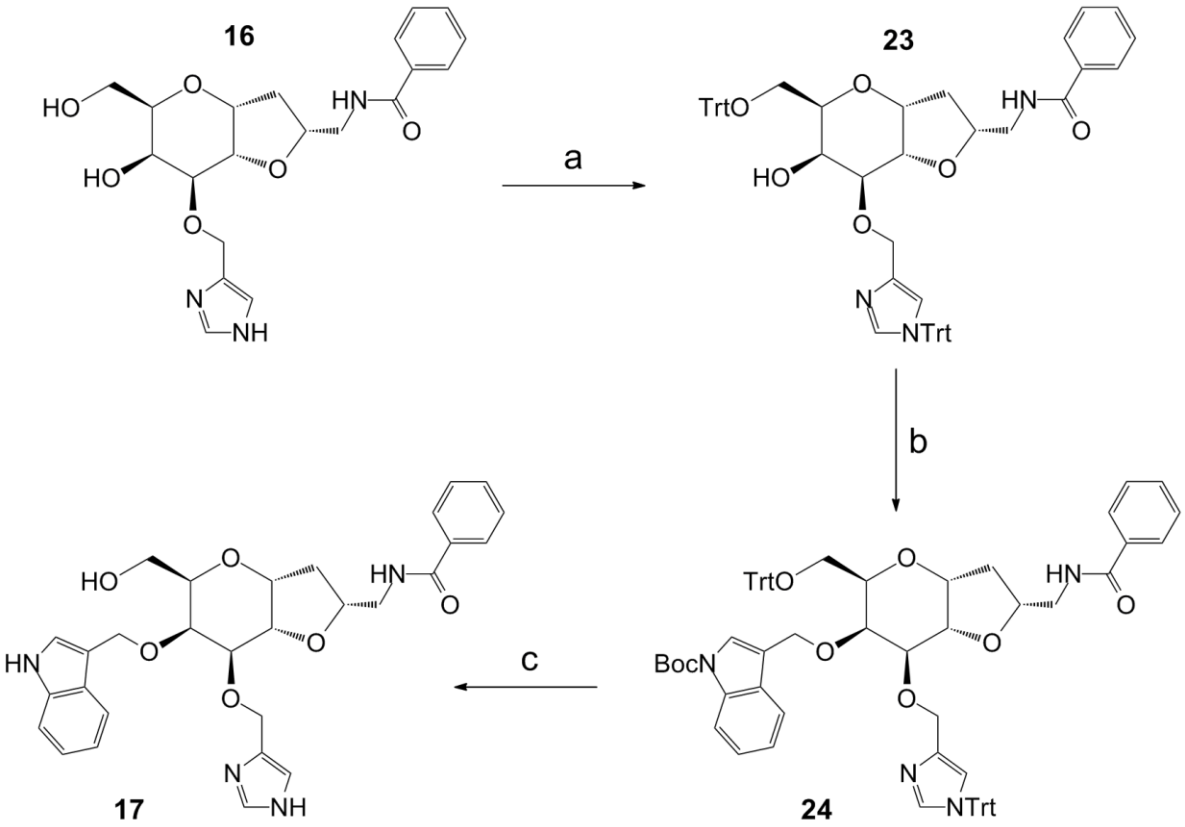

Reagents and conditions: a) TrtCl, DMAP, pyridine, 50°C, overnight, 42%; b) **6**, NaH 60%, DMF, overnight, 21%; c) HCl-satured silica, 80°C, *in vacuo*, overnight, 22%.

During the alkylation step that produced compound **24**, a minor by-product was detected. It could not be characterized by NMR spectroscopy because of its reduced quantity, but analysis by mass-spectrometry revealed that it is the product of the overalkylation of compound **23**. Because of its small occurrence, it was considered of less importance.

3.3.4. Biological tests performed with compounds 16 and 17

The activation of the GRP receptor, as a typical G-protein coupled receptor, results in the increase of intracellular calcium levels, by activation of phospholipase C. In collaboration with the group of Prof. Cavaletti from our university, biological tests were performed in PC-3 cells, a human prostate

carcinoma cell line that overexpress the GRP receptor, to follow the influence of our compounds in the intracellular calcium mobilization. The results gave us some important insights about the activity of compounds **16** and **17**.

Calcium is an important component in the signalling response of prostate carcinomas to diverse extracellular stimuli. The level of Ca^{2+} is an important second messenger involved with the initiation of many cellular processes including proliferation, migration, and invasion. Androgen independent prostate tumour cells, such as PC3 cells, express several receptors functionally coupled to rapid elevations of Ca^{2+} and bombesin elicits greater calcium signaling responses in PC3 cell line as compared to the immortalized human prostate epithelial cells.[120]

As a positive control for the experimental settings, we used the ability of bombesin to stimulate the increase of intracellular calcium in PC-3 cells. In figure 35, it can be observed a fast and strong increase in the intracellular Ca^{2+} levels after the administration of 100 nM of bombesin (time = 0 in figure 35). The maximal response was reached between 10 and 20 seconds after the treatment.

Figure 35: Effects of bombesin (100 nM) and compounds **16** and **17** (100 to 300 nM) on free intracellular calcium levels in PC-3 prostatic carcinoma cells.

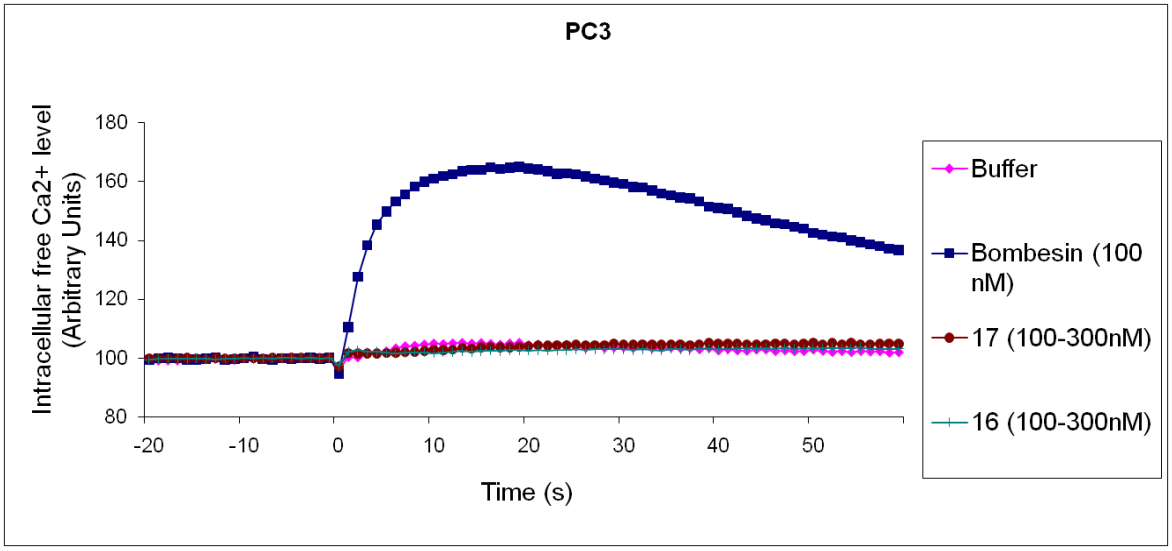

The behavior of GRP receptor agonists should be similar to the activity profile observed for bombesin. Partial agonists are expected to exert an intermediate response compared to bombesin. In the case of compounds **16** and

17, the intracellular level of calcium remained unchanged, resulting in a profile very similar to the buffer. Therefore, as no response was observed, compounds **16** and **17** cannot be considered agonists of the GRP receptor. However, these results do not exclude the possibility that the compounds could still be ligands for the GRP receptor. Fortunately, these possibility was confirmed for compound **17**. In another experiment, after the administration of compound **17** (50 nM) to PC-3 cells, these were treated with bombesin (100 nM) and the response was measured. As result, bombesin induced a considerably lower intracellular Ca^{2+} mobilization in cells pre-treated with **17**, as demonstrated by the dark blue line in figure 36.

Inhibition of PC-3 response to 100 nM administration of bombesin was achieved with compound **17** at 50 nM, which is half the concentration of bombesin. This result strongly suggests that target compound **17** could be an antagonist of the GRP receptor, and therefore we are able to propose that this compound is a ligand for this receptor. Further experiments will be performed to evaluate the binding affinity of **17** for the GRP receptor.

Figure 36: Effects of bombesin (100 nM) alone and after administration of compound **17** (50 nM) on free intracellular calcium levels in PC-3 prostatic carcinoma cells

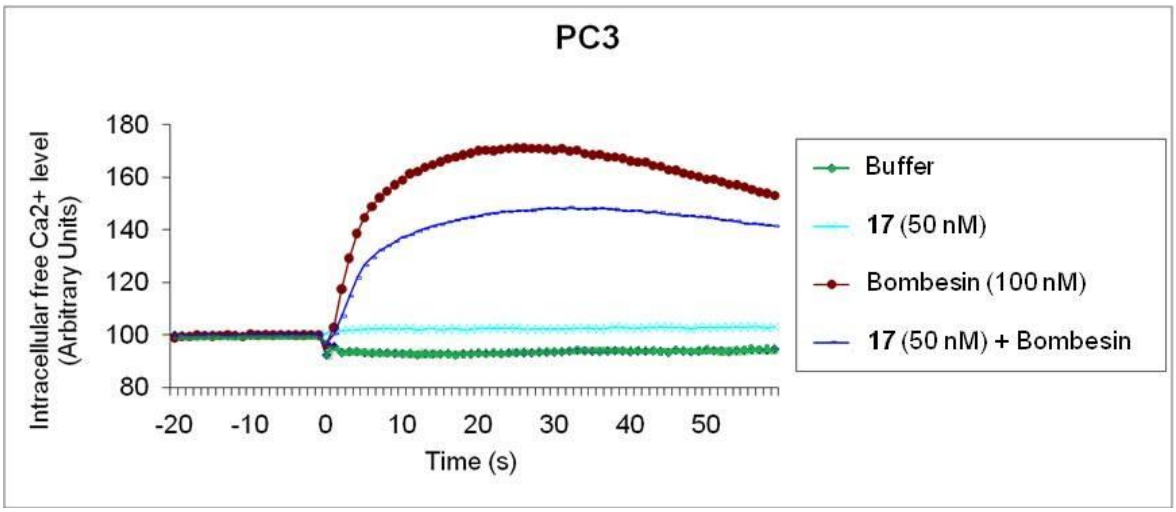

In order to evaluate the antagonist activity of compound **17**, an additional experiment is needed and will soon be performed. It has been demonstrated that bombesin is able to induce Elk-1 activation in prostate cancer cells. Elk-1 is a

transcription factor well-correlated to the proliferation of cancer cells. GRP receptor antagonists alone do not have an effect on Elk-1 activation, but abolish bombesin-induced Elk-1 activation.[121] In order to test the ability of **17** to inhibit bombesin-induced Elk-1 activation, western blot analysis that specifically recognize active (phosphorylated) Elk-1 will be performed. As a positive control for experimental settings, our collaborators tested the ability of bombesin (100 nM) to stimulate Elk-1 activation in PC-3 cells. The results are presented in figure 37. Our experiments confirm the activation of Elk-1 after treatment with bombesin at 100 nM. Experiments to verify the level of phosphorylation of Elk-1 in PC-3 cells pre-treated with compound **17** at 50 nM followed by the treatment with bombesin 100 nM are currently in progress.

Figure 37: Bombesin-induced Elk-1 activation in prostate cancer cells:[121] bombesin at 100 nM induced Elk-1 activation after 30 and 60 minutes of treatment

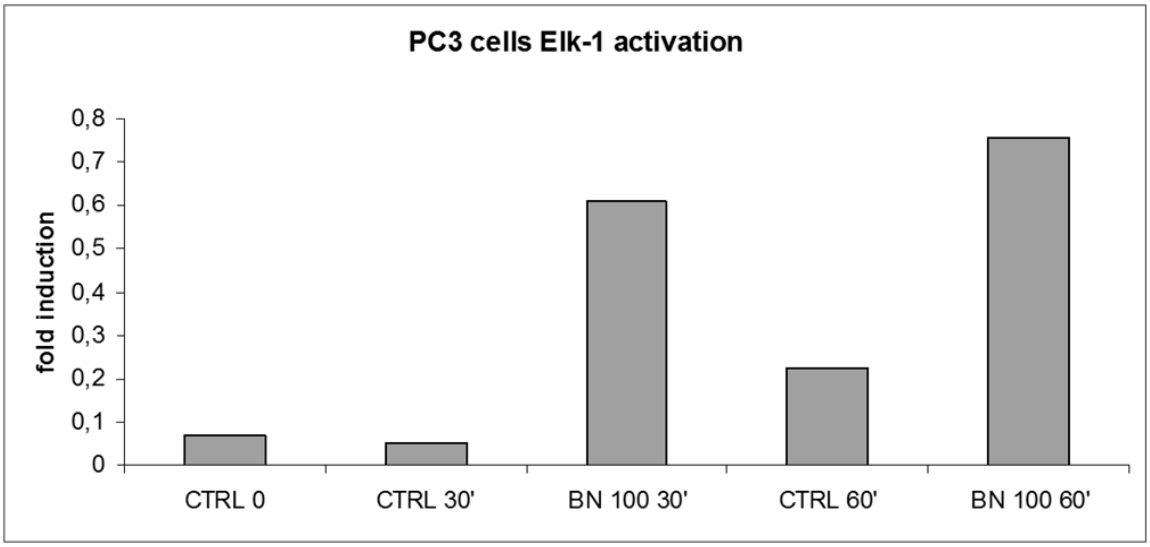

Legend: CTRL 0, CRTL 30' and CRTL 60' = untreated cells analyzed at 0, 30 and 60 minutes, BN 100 30' and 60' = cells treated with bombesin at 100 nM, analyzed at 30 and 60 minutes

3.3.5. Optimization of the synthesis of target compounds

The synthesis presented in the last topics was performed to produce the target compounds as soon as possible for biological evaluation. Unfortunately, it did not produce a good amount of compound **17** for the synthesis of the final

compound **1b**, which did not allow us to perform the reactions presented in figure 38.

Figure 38: Synthesis of compound **1b**, starting from compound **17**

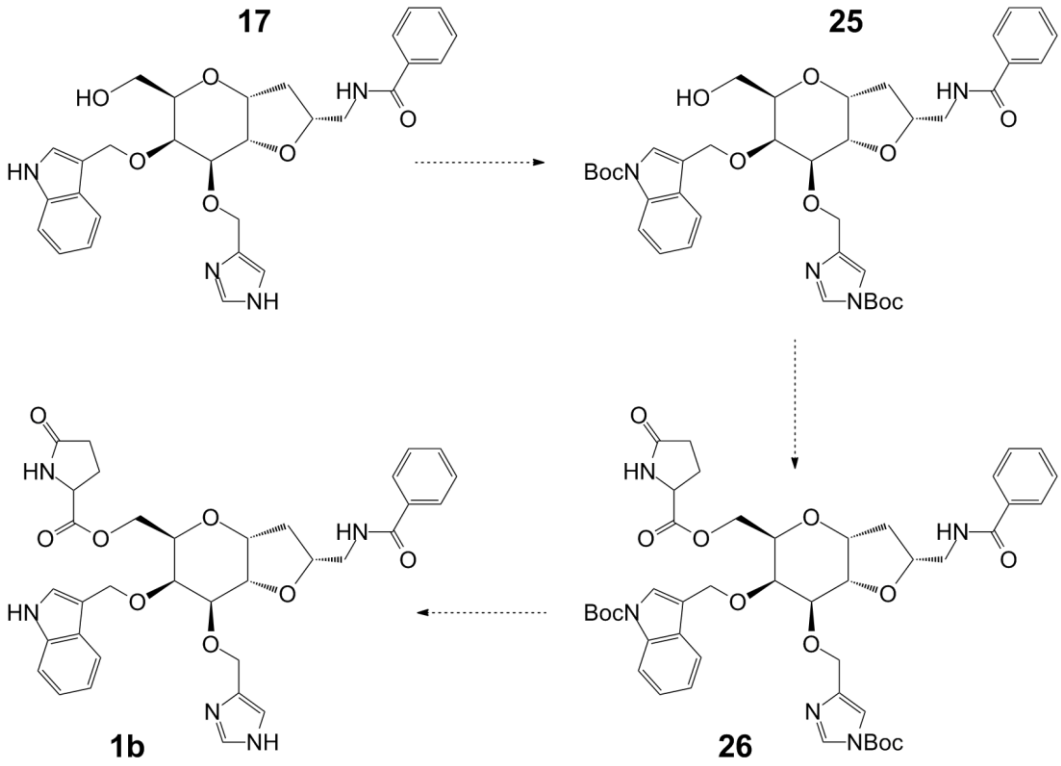

Legend: dashed arrows were used to indicate that the reactions could not be performed.

The achievement of an interesting biological activity for compound **17** gave us a compelling justification to optimize the synthesis of these target compound, and to look for a common route to synthesize both **17** and the final compound with all four pharmacophores (**1b**) with higher yield than the previous method. As already described, attempts to increase the yield of the alkylation steps using building blocks **6**, **7** and **22** were vain. We suspected that the presence of the benzamide group represented an obstacle during these steps, as we observed the formation of by-products resulting from *N*-alkylation in forced reaction conditions.

Taking into account the possibility that the amide functional group of **20** and **23** could hamper the alkylation steps, we decided to shift the attachment of this

pharmacophore, benzamide, to the last steps of our synthesis. The new synthetic pathway was performed in a pretty similar sequence as the previous pathway, but leaving the reduction of the azide to amine, and derivatization with benzoyl chloride to be performed after the alkylation steps (Figure 39).

Figure 39: Synthetic method performing the alkylation steps before the formation of the amide

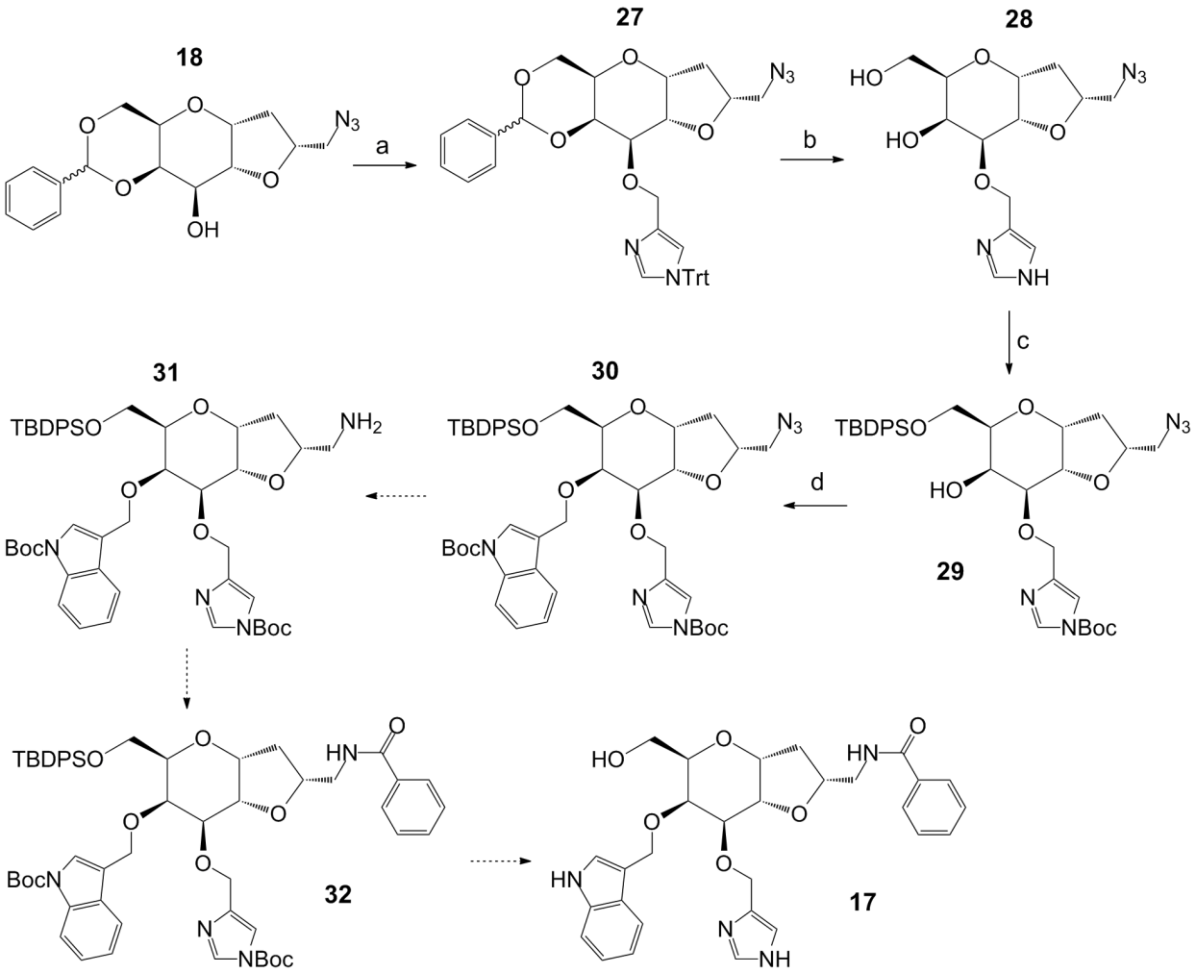

Reagents and conditions: a) **7**, NaH 60%, 0.5h, 87%; b) TFA/CH_2Cl_2 1:4, 0.5h, 87%; c) i. $(Boc)_2O$, TEA, methanol/dioxane/H_2O 6:1:4, 2.5h, 60%; ii. TBDPSCl, imidazole, DMF, 3h, 80%; d) **6**, NaH 60%, THF or DMF, overnight, 55% (by-product). Dashed arrows indicate the reactions that could not be performed.

In the beginning, the new synthetic method showed good yields. Alkylation with building block **7** and compound **18**, which have the azide instead of

benzamide, was performed with 87% yield. Comparing to the alkylation of **20**, which contains benzamide, there was a 4-fold optimization in reaction yield. This difference could be related to the presence of benzamide in **20** and azide in **18**, as this is the only difference between both starting materials.

Deprotection of **27** with TFA gave also good results, not too far from those reported for the previous synthetic method. From the deprotected compound **28**, we decided to change the protecting groups used in the previous synthetic method, because of the low protection yield and also to acquire orthogonality, an important property for the production of target compound **1b**. This is explained by the use of compound **32** to produce not only target compound **17** by total deprotection (Figure 39), but also target compound **1b** from orthogonal deprotection of OH-6 and its derivatization with building block **8**, followed by total deprotection. In order to increase the yield of protection of the imidazole group, *tert*-butyl carbamate (Boc) was selected, giving the protected product with good yield. To fulfill the requirements for orthogonality, regioselective protection of OH-6 was performed with a hindered silyl protecting group (TBDPS), which can be deprotected with F^- (TBAF) without affecting Boc protections. The overall yield involving both protection steps was satisfying (50%). This procedure afforded compound **29**, displaying free OH-4 for derivatization with indole building block **6** (Figure 39).

Several variations on reaction conditions for the alkylation of **29** with building block **6** were tested to generate compound **30**. However, in all cases the main product obtained was not the expected product, but a by-product that could result from the loss of Boc-protection of compound **30** (compound **30b**, Figure 40). Attempts to explain the Boc-deprotection of imidazole did not find definitive reasons to support the structure of compound **30b**, unless the Boc-transfer from imidazole to the alkoxide (RO^-) from deprotonated **29**. Not convinced by this explanation, we suspected that *N*-alkylation of imidazole could cause Boc-deprotection, resulting in the formation of by-product **30c** (Figure 40).

Figure 40: Possible structures for the main compound produced by the alkylation of compound **29** with building block **6**

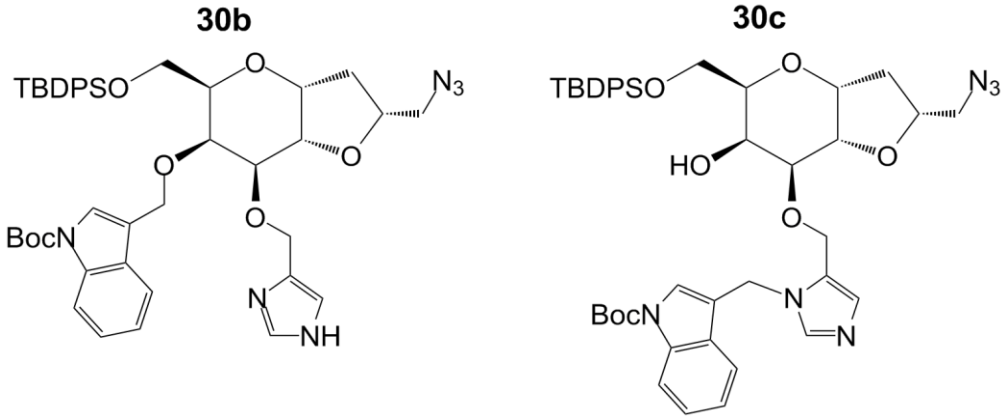

Unfortunately, the structure of the by-product could not be confirmed by either NMR spectroscopy or mass-spectrometry, as both compounds have exactly the same molecular mass and probably a very similar spectroscopic profile. Anyway, we concluded from this result that the use of Boc-protection for the imidazole ring was not favorable for the alkylation with **6**. Consequently, this synthetic strategy was rejected and we decided to use again the trityl protecting group instead of Boc-protection.

The alternative synthetic strategy is illustrated in figure 41. In order to verify the ability of trityl as an imidazole protecting group for the synthesis of compound **17**, we decided to work with both imidazole ring and OH-6 protected with trityl. Compound **28**, already obtained from the other procedure, was used as the starting material. Protection of the primary alcohol and the imidazole nitrogen was achieved with a similar yield to that reported for the synthesis of analog compound **23**. Alkylation with building block **6** was performed to evaluate the performance of the trityl double protection. The expected product, compound **34a**, was obtained in low yield. The disappointing result was explained by the presence of some by-products occurring in the reaction, some of them difficult to be separated from compound **34a**.

Figure 41: Synthetic method performing the alkylation steps before the formation of the amide, using trityl as the imidazole protecting group

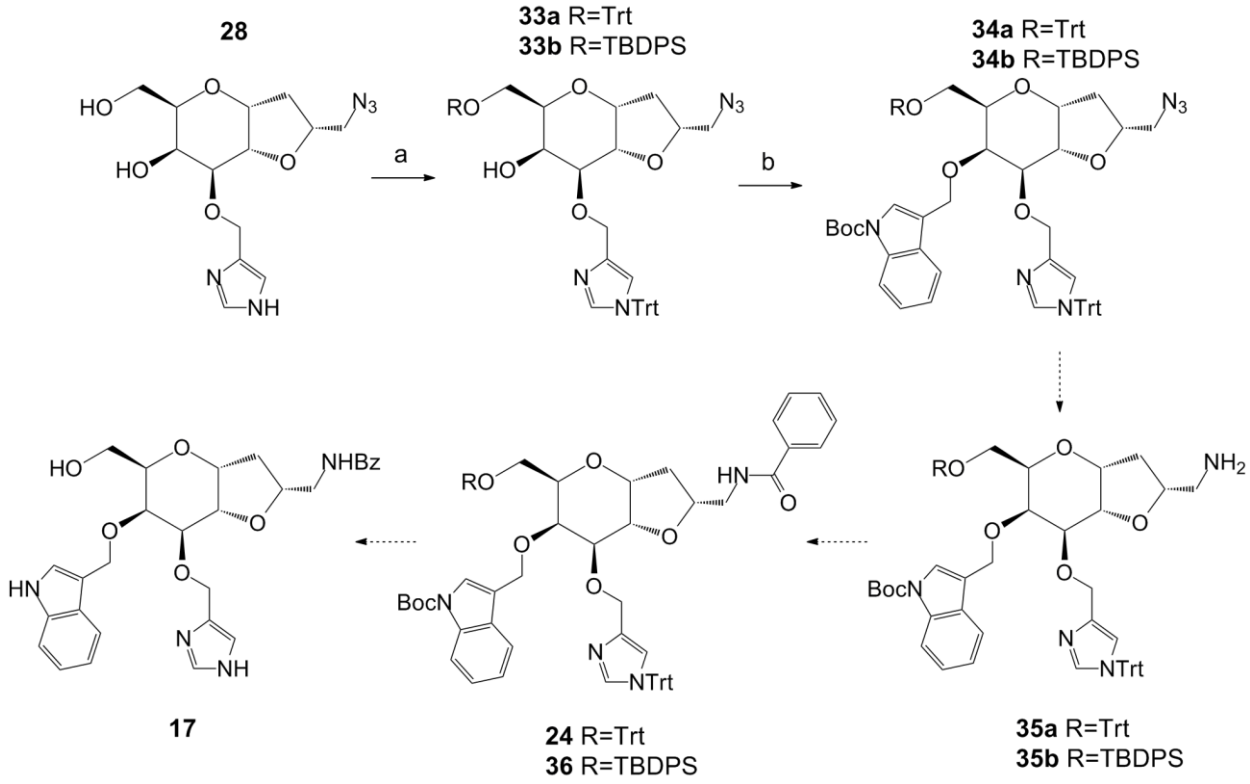

Reagents and conditions: a) For **33a**: TrtCl, DMAP, pyridine, 50-60°C, 7.5h, 34%; For **33b**: i. TrtCl, TEA, DMF, overnight, 62%; ii. TBDPSCl, imidazole, DMF, 2.5h, 33%; b) **6**, NaH 60%, THF, DMF, overnight, 14% for **34a** (partially pure). Dashed arrows indicate the reactions that could not be performed.

The structures of some by-products of the present alkylation step were hypothesized from mass-spectrometry analyses and are shown in figure 42. The major compounds obtained from this alkylation are the expected compound **34a** and its major by-product **34k**. This by-product was clearly formed by the Boc-transfer from the building block to compound **33a**. Changes in the reaction conditions were not successful to overcome the formation of **34k**, usually occurring in an equivalent yield to compound **34a**. Minor by-products were formed by the loss of trityl group from the expected product (**34y**), trityl displacement by Boc-transfer in the expected product (**34w**), and trityl displacement by the alkylating agent (**34z**). The yield of compound **34a** was so low to make this synthetic procedure become not interesting for our synthetic optimization purpose.

Figure 42: Compound **34a** and suggested structures of by-products found after the alkylation step

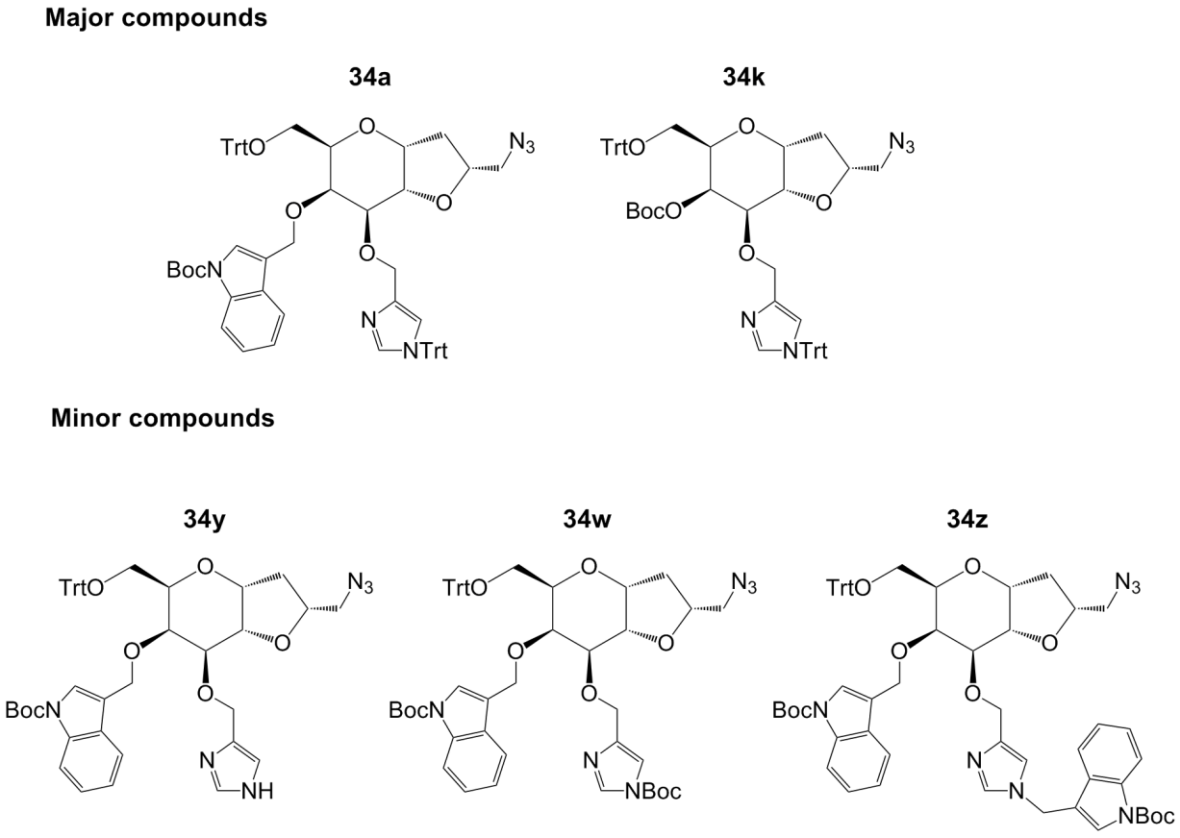

Concomitantly, orthogonal protection of imidazole and OH-6 was performed with compound **28**. The protection of the NH group of imidazole was performed with good yield, using the same reaction conditions for the synthesis of building block **7**. On the other hand, subsequent protection of OH-6 with the hindered silyl group TBDPS produced expected compound **34b** in low yield. The major compound of this reaction was the product with two TBDPS groups attached to the trityl-protected starting material **28'** (Figure 43).

Figure 43: Products formed during OH-6 protection of trityl-protected compound **28'**

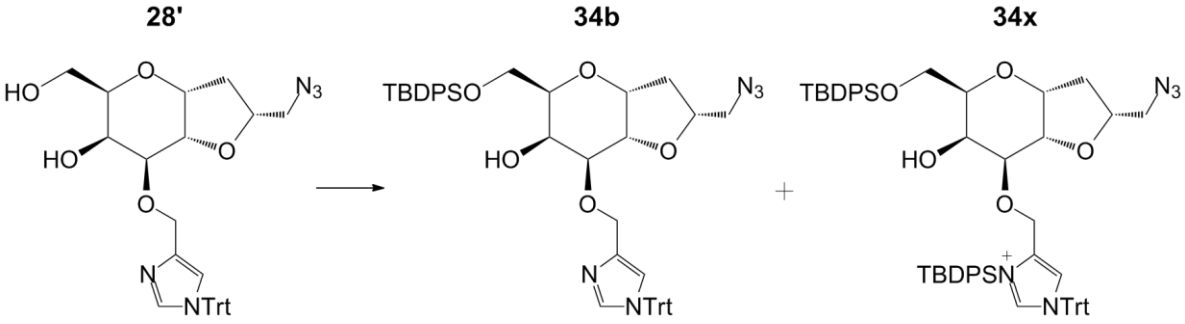

Reagents and conditions: TBDPSCl, imidazole, CH_2Cl_2, 2.5h, 33%.

In the mechanism of silylation of primary alcohols with TBDPSCl and imidazole as catalyst (Figure 44), we observe that the reaction proceeds via *N-tert*-butyldiphenylsilyl imidazole, a very reactive silylating agent. In our case, the imidazole ring present in **28'** also bound the TBDPS group during the reaction. However, the resulting compound seemed much less reactive than the original intermediate of the silylation, as it could be isolated after work-up in high yield. From this result, we could conclude that the silyl protection of OH-6 is not recommended in this situation, when a trityl-protected imidazole group is present.

Figure 44: Mechanism of silylation of a primary alcohol with TBDPS and imidazole

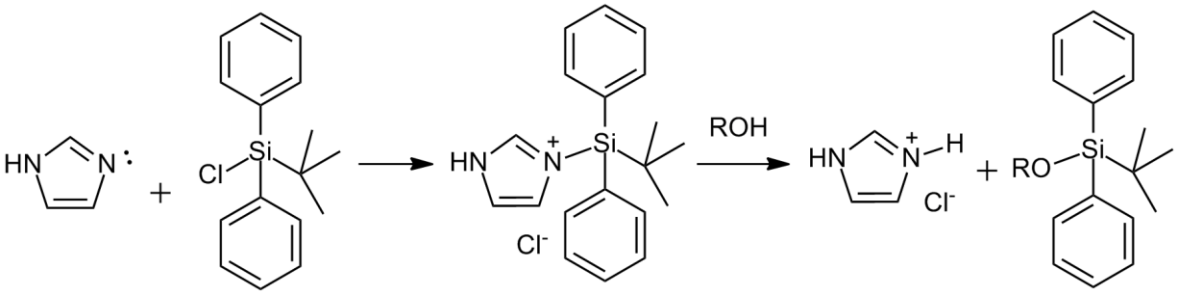

The synthetic method presented in figure 41, using trityl-protection for the imidazole group and subsequent alkylation with building block **6**, proved to be an inefficient strategy for the optimized production of target compounds **17** and **1b**.

Taking into account all results from the attempts to optimize the synthesis of compounds **17** and **1b**, some important remarks can be pointed out:

- Alkylations with building blocks **6** and **7** are recommended to be performed before the formation of the benzamide group.
- Alkylation with building block **6** should not be performed in the presence of the *N*-protected imidazole group, to avoid *N*-alkylation.
- Silylation cannot be performed in the presence of the *N*-protected imidazole group.
- Building block **6** should be reconsidered because of the occurrence of Boc-transfer during alkylations.

Guided by these rules, we understood that the small modifications performed in the reaction methods could not be the right solution for the optimization of the synthesis of target compounds. Therefore, we planned a whole different synthetic method that obeys to every single recommendation that we pointed out.

The strategy involves the use of a different building block for indole group attachment; the silylation of OH-6 and attachment of the indole building block before the attachment of the imidazole building block; and the formation of the benzamide group after the alkylation steps of the synthesis.

In order to perform the attachment of the indole building block first, we developed a protecting scheme that rendered only OH-4 unprotected. This was achieved by the regioselective protection of OH-3 with an allyl group, via a dibutylstannylene acetal intermediate, and the subsequent protection of OH-6 with the hindered silyl group TBDPS (Figure 45). This procedure afforded compound **38** as a pure diastereoisomer, which was ready for the attachment of the indole building block at OH-4.

Figure 45: Synthetic method developed from the experience acquired in previous attempts to optimize the synthesis of target compounds (reactions already performed)

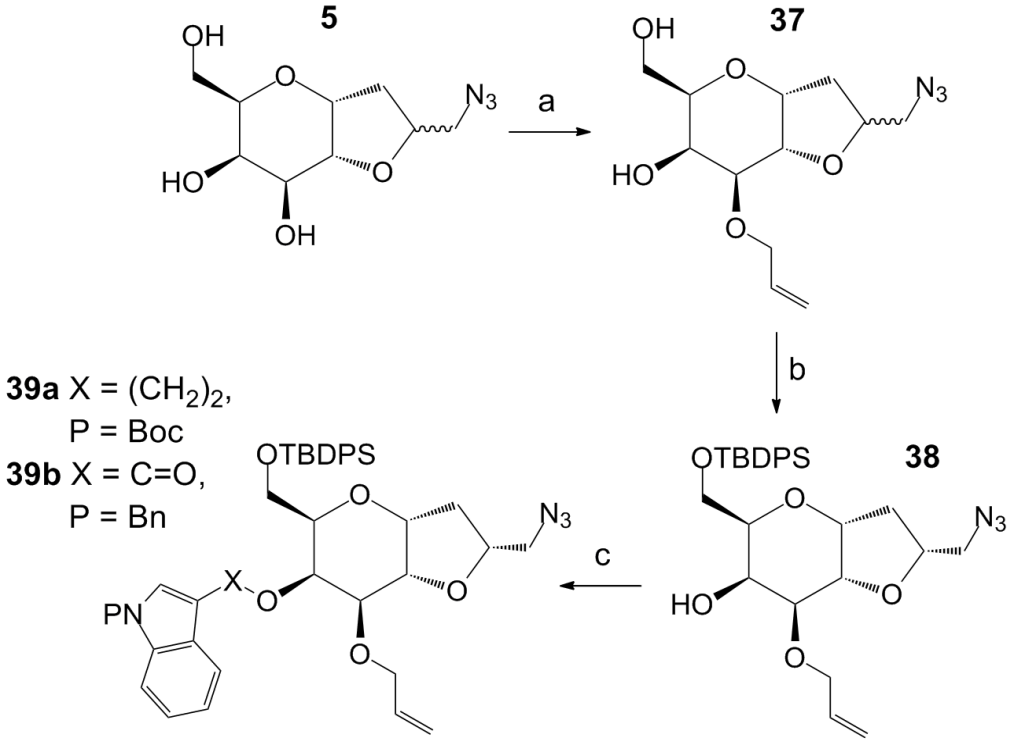

Reagents and conditions: a) i. Bu_2SnO, toluene, reflux, overnight; ii. TBAI, allyl bromide, reflux, 6h, 67%; b) TBDPSCl, imidazole, CH_2Cl_2, 0.5h, 60% (pure major isomer); c) For **39a**: **6'**, NaH 60%, TBAI, DMF, overnight, no product; For **39b**: **40**, EDC, DMAP, CH_2Cl_2, reflux, 24h, 60%.

We decided to reconsider the use of building block **6** because of frequent Boc-transfer observed during the alkylation steps of previous synthetic strategies. The ability of Boc-transfer was associated to the instability of building block **6** in the conditions used for alkylation. Thus, we suggested a mechanism for this side-reaction (Figure 46). As a good leaving group, bromide should be displaced by the alkoxide during the reaction. However, the positive charge density in the carbon that was attached to bromide is rapidly stabilized by resonance, after loss of bromide. This makes the carbonyl of Boc group a better electrophile than that carbon, and nucleophilic attack is performed on this group. This could be one of the reasons for low yields observed after alkylation with **6**.

Figure 46: Putative mechanism of Boc-transfer performed by building block **6**

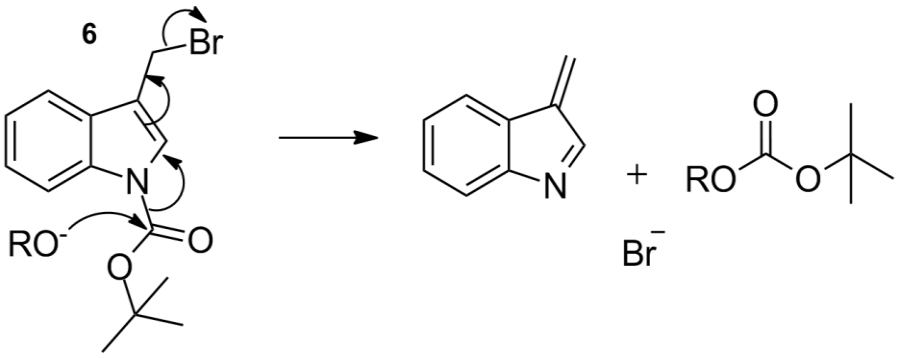

A new indole building block was synthesized, corresponding to a variation in the structure of **6**, which is an additional methylene group between the indole ring and bromide (Figure 47). It was expected that this derivative, 1-Boc-3-(2-bromoethyl)indole (**6'**), should be able to overcome the Boc-transfer problems, because of the impossibility to stabilize bromide loss by resonance. Unfortunately, every attempt to alkylate compound **38** with building block **6'** was unsuccessful, because of the prevalence of the elimination reaction over the substitution reaction (Figure 47).

Figure 47: Reaction between building block **6'** and compound **38**, dominated by the elimination reaction to afford **6b**

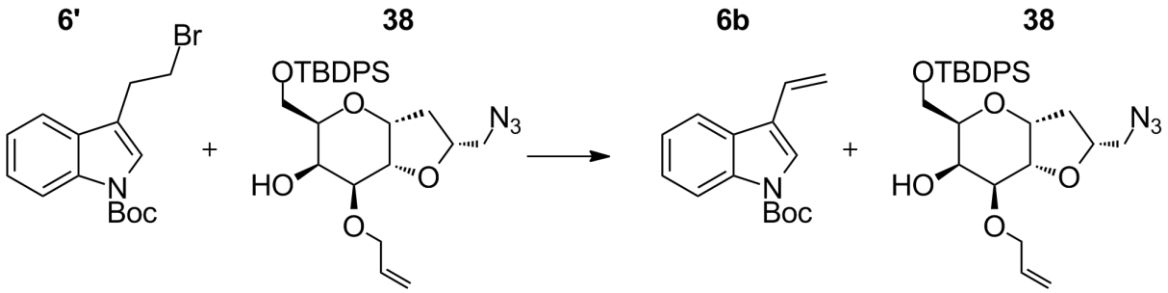

Reagents and conditions: **6'** (1.5-5 eq), NaH 60% (1.5-5 eq), DMF, TBAI, overnight.

From this point, instead of using alkylating agents as indole building blocks, we decided to use a different functional group for the attachment of this pharmacophore. In the past few years, some research groups reported the successful attachment of indole derivatives via ester linkers.[122-124] The reaction conditions used in the esterifications between carboxylic acid derivatives of indole groups and alcohols are very mild, usually the same reagents and mild conditions

used for solid-phase peptide synthesis. Based on these reports, we prepared building block **40**, a benzyl-protected indole carboxylic acid (Figure 48). Esterification of compound **38** with this new building block was performed in good yield (Figure 49), indeed, for the first time the indole pharmacophore was attached to the scaffold with more than 50% yield.

Figure 48: Synthesis of indole building block **40**

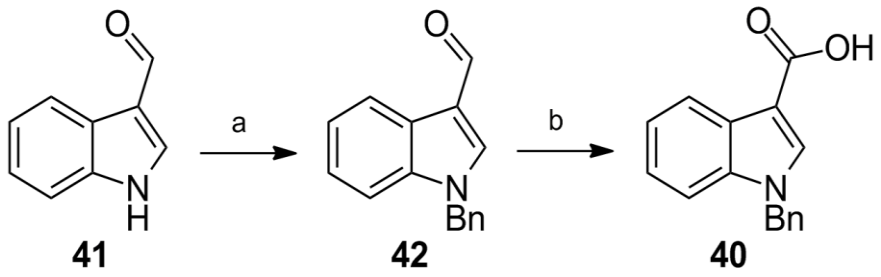

Reagents and conditions: a) BnBr, NaH 60%, DMF, 0.5h, quantitative; b) aq. $KMnO_4$, acetone, 16h, 77%.

Figure 49: Structure of building block **40** and esterification of compound **38**

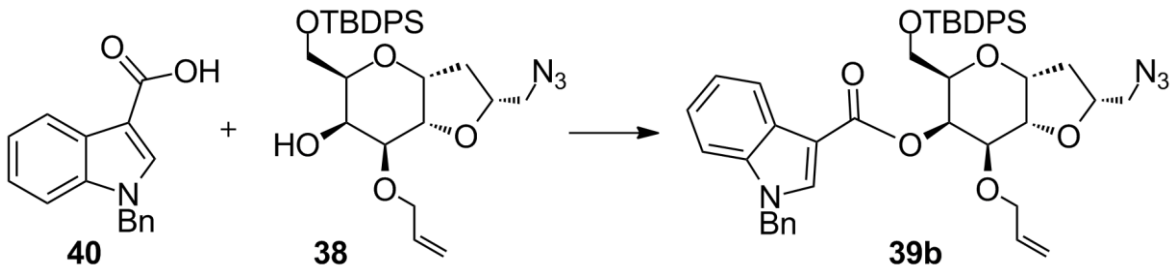

Reagents and conditions: **40**, EDC, DMAP, CH_2Cl_2, reflux, 24h, 60%.

The next steps for the attachment of the other pharmacophores are currently in progress (Figure 50). The synthetic method presented here has a good potential to obtain the target compounds in satisfactory yield, which will allow the biological evaluation of these target compounds, as demonstrated for bioactive compound **17**.

Figure 50: Synthetic method developed from the experience acquired in previous attempts to optimize the synthesis of target compounds (reactions to be performed)

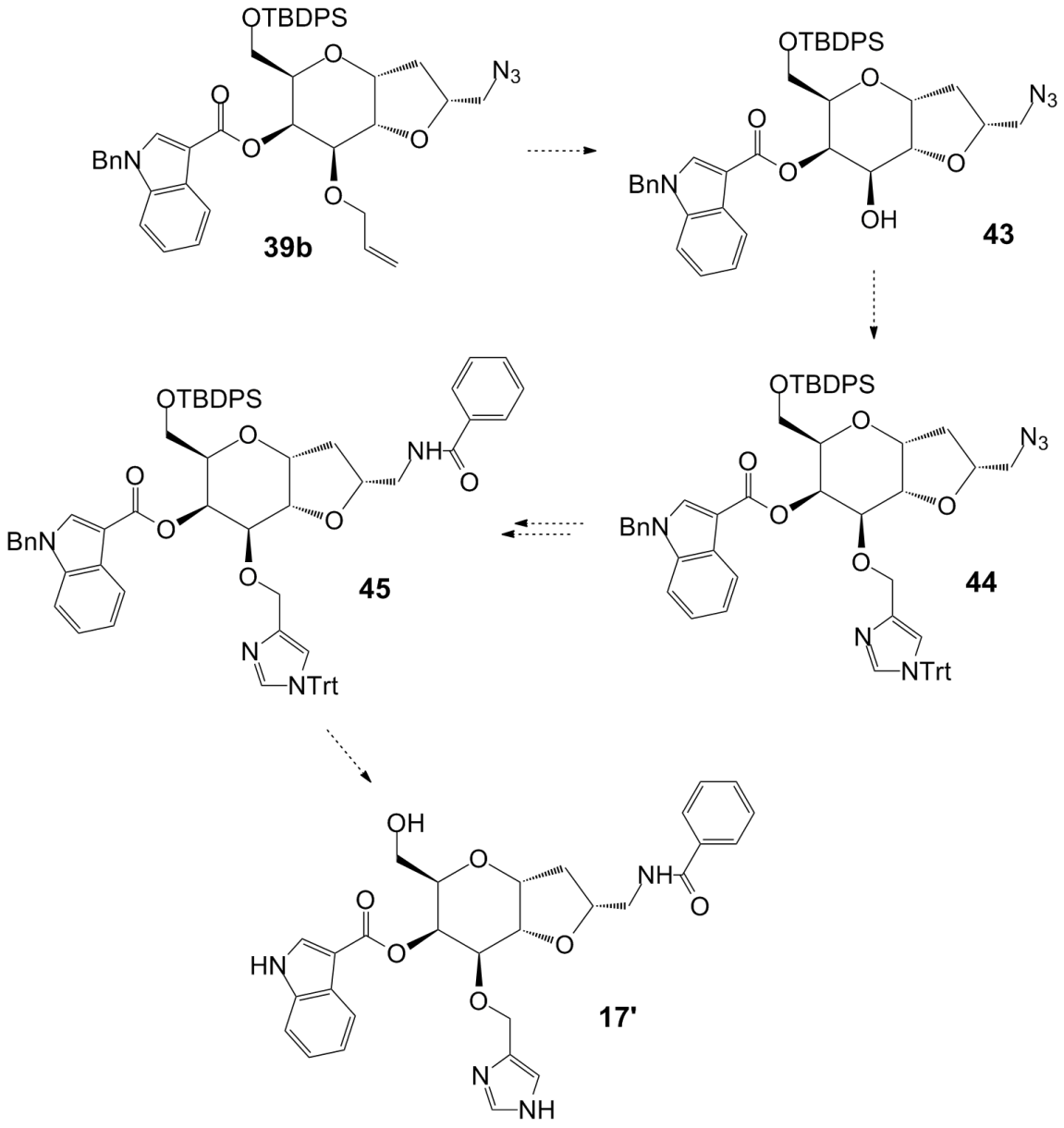

The target compound that will be prepared by the present synthetic strategy has a structure very similar to the bioactive molecule **17**, with the only difference concerning the ester linker instead of the ether for indole attachment (in other words, a C=O instead of a CH_2), for this reason it was named **17'**. In the same manner, final target compound **1b** and final target compound of the present synthetic method **1c** (Figure 51) present the same structural similarity. This

minimal difference in their structures was reflected in the ability of the target compound **1c**, with all four pharmacophores, to fit in the pharmacophore template. In figure 52, the overlay between this target compound and the GRP receptor agonist used to assemble the 3D pharmacophore template is presented. As expected, an excellent overlay was obtained, as indicated by the overlapping pharmacophores. From this result, the biological evaluation of compound **17'** is expected to afford a similar bioactivity as compound **17**.

Figure 51: Structure of final target compound **1c**

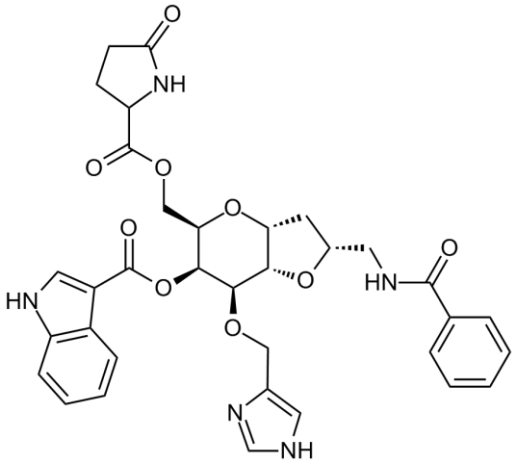

Figure 52: Overlay between the prospective GRP mimetic (in red) and the GRP receptor agonist (in grey) used to assemble the 3D template (pharmacophores indicated by the white arrows)

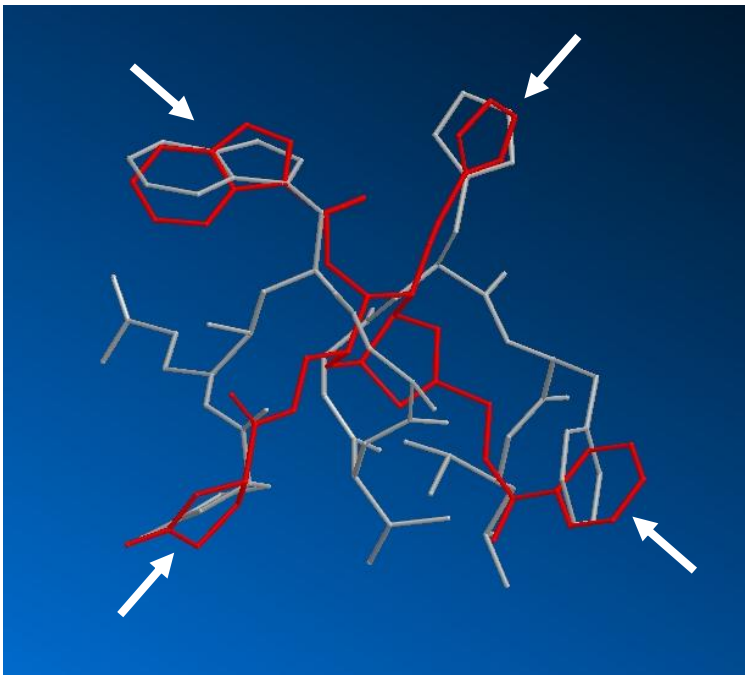

3.3.6. Synthesis of fluorescent GRP mimetics

The biological evaluation of our GRP mimetics showed that compound **17** behaved as an antagonist of the GRP receptor. Interested on the ability of this compound to afford receptor-mediated endocytosis, we planned to perform a biological test that would allow the direct observation of the internalization of GRP receptors by fluorescent microscopy. A very similar technique was used by Grady and co-workers to direct observe the endocytosis of GRP and its receptor (Figure 4, page 14). In order to perform the test, we developed a fluorescent analog of compound **17**.

The structure of this analog should share a reasonable similarity with the structure of bioactive compound **17**. The structure of the fluorescent probe should not disturb this similarity, therefore, it should be a small molecule, with good fluorescent properties. Attending to these requirements, the dansyl group was chosen as the fluorescent probe, because it is one of the simplest fluorescent dyes commonly used in chemistry and biochemistry to label peptides and proteins. Labeling is performed by reacting primary amino groups with dansyl chloride to produce blue-fluorescent sulfonamide adducts. Thus, the convenient site for dansyl labeling in the scaffold was the primary amine resulting from reduction of the azido function.

Compound **27** was used as starting material for the synthesis of the fluorescent analog of compound **17** (Figure 53). Reduction of the azido function afforded the primary amine **46**, which was labeled with the fluorescent dansyl group to afford **47**. The low yield for the labeling step was attributed to the reduction step, because of the possible generation of by-products during the hydrogenation. Then, the use of a solvent-free reaction for selective deprotection of the trityl group afforded compound **48** in a workable yield, with complete recover of remaining starting material **47**.

Figure 53: Synthesis of a fluorescent analog of bioactive compound **17**

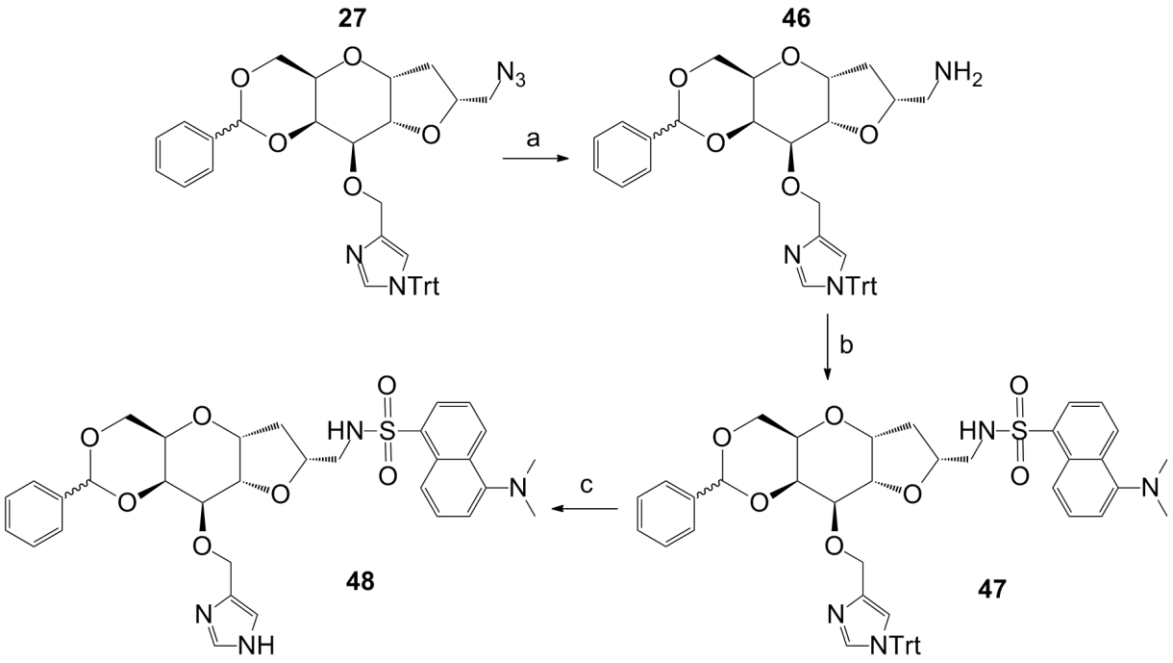

Reagents and conditions: a) Lindlar catalyst/C, H_2, AcOEt, overnight, 92%; b) dansyl chloride, TEA, CH_2Cl_2, 2h, 40%; c) silica, *in vacuo*, 100°C, 48h, 36%.

Comparing the structures of compounds **48** and **17** (Figure 54), it is possible to observe that the hydrophobic dansyl group could mimic the role of the benzamide group. In addition, it has been observed that benzene derivatives are considered hydrophobic surrogates of indole groups,[76,79,81,125,126] indicating that the benzylidene ring of **48** could act as a mimic of the indole group of **17**. Intrigued by these observations, we decided to evaluate the biological activity of compound **48**, using the same test applied in the screening of compound **17**.

Figure 54: Comparison between the structures of bioactive compound **17** and its potential analog **48**

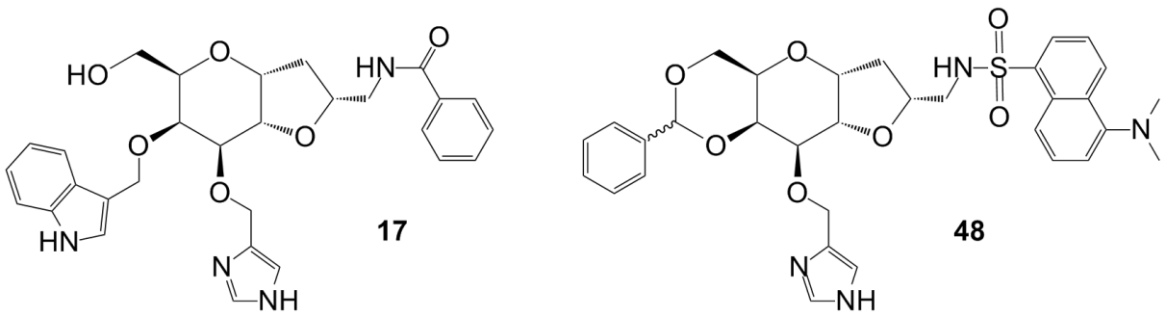

Evaluation of the ability of compound **48** to stimulate the increase of intracellular calcium in PC-3 cells showed that the fluorescent compound has no agonist activity. Treatment with compound **48** (50 nM) alone did not change the intracellular calcium level (purple profile, figure 55). Curiously, when bombesin (100 nM) was administered to the cells pre-treated with compound **48**, the response to bombesin was notably lower (light blue profile, figure 55), which is the same result observed for compound **17**. Therefore, as suggested for bioactive compound **17**, fluorescent product **48** seems to be an antagonist of the GRP receptor.

Figure 55: Effects of compound **48** (50 nM), bombesin (100 nM) alone and after administration of compound **48** (50 nM) on free intracellular calcium levels in PC-3 prostatic carcinoma cells

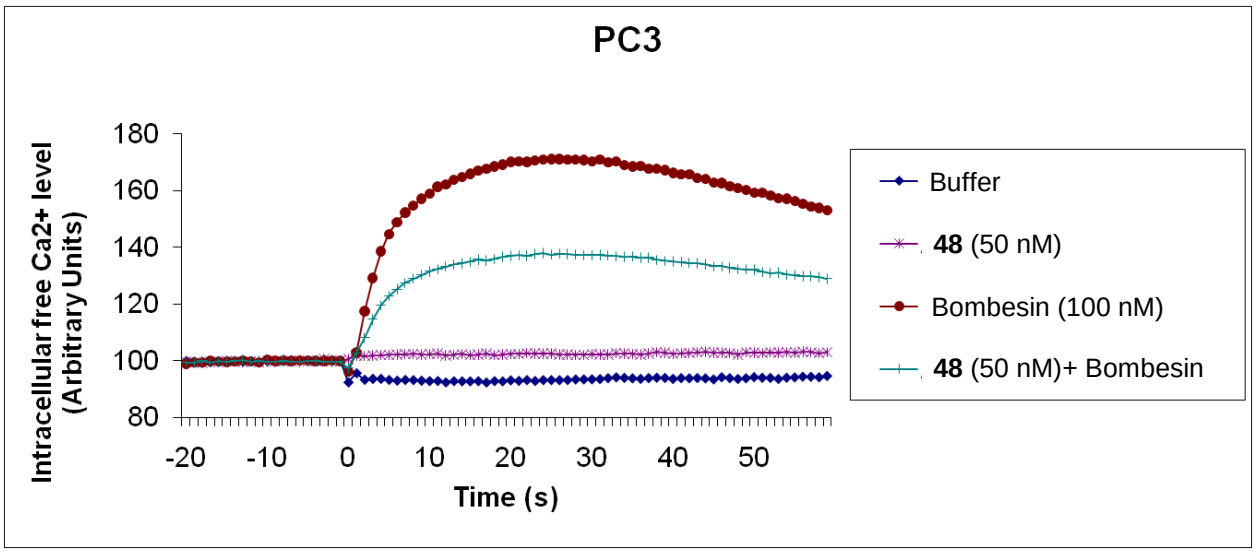

Despite their very similar structure and biological activity, the conclusion that **48** and **17** bind to the GRP receptor in the same manner seems to be premature. However, the results presented in this work provide strong evidences that **48** could be a functional analog of the prospective GRP receptor antagonist **17**.

The evaluation of receptor-mediated endocytosis of compound **48** by fluorescent microscopy is currently under development.

3.4. Design and synthesis of iminosugar-based potential Akt inhibitors

In light of the considerations described in the introductory part of this thesis, we proposed the study of a new class of inhibitors directed to the phosphoinositide-binding site of the Akt PH domain. Based on the structure of the reference inhibitor of Akt, PIA12,[100] we have initially designed a small library of iminosugar-based potential phosphatidylinositol analogues (Figure 56). Using docking calculations, this selection of potential analogues was evaluated for the ability to bind the PH domain of Akt. This work was accomplished in collaboration with the group of Prof. Luca De Gioia from our university.

The library was designed including molecules **49**-**54, 56** featuring the axial hydroxymethyl group at C3 as the inhibitor PIA12, which seems crucial for the selectivity towards Akt. Moreover, we designed also compounds **55, 57-59** with an axial carboxyl group, which should better interact with Arg^{25} in the PH domain, which in previous studies was shown to be one of the key protein residues involved in the interaction with PIP ligands. In order to possibly exploit the hydrophobic characteristics of the cleft close to the natural ligand binding site (including residues Ile^{74}, Val^{83}, Ile^{84}, see introduction), the C2 carbon atom of inhibitor PIA12 was substituted with a ring nitrogen in order to allow the chemoselective introduction of hydrophobic substituents in this position. Thus, derivatives **50**-**59** bearing a substituted ring nitrogen with different alkyl/carbamate groups were considered. Finally, we planned to substitute the labile phosphate of the natural substrate by more stable carboxymethyl group. Since the phosphatidyl moiety is not involved in the interaction with the PH domain, but is required *in vivo*

to anchor the substrate to cell membrane, we substituted the lipophilic moiety with simple ethyl ester so to avoid water solubility problems in the *in vitro* biological test.

Figure 56: Structures of the natural agonist of Akt [$PI(3,4)P_2$], the carbonate-based inhibitor PIA12 and the library of iminosugar-based phosphatidylinositol analogues

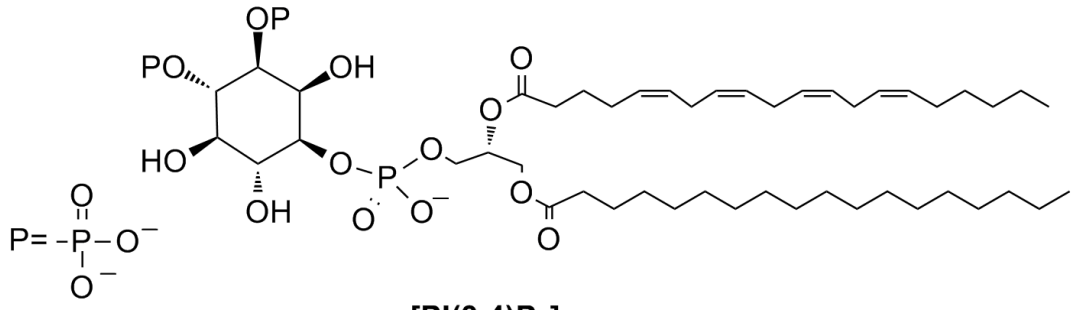

[$PI(3,4)P_2$]

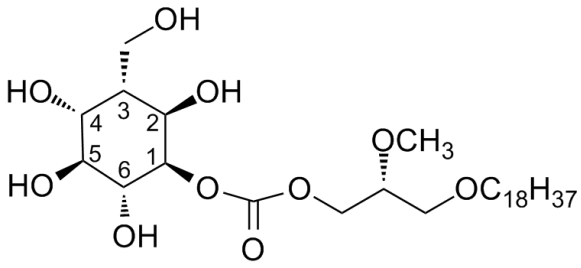

PIA12

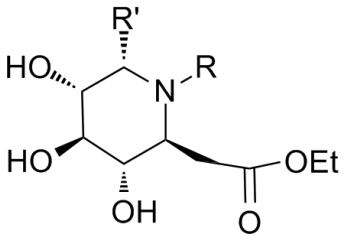

49 R=H, R'=CH_2OH
50 R=Pr, R'=CH_2OH
51 R=CH_2Cy, R'=CH_2OH
52 R=*t*Bu, R'=CH_2OH
53 R=iPr, R'=CH_2OH
54 R=Bn, R'=CH_2OH
55 R=Cbz, R'=COOH
56 R=Cbz, R'=CH_2OH
57 R=Bn, R'=COOH
58 R=3,4-dihydroxyCBZ, R'=COOH
59 R=4(COOH)CBZ, R'=COOH

In light of the above considerations, we have initially carried out docking calculations on the series of compounds members of the library. In a first series of docking experiments carried out sampling a protein region corresponding to the phosphoinositide-binding site (hereafter referred to as BOX1), it turned out that not all compounds were predicted to bind to the same protein region (see Figure 57). In particular, since the best poses for some molecules were found close to the box boundary (molecules **49**, **51**, **52** and **53**; colored in blue in Figure 57), in order to avoid possible artifacts due to boundary effects, we carried out also a second set of docking experiments, in which the docking box was shifted and centered on the

protein region where molecules **49**, **51**, **52** and **53** were docked (hereafter referred to as BOX2; see methods).

Results from docking calculations carried out on BOX 1 and 2 are collected in Table 3.

Table 3: Docking energies (in kcal/mol) computed for compounds **49**-**59** sampling the protein region labeled as BOX1 (left) and BOX2 (right). LBE and MBE stands for Lowest Binding Energy and Mean Binding Energy, respectively. MBE is computed using poses within 2 Å of the Lowest Binding energy pose

	BOX1		**BOX2**	
LIGAND	**LBE**	**MBE**	**LBE**	**MBE**
49	-4.39	-3.86	-5.45	-4.57
50	-3.68	-2.43	-4.81	-3.75
51	-3.25	-3.25	-6.16	-5.00
52	-2.86	-2.30	-4.87	-3.97
53	-3.19	-2.16	-4.88	-3.83
54	-2.84	-2.39	-5.30	-4.46
55	-6.25	-5.56	-6.25	-6.08
56	-4.31	-3.24	-5.52	-4.13
57	-4.40	-3.78	-5.64	-4.75
58	-6.94	-5.67	-7.57	-6.24
59	-7.36	-6.67	-7.05	-6.21

According to computational results, compounds **51**, **55**, **58** and **59** are predicted to have the highest affinity for the protein, followed by compounds **49**, **54**, **56** and **57**. In docking experiments carried out sampling the protein region labeled as BOX1 (Figure 57), molecules **55**, **57**, **58** and **59** were found to bind in the same pocket hosting the IP4 ligand (referred to as pocket 1 hereafter). Compounds **50**, **54** and **56** are predicted to bind in a pocket partially overlapping the binding site of the natural ligand (referred to as pocket 2), whereas, as discussed above, molecules **49**, **51**, **52**, and **53** are predicted to bind in a novel pocket not superimposed to the phosphoinositide-binding site (pocket 3). When docking calculations were carried out sampling the protein portion labeled as

BOX2, all ligands were found to bind to the same pocket, which essentially correspond to pocket 3 of the BOX1 series of calculations (see Figure 58). Notably, pocket 3 is sufficiently close to the natural ligand binding site to suggest that the interaction between the tested ligands and the protein might indirectly affect binding of the natural ligands. All molecules except molecule **59** show better docking scores for the BOX2 binding site. However, molecules **55**, **58** and **59** show very similar affinity for both BOX1 and BOX2 sites. In addition, the analysis of docking results shows that molecules featuring higher hydrophobic character have significantly higher affinity for pocket 3, an observation that can be easily rationalized since this binding site presents hydrophobic aminoacids (see interactions maps; Figures 59 and 60).

Some other details of docking calculations are noteworthy. The phosphoinositide-binding site, which is particularly rich of polar aminoacids (Lys^{14}, Asn^{53}, Asn^{54}, Arg^{86}), interacts strongly with the polar R and R' groups of molecule **59** (Figure H). Molecules **51** and **54** show the highest docking score differences when comparing results obtained sampling BOX1 and BOX2. In fact, molecules **51** and **54** are characterized by the less hydrophilic and bulkiest substituents in the R position. The binding site identified sampling the BOX2 region presents a number of hydrophobic aminoacids (Ile^{74}, Val^{83}, Ile^{84}) that can interact with hydrophobic ligand substituents. However, the strongest interactions between ligand and Akt-PH domain have electrostatic nature, in fact docking experiments highlighted strong interactions of tested molecules with Arg^{15}, Glu^{17}, Lys^{20}, Glu^{85} (see Figure 60).

In light of docking results, four molecules, which are predicted to bind to the three different binding pockets, have been selected and synthesized, and a preliminary *in vitro* biological inhibition assay has been carried out.

Figure 57: Inositol-(1,3,4,5)-tetrakisphosphate (green); ligands **49**, **51**, **52**, **53** (blue); ligands **50**, **54**, **56** (white); ligands **55**, **57**, **58**, **59** (red)

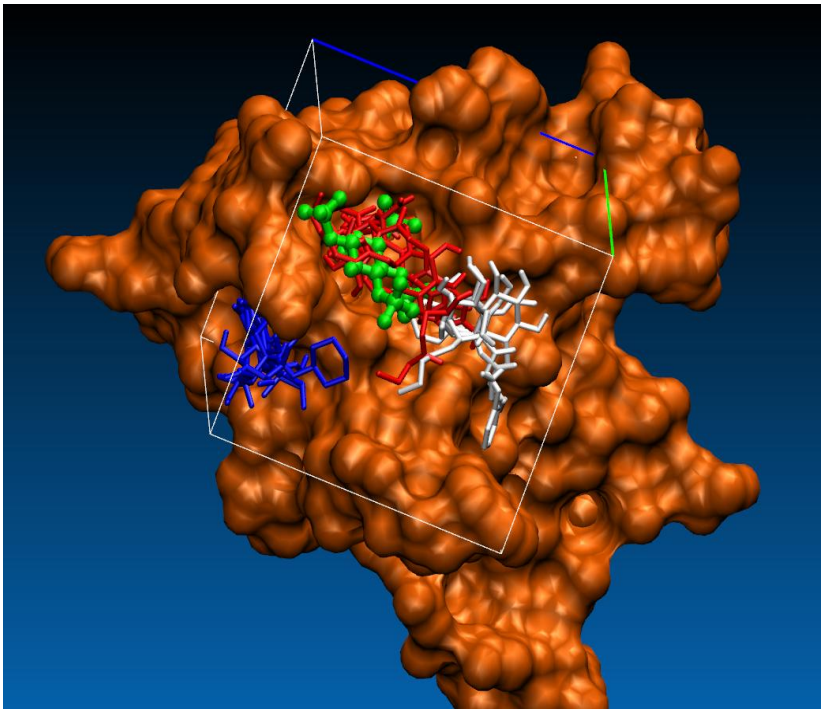

Figure 58: Blue: ligands **49** - **55**; Green: inositol-(1,3,4,5)-tetrakisphosphate.

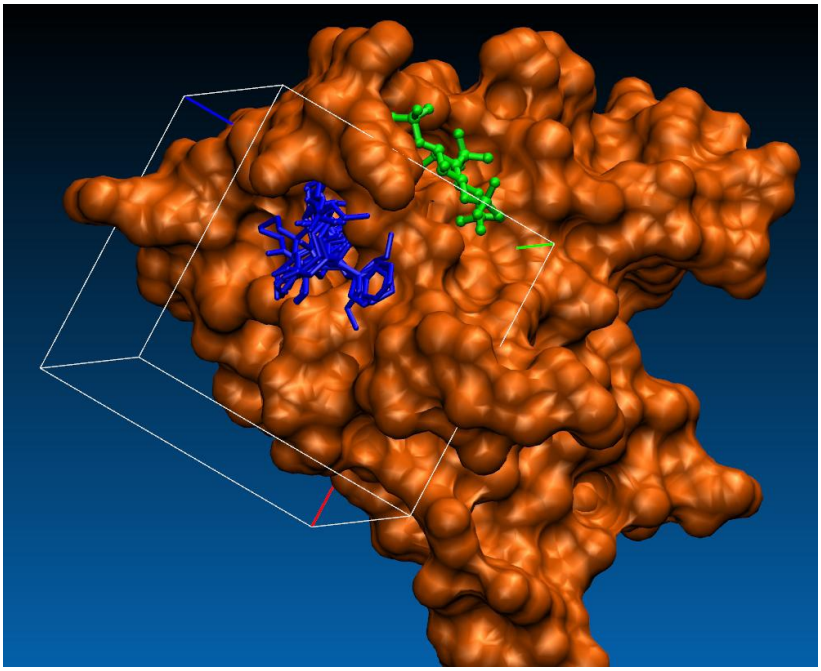

Figure 59: Map of interactions of molecule **59** with the protein, as obtained by docking calculations carried out sampling the protein region labeled as BOX1.

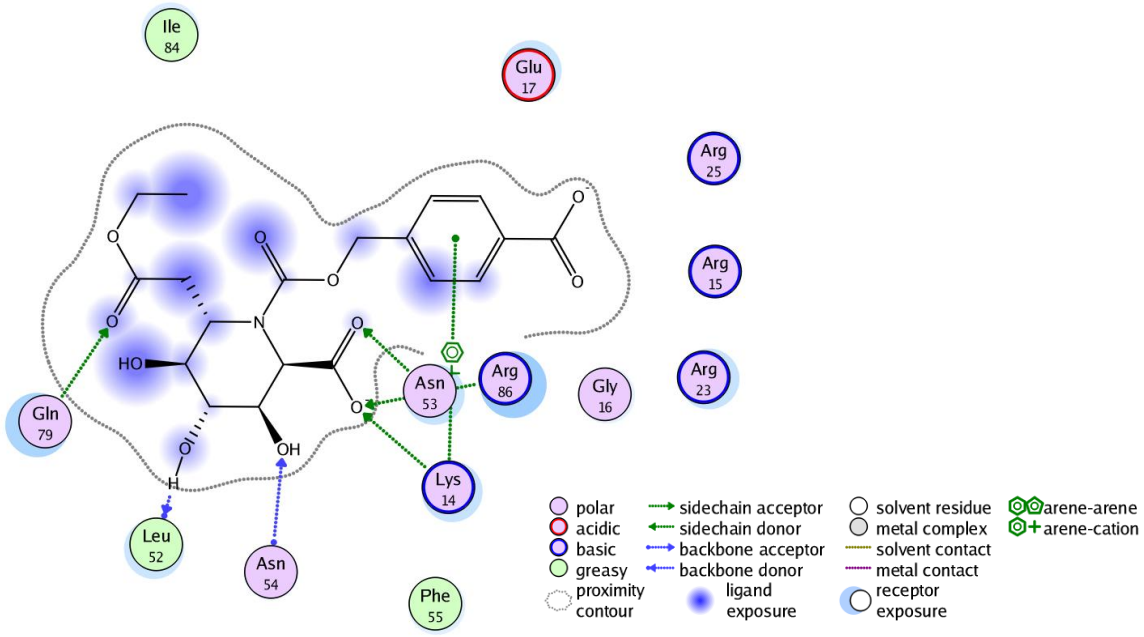

Figure 60: Map of interactions of molecule **58** with the protein, as obtained by docking calculations carried out sampling the protein region labeled as BOX1.

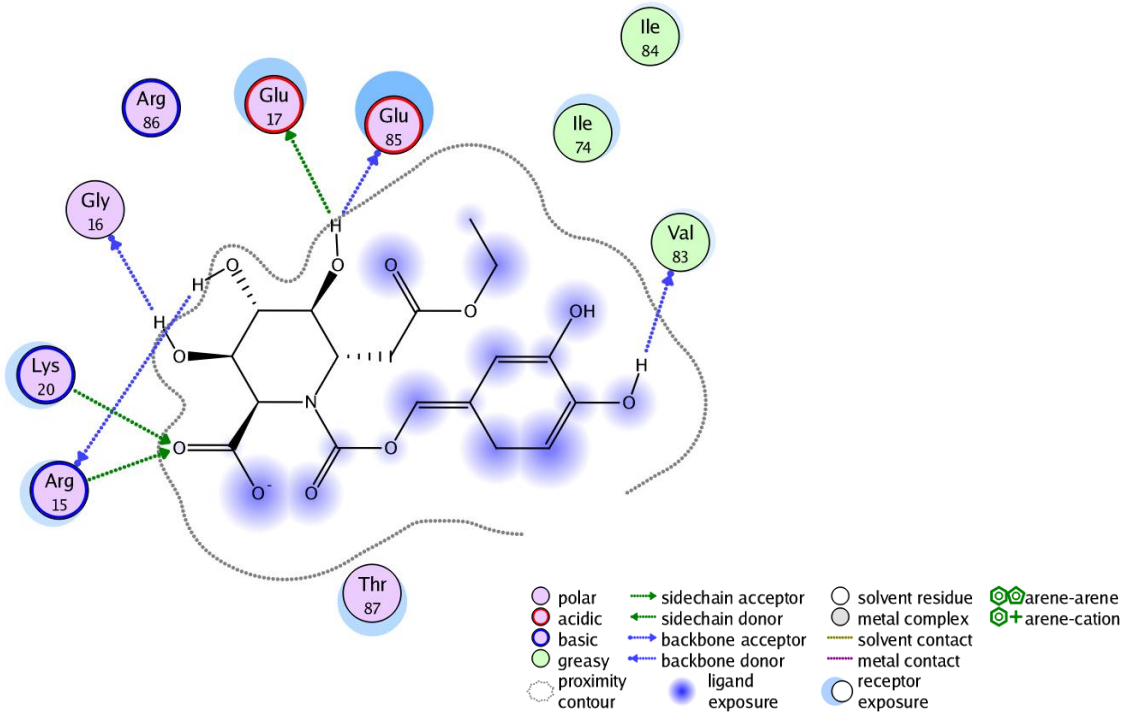

In order to explore the different binding sites identified by the computational study, we planned to synthesize selected compounds and to carry out an *in vitro* preliminary biological inhibition assay. Compounds **51** and **55** were selected from the group with the highest affinity for the protein and also as representatives of the groups of compounds that bind pockets 3 and 1, respectively. Compound **49** was also selected to evaluate pocket 3, with the second highest affinity in the group of compounds binding to this pocket. Compound **50** was selected to evaluate the biological activity of the group of compounds that bound to pocket 2 in the computational experiments. The reason for this choice is the lowest binding affinity of **50** that resulted from the experiment in BOX 2, corresponding to the binding to pocket 3. Therefore compound **50** have the lowest probability to bind pocket 3, which raises the probability to bind to pocket 2. Even though the highest affinities were obtained by compounds **58** and **59**, the difficulty to purchase commercially available starting materials for their synthesis hampered their preparation.

The synthesis was designed in order to obtain all the target compounds from a common precursor, (Figures 61 and 62) which could be differently functionalized on the ring nitrogen and selectively oxidized at the primary OH. Commercially available tetrabenzylglucose was reduced to the diol **60**, which was protected at the primary hydroxyl. In order to obtain the correct stereochemistry at C6 of the target molecules, inversion of configuration was achieved through a Mitzunobu reaction with concomitant introduction of the azido function, precursor of the ring nitrogen (compound **62**). Removal of the TBDPS group and oxidation of the free OH afforded aldehyde **64**. The introduction of the carboxymethyl moiety was done exploiting a nucleophilic attack of ethyl acetate derived enolate on aldehyde **64**, this reaction afforded azido alcohol **65** as an inseparable diastereoisomeric mixture in an approximate S/R 2:1 ratio, determined on the final cyclised products by NMR, as described below. Reduction of the azido function and cyclization through an intramolecular Mitzunobu reaction led to the desired iminosugar scaffold **67**.

Figure 61: Synthesis of the common precursor of target compounds **49**, **50**, **51** and **55**

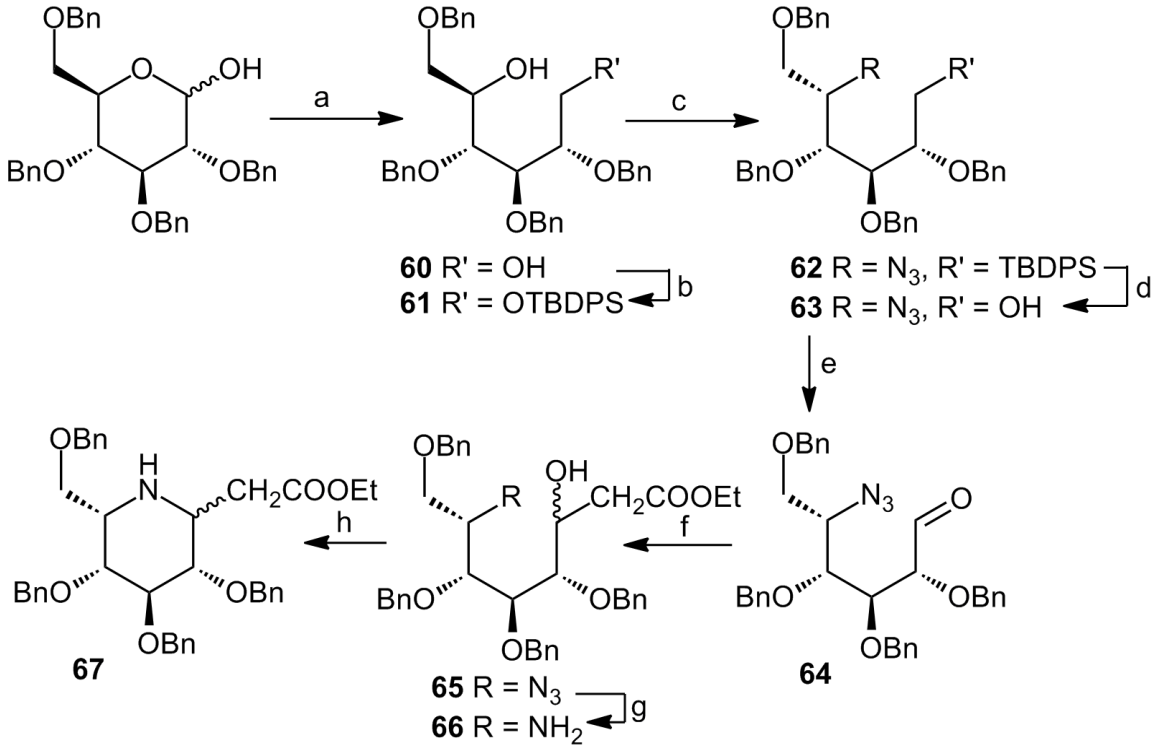

Reagents and conditions: a) $NaBH_4$, CH_2Cl_2/EtOH 1:1, 48h, quantitative; b) Imidazole, TBDPSiCl, CH_2Cl_2, 1h, 97%; c) PPh_3, DIAD, DPPA, THF, 2h, 75%; d) TBAF 1M, THF, 3h, 90%; e) Dess-Martin periodinane, CH_2Cl_2, 40 min, 79%; f) DIPA, *t*-BuLi 1M, AcOEt, THF, 1h, 95%; g) Lindlar catalyst/C, H_2, AcOEt, overnight, 86%; h) PPh_3, DIAD, THF, overnight, 70%.

The first member of the library was obtained by deprotection of **67** through a catalytic hydrogenation ($Pd(OH)_2$/C, H_2). Target compound **49** was efficiently separated by flash chromatography from the minor isomer (Figure 62). Compound **55** was obtained directly from pure compound **49**. First, the ring nitrogen was functionalised as a carboxybenzylcarbamate (CbzCl, $NaHCO_3$, MeOH), then the primary hydroxyl was selectively oxidized to the corresponding carboxylic acid (TEMPO, KBr, NaOCl 5%, H_2O) affording compound **55** in a 21% overall yield. The synthesis of derivative **50** and **51** was carried out by reductive amination on precursor **67** with propionaldehyde and cyclohexanecarboxyaldehyde respectively, followed by catalytic hydrogenation. This time the diastereoisomeric mixtures were

efficiently separated before the deprotection step, resulting in pure compounds **69** and **70**.

Figure 62: Synthesis of target compounds **49**, **50**, **51** and **55** from the common precursor **67**

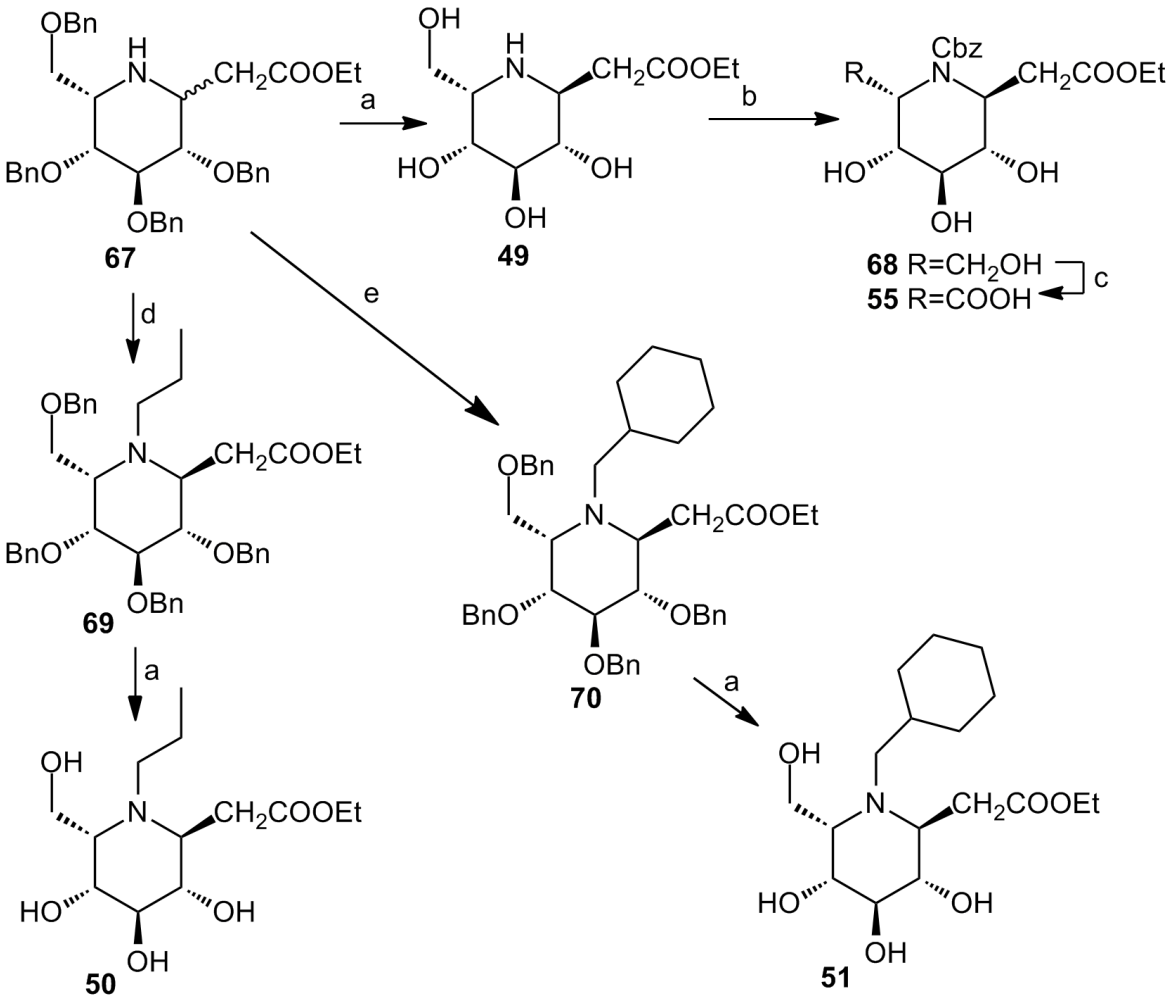

Reagents and conditions: a) $Pd(OH)_2/C$, CH_3COOH, H_2, MeOH, overnight, 67% (**49**), quantitative (**50** and **51**), ; b) CBZCl, $NaHCO_3$, MeOH, overnight, 25%; c) TEMPO, KBr, NaOCl 5%, H_2O, 4h, 84%; d) propionaldehyde, CH_3COOH, Na_2SO_4, $Na(OAc)_3BH$, 1,2-dichloroethane, overnight, 52% (major isomer); e) cyclohexanecarboxyaldehyde, CH_3COOH, Na_2SO_4, $Na(OAc)_3BH$, 1,2-dichloroethane, overnight, 79%.

The stereochemistry at the C2 carbon was determined, as said previously, on the deprotected compounds. As illustrative example, we report the NMR values of the coupling constants of compound **49** (major isomer) (Figure 63). The values ($J_{3,2}$ = 8.7, $J_{4,3}$ = 8.7, Hz) are indicative for a *trans*-diaxial disposition of the protons,

which, thus, indicates a $^4C_1$ conformation; moreover, the diaxial disposition of C(2)-H/C(3)-H allows us to determine the absolute (*S*) configuration of the C(2) center.

Figure 63: NMR values of the coupling constants of compound **49**

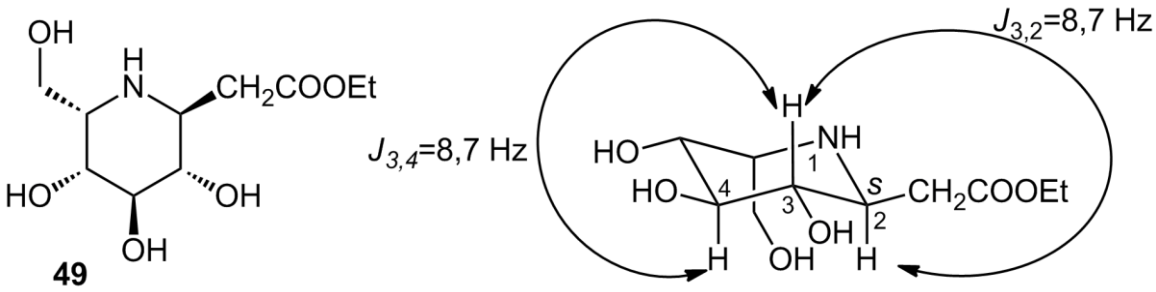

3.4.1. Preliminary biological evaluation of target compounds

In order to investigate the ability of compounds **49**, **50**, **51** and **55** to inhibit the enzyme Akt, these compounds were gently tested in collaboration with Prof. Barbara Costa (from our institution), using the Akt Activity Assay Kit® (Assay Designs, Inc.). The results are presented in figure 64.

Figure 64: Percentage of inhibition of Akt observed for the target iminosugar-based compounds, tested in two different concentrations: 100 and 700 μM

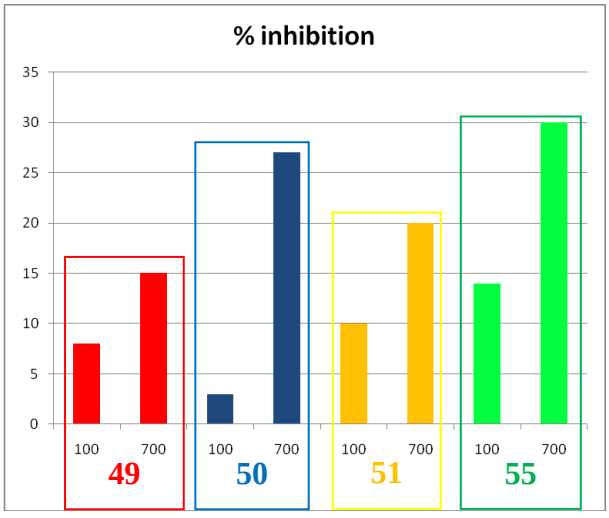

Compound **49** presented low inhibitory activity (8-15%) in both concentrations (100 and 700 μM). Compounds **50**, at the highest concentration, and **51** showed better inhibitory activities than **49**. The best inhibitor was compound **55**, which exerted the highest inhibitory activities (up to 30% of inhibition) in both concentrations tested. These results provided some insight into the structure/activity relationships: the presence of a hydrophobic group bound to the nitrogen atom (compounds **50**, **51** and **55**) proved to enhance the inhibitory activity. The concomitant use of the *N*-bound hydrophobic group and an axial carboxylic group in compound **55** resulted in a further enhancement. In addition, the carboxymethylene group showed to function as an efficient surrogate of the phosphate moiety of PIP_2. Bioactive product **55** was considered a promising lead compound for the development of new and more powerful Akt inhibitors.

Some accordance between theoretical and experimental results is reported, as demonstrated by **55**. When compared to the other target compounds **49**, **50** and **51**, compound **55** displayed the best binding affinities in computational studies and the best inhibitory activity from *in vitro* experiments.

Conclusions

4.1. Design and synthesis of GRP mimetics

The aim of this part of my Ph.D. work was the preliminary study of ligands for the GRP receptor, for their potential as carrier molecules able to deliver therapeutic drugs to cancer cells. From the studies performed on non-peptide GRP mimetics, some important remarks are noteworthy. The work performed on the 3D structure of the C-terminal decapeptide of GRP and the GRP agonist peptide allowed us to design compounds that exhibited structural similarity to the Gastrin-Releasing Peptide, which was demonstrated by computational methods.

We suggest that the structural similarity of our compounds could be associated to functional similarity, as demonstrated by the antagonist behaviour exerted by compound **17** on prostate carcinoma cells that overexpress the GRP receptor. It is important to mention that the structure-based *de novo* design performed in this work allowed us to obtain a potentially bioactive compound in preliminary attempts, which is at least notable. The achievement of detectable biological activity with nanomolar concentrations of **17** indicates its potential as a candidate lead compound for further development of a new ligands for the GRP receptor.

In addition, considering that compound **17** was designed from a template based on the helical conformation of GRP, some support to this receptor-binding conformation of GRP can be stated.

The result that compound **48**, a structural analog of **17**, also displays the same antagonist behaviour enhances the evidence that the structural similarity of our compounds could be translated in functional similarity.

However, further biological experiments are needed to confirm their biological activity and also to evaluate their potential as carrier molecules for tumor

drug targeting. These experiments are currently in progress, as demonstrated for Elk-1 activation in PC-3 cells.

Optimization of the synthetic strategies to access the target compounds in higher yields proved to be more difficult than expected. Nonetheless, our current efforts are concentrated in the search for better synthetic procedures, as demonstrated for the last synthetic strategy using a carboxylic acid derivative of the indole group.

4.2. Design and synthesis of iminosugar-based Akt inhibitors

The potential of the proto-oncogenic Akt kinase for cancer therapy prompted us to design and produce iminosugar-based analogues of phosphatidyl inositol phosphates (PIP_2 and PIP_3) as prospective Akt inhibitors. In collaboration with Prof. Luca De Gioia a small library of iminosugar derivatives was evaluated by docking experiments carried out sampling a protein region corresponding to the phosphoinositide-binding site of Akt. Four prospective compounds were selected and synthesized.

We developed a synthetic procedure composed by high-yielding reactions. The synthesis was designed in order to obtain all the target compounds from a common precursor, which could be differently functionalized on the ring nitrogen and selectively oxidized at the primary OH.

Biological evaluation showed that our compounds exerted low to moderate inhibitory activity for Akt. The structural variability of the small library of compounds demonstrated that the presence of hydrophobic groups bound to the nitrogen atom of the iminosugar tend to enhance the inhibitory activity. Therefore, our suggestion to exploit the hydrophobic characteristics of the cleft close to the natural ligand binding site was supported by experimental results.

In addition, the best inhibitory activity observed for compound **55**, with an axial carboxyl group, gives support to the interaction with Arg^{25} in the PH domain, which in previous studies was shown to be one of the key protein residues involved in the interaction with PIP ligands. We suggest that this compound should be used for further development of Akt inhibitors.

Experimental procedures

5.1. Computational studies

Molecular modeling of GRP10 and the agonist [Glp^{6},Phe^{13},Leu^{14}-NH_2]bombesin(6-14) was performed on the ChemBio3D Ultra (ChemBioOffice Ultra version 12.0), using the MM2[113] force field. Initial peptide structures were prepared using ChemBioDraw and transferred to ChemBio3D. Dihedral angles φ and ψ reported in the studies of Prakash[87] and Malikayl[92] (Table 2), were inserted in the measurement table as the optimal dihedral angles for GRP10 and the peptide agonist, respectively. The energy of each peptide was minimized using the default molecular mechanics calculations (MM2 force field), with a minimum RMS gradient of 0.100. This procedure provided the minimized conformation of the peptides in accordance with the reference papers.

The same procedure was performed for the molecular modeling of the potential GRP mimetics presented in this work, except by the use of dihedral angles.

The 3D pharmacophore template was assembled from the superimposition of both peptides. This procedure was performed by overlaying the centroids of the most important pharmacophores of both peptides in the following pairs: the indole groups of both GRP10 and the peptide agonist, the C-terminal imidazole groups of both peptides, the N-terminal imidazole group of GRP10 and the pyrrolidone group of the peptide agonist, the isobutyl group of GRP10 and the phenyl group of the peptide agonist. The pharmacophore pairs were superimposed using an overlay feature of ChemBio3D that optimize the superimposition with energy minimization without changing the dihedral angles. After the overlay, the 3D pharmacophore template was generated by making visible just the peptide pharmacophores, while peptide backbones and other side-chains were hidden. The same procedure was used for scaffold hopping.

5.2. Chemistry

General remarks: All solvents were dried with molecular sieves, for at least 24 h prior to use. Thin layer chromatography (TLC) was performed on silica gel 60 F_{254} plates (Merck) with detection using UV light when possible, or by charring with a solution of concd. H_2SO_4/EtOH/H_2O (10:45:45) or a solution of $(NH_4)_6Mo_7O_{24}$ (21 g), $Ce(SO_4)_2$ (1 g), concd. H_2SO_4 (31 mL) in water (500 mL). Flash column chromatography was performed on silica gel 230-400 mesh (Merck). ^{1}H and ^{13}C NMR spectra were recorded at 25 °C with a Varian Mercury 400 MHz instrument using $CDCl_3$ as the solvent unless otherwise stated. Chemical shift assignments, reported in ppm, are referenced to the corresponding solvent peaks. Mass spectra were recorded with a MALDI2 Kompakt Kratos instrument, using gentisic acid (DHB) as the matrix. Optical rotations were measured at room temperature using a Krüss P3002 electronic polarimeter and are reported in units of 10^{-1} deg·cm^2·g^{-1}.

5.2.1. Synthesis of the scaffold

1-(α-D-Galactopyranosyl)-2-propene (3) was synthesized according to the reference paper.[116]

(2*S*/*R*,3a*R*,5*R*,6*R*,7*S*,7a*R*)-5-hydroxymethyl-2-iodomethyl-hexahydrofuro[3,2-*b*]pyran-6,7-diol (4): to a solution of **3** (8.0 g, 38.6 mmol) in DMF (6 mL), NIS (13.0 g, 57.9 mmol) was added. After stirring for 1.5h, the solvent was evaporated *in vacuo*. Purification by flash chromatography (AcOEt) afforded compound **4** (11.7 g, 91%) as a mixture of isomers. ^{1}H-NMR (7:3 mixture of diastereomers, asterisks denote resonances from minor anomer, atom numbers in accordance to the reference paper,[116] 400 MHz, CD_3OD): δ = 4.57–4.52 [m, H(3a), H(3a*)], 4.19–4.13 [m, H(2*)], 4.15–4.07 [m, H(2)], 3.97–3.95 [dd, *J* = 3.0, 4.0 Hz, H(6)], 3.96–3.95 [m, H(6*)], 3.94–3.91 [dd, *J* = 4.5, 5.3 Hz, H(7a)], 3.92–3.87 [m, H(7a*), H(7), H(7*)], 3.83–3.76 [m, H(5), H(5*), C*H*OH, C*H*OH*], 3.70–3.66 (dd, *J* = 3.8, 11.9 Hz, C*H*OH*), 3.69–3.65 (dd, *J* = 3.8, 11.6 Hz, C*H*OH), 3.36–3.33 (m, C*H*I, C*H*I*), 2.31–2.24 [m, H(3)], 2.23–2.18 [ddd, *J* = 2.6, 6.4 Hz, H(3*)], 1.97–1.90 [ddd, *J* =

4.2, 5.9 Hz, H(3)], 1.86–1.79 [m, H(3*)] ppm. MS-ESI: *m/z* 331.0 $[M+H]^+$ calcd. $C_9H_{16}IO_5$ 331.0037.

(2*S*/*R*,3a*R*,5*R*,6*R*,7*S*,7a*R*)-2-azidomethyl-5-hydroxymethyl-hexahydrofuro[3,2-*b*] pyran-6,7-diol (5): to a stirred solution of **4** (7.1 g, 21.6 mmol) in DMF (5 mL) was added NaN_3 (2.8 g, 43.3 mmol). The reaction mixture was stirred overnight at 100°C, then the solvent was evaporated. Purification by flash chromatography (CH_2Cl_2/ethanol 15:1) afforded compound **5** (3.6 g, 68%) as a mixture of isomers. ^{1}H-NMR (7:3 mixture of anomers, asterisks denote resonances from minor anomer, atom numbers in accordance to the reference paper,[116] 400 MHz, D_2O): *δ* = 4.54–4.48 [m, H(3a), H(3a*)], 4.32–4.48 [m, H(2*)],4.14–4.06 [m, H(2)], 3.99–3.96 [dd, *J* = 5.2, 6.7 Hz, H(7a)], 3.84–3.52 [m, H(5), H(6), H(7), C*H*$_2$OH, H(5*), H(6*), H(7*), H(7a*), C*H*$_2$OH*], 3.46–3.40 (m, C*H*N_3, C*H*N_3*), 3.28–3.15 (m, C*H*N_3, C*H*N_3*), 2.12–2.02 [m, H(3), H(3*)], 1.88–1.78 [m, 2 H, H(3), H(3*)] ppm. MS-ESI: *m/z* 268.1 $[M+H]^+$ calcd. $C_9H_{16}IO_5$ 268.0904.

5.2.2. Synthesis of building blocks

3-(bromomethyl)-1-(*tert*-butoxycarbonyl)indole (6): building block **6** was synthesized from indole-3-carboxaldehyde by the procedure of Schollkopf and co-workers.[117]

3-(2-bromoethyl)-1-(*tert*-butoxycarbonyl)indole (6'): this building block was obtained from 3-(2-hydroxyethyl)indole in two steps according to the procedure described by Yang and colleagues.[127]

1-benzyl-indole-3-carboxylic acid (40): building block **40** was produced from indole-3-carboxaldehyde by the method described by Battaglia and co-workers.[128]

4-(hydroxymethyl)-1-trityl-imidazole (14): compound **14** was synthesized from 4-(hydroxymethyl)imidazole according to the procedure of Tanaka and co-workers.[129]

4-(chloromethyl)-1-trityl-imidazole (7): synthesized from compound **14** by the procedure of Peng and co-workers.[130]

4-(bromomethyl)-1-trityl-imidazole (22): building block **22** was produced from compound **14** using the procedure described by Abecassis and colleagues.[131]

Yields, NMR spectra and spectrometric data were in accordance to the data reported by the reference papers.

5.2.3. Synthesis of GRP mimetics

In order to better describe ^{1}H-NMR chemical shift assignments, proton numbers used in this topic are expressed according to figure 31.

(4a*R*,5a*R*,7*R*,8a*R*,9*R*,9a*R*)-7-(azidomethyl)-2-phenyloctahydrofuro[2',3':5,6] pyrano[3,2-d][1,3]dioxin-9-ol (18): to a solution of compound **5** (3.60 g, 14.7 mmol) in dry DMF (20 mL) under argon, camphorsulfonic acid (1.36 g, 5.9 mmol) and benzaldehyde dimethylacetal (2.64 mL, 17.6 mmol) were added. The reaction mixture was taken to 70°C under vacuum, stirring for 30 min. Then, it was neutralized with triethylamine and the solvent was removed *in vacuo*. Compound **18** (3.24 g, 66%) was purified by flash chromatography (petroleum ether/ethyl acetate 3:7 → 2:8). ^{1}H-NMR (400 MHz, $CDCl_3$) δ = 7.48-7.42 (m, 2H, *H*Ar), 7.41-7.34 (m, 3H, *H*Ar), 5.52 (s, C*H*Ph), 5.03 [dt, *J* = 7.7, 4.0 Hz, H(1)], 4.37 [t, *J* = 2.6 Hz, H(5)], 4.34 [s, H(6a)], 4.13-4.10 [m, H(2')], 4.08 [d, *J* = 2.1 Hz, H(6b)], 3.99-3.95 [m, H(2)], 3.90 [dd, *J* = 5.6, 2.5 Hz, H(3)], 3.70 [s, H(4)], 3.47 [q, *J* = 4.2 Hz, H(3'a)], 3.31 [dd, *J* = 12.9, 5.8 Hz, H(3'b)], 2.29 [dt, *J* = 14.5, 7.3 Hz, H(1'a)], 1.86 [ddd, *J* = 13.7, 7.0, 3.5 Hz, H(1'b)]. MS-ESI: *m/z* 356.3 $[M+Na]^+$ calcd. $C_{16}H_{19}N_3O_5Na$ 356.3

(4a*R*,5a*R*,7*R*,8a*R*,9*R*,9a*R*)-7-(aminomethyl)-2-phenyloctahydrofuro[2',3':5,6] pyrano[3,2-d][1,3]dioxin-9-ol (19): a catalytic amount of Lindlar catalyst was added to a solution of compound **18** (0.81 g, 2.4 mmol) in ethyl acetate (7 mL) under argon. The reaction mixture was submitted to catalytic hydrogenation. After 15h stirring the reaction mixture was filtered and evaporated to dryness to obtain compound **19** (0.75 g, quantitative) as a white powder. ^{1}H-NMR (400 MHz, $CDCl_3$) δ = 7.49-7.42 (m, 2H, *H*Ar), 7.42-7.31 (m, 3H, *H*Ar), 5.49 (s, C*H*Ph), 5.03-4.99 [m, H(1)], 4.33 [d, *J* = 4.5 Hz, H(6a)], 4.30 (d, *J* = 3.9 Hz, H(5), 4.06 [d, *J* = 12.8 Hz, H(6b)], 3.99 – 3.85 [m, H(2), H(2')], 3.74 [dd, *J* = 11.6, 4.0 Hz, H(3)], 3.65 [s, H(4)], 3.01-2.78 [m, H(3'a), H(3'b)], 2.31-2.21 [m, H(1'a)], 1.72-1.63 [m, H(1'b)]. MS-ESI: *m/z* 308.2 $[M+H]^+$ calcd. $C_{16}H_{22}NO_5$ 308.3

***N*-(((4a*R*,5a*R*,7*R*,8a*R*,9*R*,9a*R*)-9-hydroxy-2-phenyloctahydrofuro[2',3':5,6] pyrano[3,2-d][1,3]dioxin-7-yl)methyl)benzamide (20):** a solution of **19** (1.90 g, 6.2 mmol) and triethylamine (2.59 mL, 18.6 mmol) in dry methanol (16 mL) was taken to 0°C. Then, benzoyl chloride (1.44 mL, 12.4 mmol) was added dropwise. The reaction mixture was left to reach room temperature, and after stirring for 30 min the solvent was removed under vacuum. Flash chromatography (petroleum ether/ethyl acetate 3:7 → 2:8) afforded compound **20** (2.28 g, 90%). ^{1}H-NMR (400 MHz, $CDCl_3$) δ = 7.81 (s, Ar*H*), 7.79 (s, Ar*H*), 7.50-7.35 (m, 8H, Ar*H*), 5.52 (s, C*H*Ph), 5.05 [dt, *J* = 7.4, 3.6 Hz, H(1)], 4.36 [s, H5)], 4.35 [d, *J* = 9.1 Hz, H(6b)], 4.24-4.14 [m, H(2')], 4.09 [dd, *J* = 12.7, 2.1 Hz, H(6b)], 3.97 [t, *J* = 5.0 Hz, H(2)], 3.87 [dd, *J* = 5.3, 2.6 Hz, H(3)], 3.83 [dd, *J* = 6.1, 2.8 Hz, H(3'a)], 3.62 [s, H(4)], 3.54-3.45 [m, H(3'b)], 2.39 [dt, *J* = 14.4, 7.4 Hz, H(1'a)], 1.84 [ddd, *J* = 14.0, 6.9, 3.3 Hz, H(1'b)]. MS-ESI: *m/z* 412.4 $[M+H]^+$ calcd. $C_{23}H_{26}NO_6$ 412.4

***N*-(((4a*R*,5a*R*,7*R*,8a*S*,9*R*,9a*S*)-2-phenyl-9-((1-trityl-1*H*-imidazol-4-yl)methoxy) octahydrofuro[2',3':5,6]pyrano[3,2-d][1,3]dioxin-7-yl)methyl)benzamide (21): method A:** NaH 60% in mineral oil (49.0 mg, 1.2 mmol) was added portion wise to a stirred solution of compound **20** (75.2 mg, 0.18 mmol) in DMF (2 mL) at 0°C. After 10 min, building block **7** (85.3 mg, 0.24 mmol) was added, and it was stirred for 2.5h. The reaction was quenched with methanol (~1 mL), 10 min later it was diluted with CH_2Cl_2 and washed twice with H_2O. The organic layer was dried with Na_2SO_4, filtered and evaporated to dryness. Compound **21** (31.2 mg, 23%) was purified by flash chromatography (petroleum ether/AcOEt 2:8). **Method B:** to a solution of **20** (0.46 g, 1.1 mmol) in dry DMF (6 mL) at 0°C, NaH 60% in mineral oil (133 mg, 3.3 mmol) was added in 3 portions during 30 min. After stirring for 30 min, a solution of **22** (894 mg, 2.2 mmol) in dry DMF (6 mL) was added. The reaction mixture was left to reach room temperature, stirring for 20h. Then, it was quenched with methanol (2 mL) and the solvent was evaporated *in vacuo*. Flash chromatography (petroleum ether/ethyl acetate 2:8 → ethyl acetate/methanol 19:1) afforded compound **21** (189 mg, 23%). ^{1}H-NMR (400 MHz, $CDCl_3$) δ = 7.84-7.76 (m, 3H, Ar*H*), 7.47-7.28 (m, 17H, Ar*H*), 7.12-7.05 (m, 6H, Ar*H*), 6.87 (s, 1H, Ar*H*), 5.45 (s, C*H*Ph), 5.16-5.09 [m, H(1)], 4.79 [d, *J* = 12.5 Hz, OC*H*Imid.), 4.70 (d, *J* = 12.8 Hz, OC*H*Imid.), 4.37-4.29 [m, H(5), H(6a)], 4.27-4.21 [m, H(2')], 4.17

[d, *J* = 4.6 Hz, H(2)], 4.07 [s, H(6b)], 3.86 [d, *J* = 3.4 Hz, H(3)], 3.61 [s, H(4)], 3.51-3.40 [m, H(3'a), H(3'b)], 2.43-2.30 [m, H(1'a)], 1.90-1.77 [m, H(1'b)]. MS-ESI: *m/z* 734.5 $[M+H]^+$ calcd. $C_{46}H_{44}N_3O_6$ 734.9

***N*-(((2*R*,3a*R*,5*R*,6*S*,7*S*,7a*S*)-7-((1*H*-imidazol-4-yl)methoxy)-6-hydroxy-5-(hydroxymethyl)hexahydro-2*H*-furo[3,2-b]pyran-2-yl)methyl)benzamide (16):** trifluoroacetic acid (1 mL) was added slowly to a stirred solution of **21** (182 mg, 0.25 mmol) in dichloromethane (4 mL). After 30 min the solvent was removed under reduced pressure. Compound **16** (65.7 mg, 66%) was purified by flash chromatography (ethyl acetate/ methanol 85:15 → ethyl acetate/methanol/acetic acid 60:40:2). ^{1}H-NMR (400 MHz, CD_3OD) δ = 8.28 (s, 1H, Ar*H*), 8.10 (s, 1H, Ar*H*), 7.86-7.80 (m, 2H, Ar*H*), 7.57-7.41 (m, 7H, Ar*H*), 7.24 (s, 3H, Ar*H*), 4.61 (s, OCH_2Imid.), 4.59-4.53 [m, H(1)], 4.23 [dd, *J* = 12.5, 6.4 Hz, H(2')], 4.17-4.13 [m, H(4)], 3.98 [t, *J* = 4.8 Hz, H(2)], 3.92-3.79 [m, H(5), H(6a)], 3.71-3.63 [m, H(3), H(6b)], 3.63-3.55 [m, H(3'a), H(3'b)], 2.36-2.23 [m, H(1'a)], 1.94-1.81 [m, H(1'b)]. MS-ESI: *m/z* 404.3 $[M+H]^+$ calcd. $C_{20}H_{26}N_3O_6$ 404.4

***N*-(((2*R*,3a*R*,5*R*,6*S*,7*S*,7a*S*)-6-hydroxy-7-((1-trityl-1*H*-imidazol-4-yl)methoxy)-5-((trityloxy)methyl)hexahydro-2*H*-furo[3,2-b]pyran-2-yl)methyl)benzamide (23):** compound **16** (41.2 mg, 0.10 mmol) was dissolved in dry pyridine (2 mL). Trityl chloride (113.9 mg, 0.41 mmol) and 4-(dimethylamino)pyridine (2.5 mg, 0.02 mmol) were added and the mixture was stirred overnight at 50°C. Compound **23** (67.8 mg, 42%) was purified by flash chromatography (ethyl acetate). ^{1}H-NMR (400 MHz, $CDCl_3$) δ = 8.05-7.90 (m, 1H, Ar*H*), 7.68-7.45 (m, 7H, Ar*H*), 7.39-7.24 (m, 15H, Ar*H*), 7.24-7.09 (m, 12H, Ar*H*), 7.09-6.95 (m, 2H, Ar*H*), 4.97-4.83 [m, H(1)], 4.77 (d, *J* = 11.6 Hz, OC*H*Imid.), 4.73-4.65 [m, H(2')], 4.60 (d, *J* = 11.8 Hz, OC*H*Imid.), 4.31 [s, H(6a)], 4.27 [t, *J* = 6.5 Hz, H(2)], 4.20-4.10 [m, H(5)], 4.05 [d, *J* = 6.8 Hz, H(6b)], 4.02-3.84 [m, H(4)], 3.86-3.57 [m, H(3), H(3'a), H(3'b)], 2.20-2.10 [m, H(1'a)], 1.80-1.72 [m, H(1'b)]. MS-ESI: *m/z* 888.4 $[M+H]^+$ calcd. $C_{58}H_{54}N_3O_6$ 888.4

***tert*-butyl 3-((((2*R*,3a*R*,5*R*,6*S*,7*S*,7a*S*)-2-(benzamidomethyl)-7-((1-trityl-1*H*-imidazol-4-yl)methoxy)-5-((trityloxy)methyl)hexahydro-2*H*-furo[3,2-b]pyran-6-yl)oxy)methyl)-1*H*-indole-1-carboxylate (24):** to a solution of **23** (41.1 mg, 0.046 mmol) in dry DMF (1 mL) at 0°C, NaH 60% in mineral oil (5.6 mg, 0.139 mmol)

was added. After stirring for 30 min, building block **6** (43.1 mg, 0.139 mmol) was added. The reaction mixture was left to reach room temperature, stirring for 4.5h. Then, it was quenched with water (1 mL). The crude was diluted with water, followed by extraction with ethyl acetate. The organic phase was dried over Na_2SO_4 and evaporated *in vacuo*. Flash chromatography (petroleum ether/ethyl acetate 1:1 → acetate) afforded compound **24** (10.7 mg, 21%). ^{1}H-NMR (400 MHz, $CDCl_3$) δ = 8.10-7.95 (m, 1H, Ar*H*), 7.67-7.56 (m, 3H, Ar*H*), 7.55-7.44 (m, 4H, Ar*H*), 7.40 (dd, *J* = 7.6, 2.8 Hz, 2H, Ar*H*), 7.39-7.24 (m, 17H, Ar*H*), 7.24-7.09 (m, 13H, Ar*H*), 7.09-6.95 (m, 2H, Ar*H*), 5.24 (s, OC*H*$_2$Indole), 4.96-4.80 [m, H(1)], 4.75 (d, *J* = 11.7 Hz, OC*H*Imid.), 4.72-4.63 [m, H(2')], 4.59 (d, *J* = 11.9 Hz, OC*H*Imid.), 4.24 [s, H(6a)], 4.24 [t, *J* = 6.7 Hz, H(2)], 4.18-4.09 [m, H(5)], 4.05 [d, *J* = 7.1 Hz, H(6b)], 4.00-3.89 [m, H(4)], 3.88-3.67 [m, H(3), H(3'a)], 3.67-3.50 [m, H(3'b)], 2.27-2.14 [m, H(1'a)], 1.75-1.64 [m, H(1'b)], 1.57 (s, 9H, C*H*$_3$). MS-ESI: *m/z* 1117.7 $[M+H]^+$ calcd. $C_{72}H_{69}N_4O_8$ 1117.5

***N*-(((2*R*,3a*R*,5*R*,6*S*,7*S*,7a*S*)-7-((1*H*-imidazol-4-yl)methoxy)-6-((1*H*-indol-3-yl) methoxy)-5-(hydroxymethyl)hexahydro-2*H*-furo[3,2-b]pyran-2-yl)methyl) benzamide (17):** compound **24** (9.7 mg, 0.0087 mmol) was dissolved in dichloromethane (2 mL). Silica gel saturated with HCl (200 mg) was added and the solvent was removed under vacuum. The solvent-free reaction mixture was stirred at 80°C, *in vacuo*, overnight. Then, at room temperature, it was suspended in methanol (5 mL), acidified with acetic acid (0.1 mL) and filtered. This procedure was repeated 4 times. The solvent was removed under reduced pressure, followed by flash chromatography (AcOEt/methanol/water/acetic acid 80:20:10: 5) to afford pure compound **17** (1.0 mg, 22%). ^{1}H-NMR (400 MHz, CD_3OD) δ = 7.70 (s, 1H, Ar*H*), 7.53-7.32 (m, 7H, Ar*H*), 7.31-7.19 (m, 2H, Ar*H*), 7.14 (d, *J* = 6.9 Hz, 1H, Ar*H*), 7.03 (s, 1H, Ar*H*), 5.49 (s, OC*H*Indole), 5.33 (s, OC*H*Indole), 4.61 (s, OCH_2Imidazole), 4.56-4.44 [m, H(1)], 4.36-4.23 [m, H(2')], 3.95-3.93-3.77 [m, H(2), H(6a)], 3.77-3.61 (m, H(3), H(4), H(5), H(6b)] 3.61-3.47 [m, H(3'a), H(3'b)], 2.18 [dd, *J* = 14.2, 6.8 Hz, H(1'a)], 1.81-1.69 [m, H(1'b)]. MS-ESI: *m/z* 533.3 $[M+H]^+$ calcd. $C_{29}H_{33}N_4O_6$ 533.2

4-((((4a*R*,5a*R*,7*R*,8a*S*,9*R*,9a*S*)-7-(azidomethyl)-2-phenyloctahydrofuro[2',3':5, 6]pyrano[3,2-d][1,3]dioxin-9-yl)oxy)methyl)-1-trityl-1*H*-imidazole (27): NaH

60% in mineral oil (0.448 g, 11.2 mmol) was added portion wise to a stirred solution of compound **17** (0.557 g, 1.67 mmol) in DMF (10 mL) at 0°C. After 10 min, building block **7** (0.719 g, 2.0 mmol) was added, and it was stirred for 0.5h. The reaction was quenched with methanol (~1 mL) and 10 min later it was evaporated to dryness. Compound **17** (0.955 g, 87%) was purified by flash chromatography (petroleum ether/AcOEt 3:7 → 2:8). ^{1}H-NMR (400 MHz, $CDCl_3$) δ = 7.49 (s, 1H, Ar*H*), 7.46-7.38 (m, 2H, Ar*H*), 7.37-7.28 (m, 12H, Ar*H*), 7.17-7.08 (m, 6H, Ar*H*), 6.93 (s, 1H, Ar*H*), 5.45 (s, C*H*Ph), 5.18 [t, *J* = 4.6 Hz, H(1)], 4.79 (d, *J* = 12.7 Hz, OC*H*Imid.), 4.67 (d, *J* = 12.7 Hz, OC*H*Imid.), 4.52 [s, H(5)], 4.37 [dd, *J* = 5.4, 4.1 Hz, H(2)], 4.33 [d, *J* = 12.9 Hz, H(6a)], 4.26 [dt, *J* = 9.7, 4.8 Hz, H(2'), 4.07 [dd, *J* = 12.7, 1.9 Hz, H(6b)], 3.72 [dd, *J* = 5.5, 1.5 Hz, H(3)], 3.61 [s, H(4)], 3.32 [dd, *J* = 12.9, 3.7 Hz, H(3'a)], 3.14 [dd, *J* = 12.9, 5.2 Hz, H(3'b)], 2.02 [dd, *J* = 14.0, 6.0 Hz, H(1'a)], 1.88 [ddd, *J* = 13.5, 9.7, 5.5 Hz, H(1'b)]. MS-ESI: *m/z* 656.3 $[M+H]^+$ calcd. $C_{39}H_{38}N_5O_5$ 656.3

(2*R*,3a*R*,5*R*,6*S*,7*S*,7a*S*)-7-((1*H*-imidazol-4-yl)methoxy)-2-(azidomethyl)-5-(hydroxyl methyl)hexahydro-2*H*-furo[3,2-b]pyran-6-ol (28): trifluoroacetic acid (1 mL) was added slowly to a stirred solution of **27** (0.954 g, 1.45 mmol) in dichloromethane (4 mL). After 30 min the solvent was removed under reduced pressure. Compound **28** (0.411 g, 87%) was purified by flash chromatography (ethyl acetate/ methanol 9:1 → 8:2). ^{1}H-NMR (400 MHz, CD_3OD) δ = 8.35 [s, *H*(2)Imid,], 7.35 [s, *H*(5)Imid.], 4.74 (s, OCH_2Imid.), 4.62-4.57 [m, H(1)], 4.39-4.32 [m, H(2')], 4.17 [t, *J* = 4.6 Hz, H(2)], 4.16-4.13 [m, H(4)], 3.87-3.79 [m, H(6a), H(5)], 3.67 [dd, *J* = 8.1, 8.1 Hz, H(6b)], 3.61 [dd, *J* = 5.4, 2.3 Hz, H(3)], 3.43 [dd, *J* = 13.0, 3.2 Hz, H(3'a)], 3.27-3.24 [m, H(3'b)], 2.08 [ddd, *J* = 13.3, 6.5, 2.8 Hz, H(1'a)], 1.88 [ddd, *J* = 13.5, 8.4, 6.2 Hz, H(1'b)]. MS-ESI: *m/z* 326.3 $[M+H]^+$ calcd. $C_{13}H_{20}N_5O_5$ 326.3

***tert*-butyl 4-((((2*R*,3a*R*,5*R*,6*S*,7*S*,7a*S*)-2-(azidomethyl)-5-(((*tert*-butyldiphenyl silyl)oxy)methyl)-6-hydroxyhexahydro-2*H*-furo[3,2-b]pyran-7-yl)oxy)methyl)-1*H*-imidazole-1-carboxylate (29):** compound **28** (93.0 mg, 0.286 mmol) was dissolved in methanol/dioxane/H_2O 6:1:4 (4.4 mL). Then, TEA (0.24 mL, 1.70 mmol) and di-*tert*-butyl-dicarbonate (0.449 g, 2.06 mmol) were added. After 2.5h the solvent was evaporated *in vacuo* and the *N*-Boc-protected compound (71.8

mg, 60%) was purified by flash chromatography (AcOEt). Afterwards, the compound was dissolved in DMF (1 mL), and imidazole (8.2 mg, 0.12 mmol) was added, followed by the slow addition of TBDPSiCl (15.4 µL, 0.06 mmol). After 3h stirring, the reaction was quenched with methanol (0.5 mL) and the solvent was evaporated *in vacuo*. Flash chromatography (petroleum ether/AcOEt 1:1) afforded pure compound **29** (28.9 mg, 80%). ^{1}H-NMR (400 MHz, $CDCl_3$) δ = 8.05 (s, 1H, Ar*H*), 7.73-7.65 (m, 4H, Ar*H*), 7.46-7.32 (m, *7*H, Ar*H*), 4.75 (d, *J* = 12.8 Hz, OC*H*Imid.), 4.53 (d, *J* = 12.6 Hz, OC*H*Imid.), 4.47-4.37 [m, H(1), H(2')], 4.33-4.28 [m, H(5)], 4.17 [t, *J* = 4.4 Hz, H(2)], 4.02-3.94 [m, H(4), H(6a)], 3.87 [dd, *J* = 12.4, 8.7 Hz, H(6b)], 3.67 [dd, *J* = 4.8, 2.4 Hz, H(3)], 3.47 [dd, *J* = 13.0, 3.6 Hz, H(3'a)], 3.20 [dd, *J* = 12.9, 5.0 Hz, H(3'b)], 1.99 [ddd, *J* = 13.3, 6.2, 1.8 Hz, H(1'a)], 1.88-1.79 [m, H(1'b)], 1.62 (s, 9H, *t*Bu), 1.26 (s, 9H, *t*Bu). MS-ESI: *m/z* 644.8 $[M+H]^+$ calcd. $C_{34}H_{46}N_5O_7Si$ 664.8

***tert*-butyl 3-((((2*R*,3a*R*,5*R*,6*S*,7*S*,7a*S*)-2-(azidomethyl)-7-((1-(*tert*-butoxy carbonyl)-1*H*-imidazol-4-yl)methoxy)-5-(((*tert*-butyldiphenylsilyl)oxy)methyl) hexahydro-2*H*-furo[3,2-b]pyran-6-yl)oxy)methyl)-1*H*-indole-1-carboxylate (30):** compound **29** (92.1 mg, 0.14 mmol) and building block **6** (129.1 mg, 0.42 mmol) were dissolved in THF (2 mL). Then, NaH 60% in mineral oil (11.1 mg, 0.28 mmol) was added portion wise. After 2h stirring, the reaction was quenched with water (1 mL) and evaporated to dryness. Purification by flash chromatography afforded a product that was expected to be compound **30**, but the structure characterization revealed that it consisted in a by-product (68.2 mg, 55%). ^{1}H-NMR did not reveal the definitive structure of by-product. ESI-MS showed *m/z* 793.7 which reveals Boc protection loss, while for expected product calcd. $C_{48}H_{61}N_6O_9Si$ 893.4

(2*R*,3a*R*,5*R*,6*S*,7*S*,7a*S*)-2-(azidomethyl)-7-((1-trityl-1*H*-imidazol-4-yl)methoxy)-5-((trityloxy)methyl)hexahydro-2*H*-furo[3,2-b]pyran-6-ol (33a): compound **28** (0.25 g, 0.77 mmol), TrtCl (1.71 g, 6.15 mmol) and DMAP (28.2 mg, 0.23 mmol) were dissolved in pyridine (10 mL). The reaction mixture was warmed to 50-60°C and stirred for 7.5h. Then, the solvent was evaporated *in vacuo*, and compound **33a** (0.212 g, 34%) was purified by flash chromatography (petroleum ether/AcOEt 3:7 → 2:8 → AcOEt). ^{1}H-NMR (400 MHz, $CDCl_3$) δ = 7.52-7.45 (m, 5H, Ar*H*), 7.39-

7.31 (m, 9H, Ar*H*), 7.31-7.17 (m, 11H, Ar*H*), 7.16-7.07 (m, 6H, Ar*H*), 6.81 (s, 1H, Ar*H*), 4.72 (d, *J* = 12.6 Hz, OC*H*Imid.), 4.52 (d, *J* = 12.4 Hz, OC*H*Imid.), 4.45-4.37 [m, H(1)], 4.28-4.23 [m, H(4)], 4.10-4.03 [m, H(2'), H(5)], 3.96 [t, *J* = 4.6 Hz, H(2)], 3.64 [d, *J* = 3.8 Hz, H(3)], 3.51 [dd, *J* = 10.1, 7.8 Hz, H(3'a)], 3.39-3.34 [m, H(6a), H(6b)], 3.27 [dd, *J* = 10.1, 4.8 Hz, H(3'b)], 2.28-2.15 [m, H(1'a)], 1.83 [ddd, *J* = 13.2, 6.1, 2.8 Hz, H(1'b)]. MS-ESI: *m/z* 810.7 $[M+H]^+$ calcd. $C_{51}H_{48}N_5O_5$ 810.9

(2*R*,3a*R*,5*R*,6*S*,7*S*,7a*S*)-2-(azidomethyl)-5-(((*tert*-butyldiphenylsilyl)oxy) methyl)-7-((1-trityl-1*H*-imidazol-4-yl)methoxy)hexahydro-2*H*-furo[3,2-b]pyran-6-ol (33b): to a solution of compound **28** (85.5 mg, 0.26 mmol) in DMF (1 mL), TEA (55 µL, 0.39 mmol) was added. After 10 min stirring, TrtCl (87.9 mg, 0.32 mmol) was added and the reaction mixture was stirred overnight. Then, the reaction was quenched with water (1 mL) and after 10 min the solvent was evaporated *in vacuo*. Flash chromatography (AcOEt/methanol 19:1 → 9:1) afforded the *N*-trityl-protected compound (93.0 mg, 62%). This reaction was repeated in a larger scale. Afterwards, the product of both reactions was dissolved in dry CH_2Cl_2 (3 mL). Imidazole (141 mg, 2.08 mmol) and TBDPSiCl (0.29 mL, 1.13 mmol) were added. After 2.5h the reaction mixture was quenched with methanol (~1 mL), evaporated to dryness, diluted with H_2O, and extracted with CH_2Cl_2. The organic layer was dried with Na_2SO_4, filtered, and then the solvent was evaporated *in vacuo*. Purification by flash chromatography (petroleum ether/AcOEt/methanol 70:30:1 → 40:60:1) afforded pure compound **33b** (0.254 g, 22%). ^{1}H-NMR (400 MHz, $CDCl_3$) δ = 7.75-7.67 (m, 3H, Ar*H*), 7.45-7.27 (m, 17H, Ar*H*), 7.17-7.07 (m, 6H, Ar*H*), 6.74 (s, 1H, Ar*H*), 4.54 (d, *J* = 12.7 Hz, OC*H*Imid.), 4.48 [dt, *J* = 12.5, 6.2 Hz, H(1)], 4.38 (d, *J* = 12.6 Hz, OC*H*Imid.), 4.02-3.95 [m, H(2), H(2')], 3.88 [dd, *J* = 4.9, 2.7 Hz, H(3)], 3.85-3.81 [m, H(4)], 3.78-3.69 [m, H(5), H(6a), H(6b)], 3.20 [dd, *J* = 12.7, 6.6 Hz, H(3'a)], 3.14 [dd, *J* = 12.6, 4.7 Hz, H(3'b)], 2.11 [dt, *J* = 14.1, 7.1 Hz, H(1'a)], 1.65 [ddd, *J* = 13.5, 6.3, 3.4 Hz, H(1'b)], 1.08 (s, 9H, *t*Bu). MS-ESI: *m/z* 806.6 $[M+H]^+$ calcd. $C_{48}H_{52}N_5O_5Si$ 806.4

***tert*-butyl 3-((((2*R*,3a*R*,5*R*,6*S*,7*S*,7a*S*)-2-(azidomethyl)-7-((1-trityl-1*H*-imidazol-4-yl)methoxy)-5-((trityloxy)methyl)hexahydro-2*H*-furo[3,2-b]pyran-6-yl)oxy) methyl)-1*H*-indole-1-carboxylate (34a):** to a solution of building block **6** (60.1 mg, 0.20 mmol) in DMF (2 mL) at 0°C, a solution of compound **33a** (53.0 mg,

0.065 mmol) in THF (2 mL) was added dropwise. After stirring overnight, the reaction was quenched with methanol (0.5 mL) and after 0.5h evaporated to dryness. Flash chromatography (petroleum ether/AcOEt/ methanol 70:30:1) afforded partially purified compound **34a** (9.5 mg, 14% partially purified). Due to the degree of contamination of **34a** with by-products, interpretation of ^{1}H-NMR spectra was not clear. MS-ESI: *m/z* 1039.7 $[M+H]^+$ calcd. $C_{65}H_{63}N_6O_7$ 1039.5

(3a*R*,5*R*,6*S*,7*S*,7a*S*)-7-(allyloxy)-2-(azidomethyl)-5-(hydroxymethyl)hexahydro-2*H*-furo[3,2-b]pyran-6-ol (37): a solution of compound **5** (1.17 g, 4.76 mmol) and Bu_2SnO (1.30 g, 5.24 mmol) in toluene (50 mL) were refluxed overnight with a Dean-Starck apparatus for azeotropic removal of water. Then, the reaction mixture was cooled to room temperature, and TBAI (1.76 g, 4.76 mmol) and allyl bromide (0.60 mL, 7.14 mmol) were added. The reaction mixture was refluxed and stirred for 5.5h, when the solvent was evaporated *in vacuo*. Purification by flash chromatography (petroleum ether/AcOEt 2:8) afforded pure compound **37** (0.91 g, 67%). ^{1}H-NMR (400 MHz, CD_3OD) δ = 5.96 (ddd, *J* = 22.8, 10.8, 5.6 Hz, OCH_2CHCH_2), 5.32 (dd, *J* = 17.3, 1.7 Hz, OCH_2CHCH), 5.16 (dd, *J* = 10.4, 1.3 Hz, OCH_2CHCH), 4.54 [dt, *J* = 6.5, 4.4 Hz, H(1)], 4.22-4.16 (m, OCH_2CHCH_2), 4.16-4.09 [m, H(2'), H(4)], 3.96 [t, *J* = 5.1 Hz, H(2)], 3.87-3.78 [m, H(5), H(6a)], 3.67 [dd, *J* = 10.5, 3.0 Hz, H(6b)], 3.57 [dd, *J* = 5.5, 2.6 Hz, H(3)], 3.38-3.29 [m, H(3'a), H(3'b)], 2.21 [dt, *J* = 13.9, 7.2 Hz, H(1'a)], 1.83 [ddd, *J* = 13.4, 6.7, 4.1 Hz, H(1'b)]. MS-ESI: *m/z* 286.1 $[M+H]^+$ calcd. $C_{12}H_{20}N_3O_5$ 286.1

(2*R*,3a*R*,5*R*,6*S*,7*S*,7a*S*)-7-(allyloxy)-2-(azidomethyl)-5-(((*tert*-butyldiphenyl silyl)oxy)methyl)hexahydro-2*H*-furo[3,2-b]pyran-6-ol (38): compound **37** (0.96 g, 3.37 mmol) was dissolved in dry CH_2Cl_2 (3 mL). Imidazole (0.50 g, 7.40 mmol) and TBDPSiCl (0.95 mL, 3.70 mmol) were added. After 1h the reaction mixture was quenched with methanol (1 mL), evaporated to dryness, diluted with H_2O, and extracted three times with CH_2Cl_2. The organic layer was dried with Na_2SO_4, filtered, and then the solvent was evaporated *in vacuo*. Purification by flash chromatography (petroleum ether/AcOEt 8:2) afforded compound **38** (1.05 g, 60%) as a pure diastereoisomer. ^{1}H-NMR (400 MHz, $CDCl_3$) δ = 7.73-7.65 (m, 4H, Ar*H*), 7.48-7.35 (m, 6H, Ar*H*), 5.96 (ddd, *J* = 16.0, 10.9, 5.7 Hz, OCH_2CHCH_2), 5.31 (dd, *J* = 16.5, 2.3 Hz, OCH_2CHCH), 5.20 (dd, *J* = 10.4, 1.3 Hz, OCH_2CHCH), 4.50-4.42

[m, H(1)], 4.31-4.23 [m, H(4), OC*H*CHCH$_2$], 4.20-4.05 [m, H(2'), OC*H*CHCH$_2$], 4.02-3.90 [m, H(2), H(5), H(6a)], 3.84 [dd, *J* = 9.7, 5.5 Hz, H(6b)], 3.60 [dd, *J* = 5.0, 2.6 Hz, H(3)], 3.40-3.28 [m, H(3'a), H(3'b)], 2.69 (d, *J* = 2.8 Hz, O*H*), 2.20-2.10 [m, H(1'a)], 1.73 [ddd, *J* = 13.6, 6.4, 3.3 Hz, H(1'b), 1.06 (s, 9H, *t*Bu). MS-ESI: *m/z* 524.3 $[M+H]^+$ calcd. $C_{28}H_{38}N_3O_5Si$ 524.3

***tert*-butyl 3-(2-(((2*R*,3a*R*,5*R*,6*S*,7*S*,7a*S*)-7-(allyloxy)-2-(azidomethyl)-5-(((*tert*-butyldiphenylsilyl)oxy)methyl)hexahydro-2*H*-furo[3,2-b]pyran-6-yl)oxy)ethyl)-1*H*-indole-1-carboxylate (39a):** to a solution of compound **38** (43.2-54.0 mg, 0.082-0.10 mmol) in DMF (1 mL) at 0°C, different equivalents of NaH 60% in mineral oil (5.0-16.5 mg, 0.12-0.41 mmol) were added. After 20 min stirring, building block **6'** (40.1-134.0 mg, 0.12-0.41 mmol) was added alone or in the presence of a catalytic amount of TBAI. For every condition tested, the expected product was not found after 24h and work-up.

(2*R*,3a*R*,5*R*,6*S*,7*R*,7a*S*)-7-(allyloxy)-2-(azidomethyl)-5-(((*tert*-butyldiphenyl silyl)oxy)methyl)hexahydro-2*H*-furo[3,2-b]pyran-6-yl-1-benzyl-1*H*-indole-3-carboxylate (39b): to a solution of **38** (54.5 mg, 0.10 mmol) and building block **40** (28.8 mg, 0.11 mmol) in CH_2Cl_2 (3 mL), EDC (21.9 mg, 0.11 mmol) and DMAP (6.3 mg, 0.05 mmol) were added. The reaction mixture was refluxed for 24h, then it was poured into water (30 mL) and washed three times with CH_2Cl_2 (30 mL). The organic layers were mixed, dried with Na_2SO_4, filtered and the solvent was evaporated *in vacuo*. Purification by flash chromatography (petroleum ether/AcOEt/methanol 93:7:2) afforded compound **39b** (46.5 mg, 60%). ^{1}H-NMR (400 MHz, $CDCl_3$) δ = 8.08 (dd, *J* = 6.0, 2.6 Hz, 1H, Ar*H*), 7.75 (s, 1H, Ar*H*), 7.69-7.64 (m, 2H, Ar*H*), 7.54 (s, 1H, Ar*H*), 7.52 (s, 1H, Ar*H*), 7.44-7.20 (m, 10H, Ar*H*), 7.16-7.05 (m, 4H, Ar*H*), 5.93-5.80 [m, H(4), OCH$_2$C*H*CH$_2$], 5.34 (s, OC*H*$_2$Ph), 5.25 (dd, *J* = 17.3, 1.6 Hz, OCH$_2$CHC*H*), 5.11 (dd, *J* = 10.5, 1.4 Hz, OCH$_2$CHC*H*), 4.51-4.40 [m, H(1), H(2')], 4.28-4.20 [m, *J* = 5.1 Hz, H(5), OC*H*CHCH$_2$], 4.20-4.09 [m, H(2), OC*H*CHCH$_2$], 3.98-3.86 [m, H(6a), H(6b)], 3.77 [dd, *J* = 5.1, 2.7 Hz, H(3)], 3.53 [dd, *J* = 12.9, 3.7 Hz, H(3'a)], 3.25 [dd, *J* = 12.9, 4.6 Hz, H(3'b)], 2.05 [dd, *J* = 13.8, 5.7 Hz, H(1'a)], 1.96-1.85 [m, H(1'b)], 1.00 (s, 9H, *t*Bu). MS-ESI: *m/z* 756.3 $[M+H]^+$ calcd. $C_{44}H_{48}N_4O_6Si$ 756.3

((4a*R*,5a*R*,7*R*,8a*S*,9*R*,9a*S*)-2-phenyl-9-((1-trityl-1*H*-imidazol-4-yl)methoxy)octahydro-furo[2',3':5,6]pyrano[3,2-d][1,3]dioxin-7-yl)methanamine (46): to a solution of compound **27** (25.0 mg, 0.038 mmol) in AcOEt (5 mL), a catalytic amount of Lindlar catalyst was added and the reaction mixture was stirred under H_2 overnight. The catalyst was filtered through a Celite pad (eluent AcOEt) and the solvent was evaporated *in vacuo* to afford compound **46** (22.1 mg, 92%) which was used directly without purification and further characterization.

5-(dimethylamino)-*N*-(((4a*R*,5a*R*,7*R*,8a*S*,9*R*,9a*S*)-2-phenyl-9-((1-trityl-1*H*-imidazol-4-yl)methoxy)octahydrofuro[2',3':5,6]pyrano[3,2-d][1,3]dioxin-7-yl) methyl)naphthalene-1-sulfonamide (47): to a solution of compound **46** (22.1 mg, 0.035 mmol) in CH_2Cl_2 (3 mL), TEA (6 µL, 0.042 mmol) and dansyl chloride (10.4 mg, 0.039 mmol) were added. After 2h stirring, the solvent was evaporated and purification by flash chromatography (AcOEt) afforded compound **47** (11.7 mg, 40%). ^{1}H-NMR (400 MHz, $CDCl_3$) δ = 8.43 [d, *J* = 8.5 Hz, Ar*H*(dansyl)], 8.21 [d, *J* = 8.6 Hz, Ar*H*(dansyl)], 8.12 [d, *J* = 7.1 Hz, Ar*H*(dansyl)], 7.48-7.17 (m, 17H, Ar*H*), 7.11-6.98 (m, 7H, Ar*H*), 6.79 [s, H(5'')Imid.], 5.83 (s, N*H*), 5.33 (s, C*H*Ph), 4.96-4.91 [m, H(1)], 4.60 (d, *J* = 12.2 Hz, OC*H*Imid.), 4.52 (d, *J* = 12.4 Hz, OC*H*Imid.) 4.37-4.33 [m, H(5)], 4.24-4.16 [m, H(2), H(6a)], 4.12-4.06 [m, H(2')], 3.95 [d, *J* = 12.0 Hz, H(6b)], 3.54 [d, *J* = 4.3 Hz, H(3)], 3.46-3.43 [m, H(4)], 3.09-2.98 [m, H(3'a)], 2.81-2.75 [m, H(3'b), N(CH_3)$_2$(dansyl)], 1.78 [dd, *J* = 13.4, 5.3 Hz, H(1'a)], 1.69-1.58 [m, H(1'b)]. MS-ESI: *m/z* 863.3 $[M+H]^+$ calcd. $C_{51}H_{51}N_4O_7S$ 863.3

***N*-(((4a*R*,5a*R*,7*R*,8a*S*,9*R*,9a*S*)-9-((1*H*-imidazol-4-yl)methoxy)-2-phenylocta-hydrofuro[2',3':5,6]pyrano[3,2-d][1,3]dioxin-7-yl)methyl)-5-(dimethylamino) naphthalene-1-sulfonamide (48):** to a solution of compound **47** (11.7 mg, 0.014 mmol) in CH_2Cl_2 (2 mL), silica gel (200 mg) was added. The solvent was evaporated *in vacuo* and the reaction mixture was heated to 100°C and stirred for 48h. Then, at room temperature, it was suspended in methanol (5 mL), acidified with acetic acid (0.1 mL) and filtered. This procedure was repeated 4 times. The solvent was removed under reduced pressure, followed by flash chromatography (AcOEt → AcOEt/methanol 9:1) to afford pure compound **48** (3.0 mg, 36%). ^{1}H-NMR (600 MHz, MeOD) δ = 8.55 [d, *J* = 8.5 Hz, Ar*H*(dansyl)], 8.38 [d, *J* = 8.7 Hz, Ar*H*(dansyl)], 8.22 [dd, *J* = 7.3, 1.1 Hz, Ar*H*(dansyl)], 7.70 [s, H(2')Imid.], 7.60-7.56

[m, 2H, Ar*H*(dansyl)], 7.45-7.42 (m, *J* = 7.3 Hz, 2H, Ar*H*), 7.41-7.34 (m, 3H, Ar*H*), 7.23 [d, *J* = 7.5 Hz, Ar*H*(dansyl)], 7.08 [s, H(5')Imid.], 5.51 (s, C*H*Ph), 4.92-4.89 [m, H(1)], 4.59 (d, *J* = 12.3 Hz, OC*H*Imid.), 4.54 (d, *J* = 12.2 Hz, OC*H*Imid.), 4.46-4.43 [m, H(5)], 4.19 [d, *J* = 11.9 Hz, H(6a)], 4.14-4.07 [m, H(2'), H(6b)], 3.96 [dd, *J* = 5.7, 4.5 Hz, H(2)], 3.59-3.55 [m, H(4)], 3.53 [dd, *J* = 5.9, 1.8 Hz, H(3)], 3.11 [dd, *J* = 14.0, 4.3 Hz, H(3'a)], 3.01 [dd, *J* = 14.0, 5.3 Hz, H(3'b)], 2.85 (s, N(CH_3)$_2$(dansyl)], 1.84 [ddd, *J* = 13.3, 5.7, 1.5 Hz, H(1'a)], 1.68 [ddd, *J* = 13.4, 9.3, 5.9 Hz, H(1'b)]. MS-ESI: *m/z* 621.3 $[M+H]^+$ calcd. $C_{32}H_{37}N_4O_7S$ 621.2

5.2.4. Synthesis of iminosugar-based Akt inhibitors

2,3,4,6-tetra-*O*-benzyl-D-glucitol (60): $NaBH_4$ (420 mg, 11.09 mmol) was added to a stirred solution of 2,3,4,6-tetra-*O*-benzyl-D-glucopyranose (2.00 g, 3.70 mmol) in CH_2Cl_2/EtOH 1:1 (20 mL). After 48 h the solvent was evaporated *in vacuo* and the solid was treated with Na_2CO_3 (10 mL satd. solution), stirring for 10 min. The reaction mixture was diluted with CH_2Cl_2, washed with distd. water, dried with Na_2SO_4 and filtered. The solvent was evaporated *in vacuo* to afford compound **60** (2.01 g, quantitative) as a colorless syrup. $[\alpha]_D^{20}$ = +3.1 (*c* = 1.2, $CHCl_3$). ^{1}H-NMR: δ = 3.60 [dd, *J* = 11.9, 4.8, 1H, 1a-H], 3.64-3.72 [m, 2H, 6a,b-H], 3.77 [dd, *J* = 11.9, 4.3, 1H, 1b-H], 3.80-3.86 [m, 2H, 2-H, 4-H], 3.94 [dd, *J* = 6.2, 3.6, 1H, 3-H], 4.06-4.10 [m, 1H, 5-H], 4.54 (d, *J* = 11.9, 1H, C*H*Ph), 4.57-4.59 (m, 2H, C*H*Ph), 4.63 (d, *J* = 11.4, 1H, C*H*Ph), 4.66 (d, *J* = 11.5, 1H, C*H*Ph), 4.69 (d, *J* = 11.2, 1H, C*H*Ph), 4.70 (d, *J* = 11.5, 1H, C*H*Ph), 4.75 (d, *J* = 11.2, 1H, C*H*Ph), 7.20-7.40 (m, 20H, *H*Ar). ^{13}C-NMR: δ = 62.2 [C(1)], 71.1 [C(5)], 71.5 [C(6)], 73.4, 73.6, 73.8, 74.9 (4 *C*H_2Ph), 77.7, 79.4, 79.8 [C(2), C(3), C(4)], 128.0-128.7 (*C*HAr), 138.0, 138.1, 138.2, 138.4 (*C*qAr). MS-ESI: *m/z* = 543.2757 $[M+H]^+$, calcd. for $C_{34}H_{38}O_6$ = 542.2668.

2,3,4,6-tetra-*O*-benzyl-1-*O*-*tert*-butyldiphenylsilyl-D-glucitol (61): compound **60** (2.00 g, 3.68 mmol) was dissolved in dry CH_2Cl_2 (12mL) under argon. Imidazole (550 mg, 8.10 mmol) and TBDPSiCl (1.04 mL, 4.05 mmol) were added. After 1 h the reaction mixture was quenched with methanol (0.5 mL), diluted with H_2O, and extracted with CH_2Cl_2. The organic layer was dried with Na_2SO_4, filtered, and then

the solvent was evaporated *in vacuo*. Purification by flash chromatography (petroleum ether/ethyl acetate 8:2) afforded pure compound **61** (2.79 g, 97%). $[\alpha]_D^{25}$ = +12.8 (*c* = 1.0, $CHCl_3$). ^{1}H-NMR: δ = 1.08 [s, 9H, C(C*H*$_3$)$_3$], 2.97 (d, *J* = 4.9, 1H, O*H*), 3.62-3.64 [m, 2H, 6a,b-H], 3.76-4.03 [m, 6H, 1a,b-H, 2-H, 3-H, 4-H, 5-H], 4.48-4.59 (m, 5H, 5 C*H*Ph), 4.64-4.70 (m, 3H, 3 C*H*Ph), 7.20-7.80 (m, 30H, *H*Ar). ^{13}C-NMR: δ = 19.7 [*C*(CH$_3$)$_3$], 27.3 [C(*C*H$_3$)$_3$], 63.5, 71.6 [C(1), C(6)], 71.4 [C(5)], 73.4, 73.6, 73.7, 74.6 (4 *C*H$_2$Ph), 77.8, 78.3, 79.9 [C(2), C(3), C(4)], 127.8-129.9 (*C*HAr), 133.5, 133.6 (*C*qAr), 135.8 (*C*HAr), 138.3, 138.3, 138.4, 138.6 (4 *C*qAr). MS-ESI: *m/z* = 781.3900 $[M+H]^+$, calcd. for $C_{50}H_{56}O_6Si$ = 780.3846.

5-azido-2,3,4,6-tetra-*O*-benzyl-1-*O*-*tert*butyldiphenylsilyl-5-desoxy-L-iditol (62): compound **61** (5.28 g, 6.76 mmol) was dissolved in dry THF (20 mL) under argon. Triphenylphosphine (5.32 g, 20.30 mmol) was added. The reaction was cooled to 0ºC and DIAD (3.93 mL, 20.30 mmol) was added dropwise, a yellow precipitate is formed. Diphenylphosphorilazide (4.68 mL, 21.64 mmol) was added. After 2 h the solvent was evaporated *in vacuo*. Purification by flash chromatography (petroleum ether/ethyl acetate 9:1) afforded pure compound **62** (4.10 g, 75.2% yield). $[\alpha]_D^{25}$ = -1.7 (*c* = 1.2, $CHCl_3$). ^{1}H-NMR: δ = 1.07 [s, 9H, C(C*H*$_3$)$_3$], 3.23-3.26 [m, 1H, 5-H], 3.34 [dd, *J* = 9.5, 4.8, 1H, 6a-H], 3.54-3.58 [m, 2H, 2-H, 6b-H], 3.82 [dd, *J* = 7.8, 3.0, 1H, 4-H], 3.86-3.91 [m, 2, 1a,b-H], 4.04 [dd, *J* = 7.8, 2.8, 1H, 3-H], 4.31 (d, *J* = 11.8, 1H, C*H*Ph), 4.38 (d, *J* = 11.9, 1H, C*H*Ph), 4.39 (d, *J* = 11.9, 1H, C*H*Ph), 4.54 (d, *J* = 11.5, 1H, C*H*Ph), 4.62 (d, *J* = 11.8, 1H, C*H*Ph), 4.66 (d, *J* = 11.2, 1H, C*H*Ph), 4.76 (d, *J* = 11.2, 1H, C*H*Ph), 4.78 (d, *J* = 11.5, 1H, C*H*Ph), 7.20-7.80 (m, 30H, *H*Ar). ^{13}C-NMR: δ = 19.6 [*C*(CH$_3$)$_3$], 27.3 [C(*C*H$_3$)$_3$], 61.6 [C(5)], 62.6, 70.2 [C(1)], 72.7, 73.5, 75.2, 75.6 (4 *C*H$_2$Ph), 78.1 [C(2)], 78.6 [C(4)], 79.3 [C(3)], 127.8-130.1 (*C*HAr), 133.40 (*C*qAr), 135.8-135.9 (*C*HAr), 138.0, 138.1, 138.3, 138.4 (4 *C*qAr). MS-ESI: *m/z* = 806.3798 $[M+H]^+$, calcd. for $C_{50}H_{55}N_3O_5Si$ = 805.3911.

5-azido-2,3,4,6-tetra-*O*-benzyl-5-desoxy-L-iditol (63): compound **62** (4.10 g, 5.09 mmol) was dissolved in dry THF (15 mL) under argon. A solution of TBAF 1M (15.26 mL, 15.26 mmol) was added slowly. After 3 h the solvent was evaporated *in vacuo*. Purification by flash chromatography (petroleum ether/ethyl acetate 8:2) afforded pure compound **63** (2.61 g, 90.4% yield). $[\alpha]_D^{25}$ = +11.0 (*c* = 1.1, $CHCl_3$).

^{1}H-NMR: δ = 3.40 [dd, *J* = 9.4, 4.8, 1H, 6a-H], 3.47-3.55 [m, 3H, 2-H, 5-H, 6b-H], 3.56-3.61 [m, 1H, 1a-H], 3.67-3.73 [m, 1H, 1b-H], 3.77-3.83 [m, 2H, 3-H, 4-H], 4.32 (d, *J* = 11.8, 1H, C*H*Ph), 4.36 (d, *J* = 11.8, 1H, C*H*Ph), 4.49 (d, *J* = 11.5, 2H, 2 C*H*Ph), 4.54 (d, *J* = 11.5, 1H, C*H*Ph), 4.56 (d, *J* = 11.2, 1H, C*H*Ph), 4.62 (d, *J* = 11.2, 1H, C*H*Ph), 4.69 (d, *J* = 11.5, 1H, C*H*Ph), 7.15-7.30 (m, 20H, *H*Ar). ^{13}C-NMR: δ = 61.4 [C(5)], 61.7 [C(1)], 69.8 [C(6)], 72.7, 73.6, 75.0, 75.1 (4 *C*H_2Ph), 78.2, 78.3, 79.2 [C(2), C(3), C(4)], 127.9-128.7 (*C*HAr), 137.8, 137.9, 137.9, 138.0 (4 *C*qAr). MS-ESI: *m/z* = 568.2789 $[M+H]^+$, calcd. for $C_{34}H_{37}N_3O_5$ = 567.2733.

5-azido-2,3,4,6-tetra-*O*-benzyl-5-desoxy-L-idose (64): compound **63** (2.61 g, 4.60 mmol) was dissolved in CH_2Cl_2 (20 mL). Dess-Martin periodinane (2.93 g, 6.90 mmol) was added slowly. After 40 min a 1:1 solution of satd. $NaHCO_3$/$Na_2S_2O_3$ 10% (100 mL) was added. After stirring for 30 min the reaction mixture was diluted with CH_2Cl_2 and then washed with water. The organic layer was dried with Na_2SO_4, filtered and the solvent was evaporated *in vacuo*. Purification by flash chromatography (petroleum ether/ethyl acetate 8:2) afforded pure aldehyde **64** (1.98 g, 79.1% yield), which suddenly was used in the next reaction due to its low chemical stability, without further characterization.

Ethyl (3R,4S,5S,6R,7R)-7-azido-4,5,6,8-tetra(benzyloxy)-3-hydroxy-octanoate and Ethyl (3S,4S,5S,6R,7R)-7-azido-4,5,6,8-tetra(benzyloxy)-3-hydroxy-octanoate (65): diisopropylamine (4.94 mL, 34.99 mmol) was dissolved in dry THF (10 mL) under argon. At 0ºC, a solution of *tert*-butyllithium 1M (21.87 mL, 34.99 mmol) was added. After 0.5 h stirring, the temperature was taken to -78ºC and dry ethyl acetate (3.42 mL, 34.99 mmol) was added. After 0.5 h stirring, a solution of compound **64** (1.98 g, 3.50 mmol) in dry THF (5 mL) was added. After 1 h, the reaction was treated with a satd. solution of NH_4Cl (30 mL), taken to room temperature and neutralized with HCl 5%. The reaction mixture was dissolved with CH_2Cl_2 and washed with water. The organic layer was dried with Na_2SO_4, filtered and the solvent was evaporated *in vacuo*. Purification by flash chromatography (petroleum ether/ethyl acetate 8:2) afforded compound **65** as a mixture of stereoisomers (2.18 g, 95.1% yield, 3R/3S = 2:1). ^{1}H-NMR: δ = 1.23 (m, 3H, OCH_2CH_3), 2.30 [dd, *J* = 15.8, 4.3, 0.4H, 2a-H(3R)], 2.49-2.56 [m, 1H, 2b-H(3S), 2a-H(3R)], 2.72 [dd, *J* = 16.0, 3.6, 0.6H, 2b-H(3R)], 3.50-3.68 [m, 4H, 4-H, 5-H, 6-

H, 7-H (3R, 3S)], 3.86 [dd, *J* = 6.0, 3.7, 0.4H, 8a-H(3S)], 3.87-3.92 [m, 0.4H, 8b-H(3S)], 3.96 [dd, *J* = 7.0, 3.0, 0.6H, 8a-H(3R)], 4.00 [dd, *J* = 7.0, 3.6, 0.6H, 8b-H(3R)], 4.09-4.18 [m, 2H, C*H*$_2$CO$_2$Et (3R, 3S)], 4.20-4.26 [m, 0.4H, 3-H(3S)], 4.26-4.32 [m, 0.6H, 3-H(3R)], 4.40-4.49 (m, 2H, C*H*$_2$Ph), 4.51 [d, *J* = 11.3, 0.4H, C*H*Ph(3S)], 4.59-4.72 (m, 4.2H, C*H*Ph), 4.77 [d, *J* = 11.8, 0.4H, C*H*Ph(3S)], 4.80 [d, *J* = 11.6, 0.6H, C*H*Ph(3R)], 4.81 [d, *J* = 11.4, 0.4H, C*H*Ph(3S)], 7.23-7.40 (m, 20H, *H*Ar). ^{13}C-NMR: δ = 14.4 (OCH$_2$*C*H$_3$), 38.7, 39.1 [C(2)], 60.8 (O*C*H$_2$CH$_3$), 61.3, 61.4 [C(7)], 67.5, 69.0 [C(3)], 69.6, 69.9, 73.2, 73.3, 73.4, 74.1, 74.5, 74.7, 74.8, 75.0 [*C*H$_2$Ph, C(8)], 77.8, 78.1, 78.1, 78.9, 79.0, 79.7 [C(4), C(5), C(6)], 127.9-128.7 (*C*HAr), 137.6, 137.7, 137.8, 137.9, 138.0, 138.1, 138.2 (*C*qAr), 172.2, 172.6 [*C*(1)]. MS-ESI: *m/z* = 654.3748 $[M+H]^+$, calcd. for $C_{38}H_{43}N_3O_7$ = 653.3101.

Ethyl (3R,4S,5S,6R,7R)-7-amino-4,5,6,8-tetra(benzyloxy)-3-hydroxy-octanoate and Ethyl (3S,4S,5S,6R,7R)-7-amino-4,5,6,8-tetra(benzyloxy)-3-hydroxy-octanoate (66): compound **65** (240 mg, 0.36 mmol) was dissolved in ethyl acetate (3 mL); a catalytic amount of Lindlar catalyst was added and the reaction mixture was stirred under H_2 overnight. The catalyst was filtered through a Celite pad (eluent ethyl acetate) and the solvent was evaporated *in vacuo.* Purification by flash chromatography (petroleum ether/ethyl acetate 3:7) afforded compound **66** as a mixture of stereoisomers (190 mg, 85.6%, 3R/3S = 2:1). ^{1}H-NMR: δ = 1.20-1.30 (m, 3H, OCH$_2$C*H*$_3$), 2.42 [dd, *J* = 15.8, 4.6, 0.4H, 2a-H(3S)], 2.49-2.60 [m, 1H, 2a-H(3R), 2a-H(3S)], 2.75 [dd, *J* = 16.0, 3.7, 0.6H, 2b-H(3R)], 3.12 [dt, *J* = 6.4, 2.4, 0.6H, 7-H(3R)], 3.24-3.27 [m, 0.4H, 7-H(3S)], 3.30-3.45 [m, 2H, 8a,b-H(3R), 8a,b-H(3S)], 3.61 [dd, *J* = 6.6, 3.6, 0.6H, 4-H(3R)], 3.64 [dd, *J* = 6.0, 3.4, 0.4H, 4-H(3S)], 3.77 [dd, *J* = 6.0, 3.7, 0.4H, 6-H(3S)], 3.89 [dd, *J* = 7.6, 2.5, 0.6H, 6-H(3R)], 4.04-4.15 [m, 3H, OC*H*$_2$CH$_3$, 5-H(3R,3S)], 4.28-4.36 [m, 1H, 3-H(3R,3S)], 4.03 [d, *J* = 11.9, 0.6H, C*H*Ph(3R)], 4.42 [d, *J* = 11.8, 0.4H, C*H*Ph(3S)], 4.44 [d, *J* = 11.9, 0.6H, C*H*Ph(3R)], 4.46 [d, *J* = 11.8, 0.4H, C*H*Ph(3S)], 4.51 [d, *J* = 11.2, 0.6H, C*H*Ph(3R)], 4.52 [d, *J* = 11.3, 0.4H, C*H*Ph(3S)], 4.58 [d, *J* = 11.3, 0.6H, C*H*Ph(3R)], 4.64-4.84 [m, 4.4H, C*H*Ph(3R,3S)], 7.20-7.40 (m, 20H, *H*Ar). ^{13}C-NMR: δ = 14.1 (OCH$_2$*C*H$_3$), 38.5, 38.7 [C(2)], 51.4, 51.5 [C(7)], 60.4 (O*C*H$_2$CH$_3$), 67.7, 68.8 [C(3)], 72.9, 73.4, 74.1, 74.3, 74.4, 74.5, 74.6 [*C*HPh, C(8)], 78.6, 78.9,

79.1, 79.4, 79.8, 80.1 [C(4), C(5), C(6)], 127.7, 128.6 (*C*HAr), 138.1, 138.2, 138.3, 138.5, 138.6 (*C*qAr), 172.2 [C(1)]. MS-ESI: *m/z* = 628.3371 $[M+H]^+$, calcd. for $C_{38}H_{45}NO_7$ = 627.3196.

Ethyl [(2S,3S,4R,5R,6S)-3,4,5-tris(benzyloxy)-6-[(benzyloxy)methyl]piperidin-2-yl] acetate and Ethyl [(2R,3S,4R,5R,6S)-3,4,5-tris(benzyloxy)-6-[(benzyloxy)methyl] piperidin-2-yl]acetate (67): compound **66** (170 mg, 0.27 mmol) was dissolved in dry THF (1 mL) under argon. The reaction was chilled to 0ºC and triphenylphosphine (140 mg, 0.54 mmol) was added. Then DIAD (0.10 mL, 0.54 mmol) was added dropwise and the reaction mixture was stirred overnight. The solvent was removed *in vacuo*, then purification by flash chromatography (petroleum ether/ethyl acetate 7:3) afforded compound **67** as a mixture of stereoisomers (0.12 g, 70.4%, 2S/2R = 2:1). Major isomer: ^{1}H-NMR: δ = 1.21-1.24 (m, 3H, OCH_2CH_3), 2.32 [dd, *J* = 15.5, 8.1, 1H, C*H*CO_2Et], 2.82 [dd, *J* = 15.5, 4.3, 1H, C*H*CO_2Et], 3.20-3.28 [m, 2H, 2-H, 3-H], 3.38-3.61 [m, 1H, C*H*OBn], 3.62-3.68 [m, 2H, 4-H, C*H*OBn], 3.78 [bt, *J* = 9.9, 1H, 5-H], 3.79 [dd, *J* = 9.4, 5.9, 1H, 6-H], 4.01-4.19 (m, 2H, OCH_2CH_3), 4.37-4.67 (m, 5H, C*H*Ph), 4.74 (d, *J* = 11.8, 1H, C*H*Ph), 4.91 (d, 1H, *J* = 11.6, C*H*Ph), 4.94 (d, 1H, *J* = 11.5, C*H*Ph), 7.20-7.40 (m, 20H, *H*Ar). ^{13}C-NMR: δ = 14.4 (OCH_2CH_3), 29.9 (CH_2CO_2Et), 50.7, 54.3 [C(2), C(6)], 60.8, 65.6 (OCH_2CH_3, CH_2OBn), 73.0, 73.8, 75.5, 75.7 (CH_2Ph), 80.4, 82.2, 83.5 [C(3), C(4), C(5)], 127.7-128.8 (*C*HAr), 138.3, 138.4, 138.4, 138.8 (*C*qAr), 172.2 (C=O) ppm. MS-ESI: *m/z* = 610.4024 $[M+H]^+$, calcd. for $C_{38}H_{43}NO_6$ = 609.3090.

Ethyl [(2S,3S,4R,5R,6S)-3,4,5-trihydroxy-6-(hydroxymethyl)piperidin-2-yl] acetate (49): benzylated iminosugars **67** (26.4 mg, 0.043 mmol) were dissolved in methanol (2 mL). A catalytic amount of $Pd(OH)_2$ and acetic acid (0.1 mL) were added and the reaction mixture was stirred under H_2 overnight. The catalyst was filtered through a Celite pad (eluent methanol) and the solvent was evaporated *in vacuo*. Purification by flash chromatography (ethyl acetate/methanol 8:2) afforded pure compound **49** as the major isomer (7.2 mg, 66.7%). $[\alpha]_D^{25}$ = -30.1 (*c*=0.7, MeOH). ^{1}H-NMR: δ = 1.26 (t, *J* = 7.1 Hz, 3H, OCH_2CH_3), 2.36 (dd, *J* = 16.3, 8.8 Hz, 1H, C*H*CO_2Et), 2.91 (dd, *J* = 16.3, 3.3 Hz, 1H, C*H*CO_2Et), 3.10 [t, *J* = 8.7 Hz, 1H, 3-H], 3.17 [dt, *J* = 9.0, 8.9, 3.4 Hz, 1H, 2-H], 3.20-3.27 [m, 1H, 6-H], 3.42 [t, *J* =

8.7 Hz, 1H, 4-H], 3.70 [dd, *J* = 9.2, 5.4 Hz, 1H, 5-H], 3-75-3.80 [m, 2H, 7a,b-H], 4.12-4.19 (m, 2H, OC*H*$_2$CH$_3$). ^{13}C-NMR: δ = 14.5 (OCH$_2$*C*H$_3$), 38.2 (*C*H$_2$CO$_2$Et), 52.1, 59.0, 73.3, 76.0, 76.3 [C(2), C(3), C(4), C(5), C(6)], 58.1, 61.8, (O*C*H$_2$CH$_3$, *C*H$_2$OH), 174.0 (C=O) ppm. MS-ESI: *m/z* = 250.1246 [M+H]$^+$, calcd. for $C_{10}H_{19}NO_6$ = 249.1212.

Ethyl [(2S,3S,4R,5R,6S)-3,4,5-tris(benzyloxy)-6-[(benzyloxy)methyl]-1-propyl piperidin-2-yl]acetate (69): benzylated iminosugars **67** (115.4 mg, 0.19 mmol) were dissolved in dry 1,2-dichloroethane (5 mL), then propionaldehyde (41 µL, 0.57 mmol) and acetic acid (0.108 mL, 1.89 mmol) were added. The reaction mixture was dried with Na_2SO_4 and was stirred for 0.5 h. Then Na(OAc)$_3$BH (160.4 mg, 0.76 mmol) was added, stirring overnight. The reaction mixture was neutralized with a satd. solution of $NaHCO_3$, dissolved with CH_2Cl_2 and washed with water. The organic layer was dried with Na_2SO_4, filtered and the solvent was evaporated *in vacuo*. Purification by flash chromatography (petroleum ether/ethyl acetate 9:1) afforded pure compound **69** (64.0 mg, 51.9% major isomer). Major compound **(69):** $[\alpha]_D^{25}$ = -38.6 (*c*=1.4, $CHCl_3$). ^{1}H-NMR: δ = 0.83 [t, *J* = 7.3 Hz, 3H, N(CH$_2$)$_2$C*H*$_3$], 1.17 (t, *J* = 7.1 Hz, 3H, OCH$_2$C*H*$_3$), 1.37-1.49 (m, 2H, NCH$_2$C*H*$_2$CH$_3$), 2.40-2.53 (m, 2H, C*H*CO$_2$Et, NC*H*$_2$CH$_2$CH$_3$), 2.62 (ddd, *J* = 12.6, 8.6, 6.2 Hz, 1H, NC*H*$_2$CH$_2$CH$_3$), 2.73 (dd, *J* = 15.1, 3.9 Hz, 1H, C*H*CO$_2$Et), 3.32-3.44 [m, 3H, 2-H, 3-H, 6-H], 3.66-3.74 (m, 1H, C*H*OBn), 3.74-3.81 [m, 2H, C*H*OBn, 4-H], 3.84 [dd, *J* = 10.1, 3.4 Hz, 1H, C(5)-H], 3.97-4.10 (m, 2H, OC*H*$_2$CH$_3$), 4.50-4.78 (m, 6H, 6 C*H*Ph), 4.89-4.98 (m, 2H, 2 C*H*Ph), 7.20-7-43 (m, 20H, *H*Ar) ppm. ^{13}C-NMR: δ = 11.90 [N(CH$_2$)$_2$*C*H$_3$], 14.42 (OCH$_2$*C*H$_3$), 22.52 (NCH$_2$*C*H$_2$CH$_3$), 36.15 (*C*H$_2$CO$_2$Et), 49.99 (N*C*H$_2$CH$_2$CH$_3$), 56.75, 57.93 [C(2), C(6)], 60.76, 67.84 (O*C*H$_2$CH$_3$, *C*H$_2$OBn), 72.98, 73.65, 75.00, 75.50 (4 *C*H$_2$Ph), 79.08, 80.94, 84.37 [C(3), C(4), C(5)], 127.6-129.6 (*C*HAr),138.45, 138.45, 139.05, 139.05 (*C*qAr), 172.25 (C=O) ppm. MS-ESI: *m/z* = 652.3416 [M+H]$^+$, calcd. for $C_{41}H_{49}NO_6$ = 651.3560.

Ethyl [(2S,3S,4R,5R,6S)-3,4,5-trihydroxy-6-(hydroxymethyl)-1-propylpiperidin -2-yl] acetate (50): compound **69** (64.0 mg, 0.098 mmol) was dissolved in ethyl acetate (2 mL) and methanol (4 mL). A catalytic amount of $Pd(OH)_2$ and acetic acid (0.1 mL) were added and the reaction mixture was stirred under H_2 overnight.

The catalyst was filtered through a Celite pad (eluent methanol) and the solvent was evaporated *in vacuo* to afford pure compound **50** (29.2 mg, 100%). $[\alpha]_D^{25}$ = +2.1 (*c* = 0.3, MeOH). ^{1}H-NMR: δ = 0.84 [t, *J* = 7.4 Hz, 3H, $N(CH_2)_2CH_3$], 1.25 (t, *J* = 7.1 Hz, 3H, OCH_2CH_3), 1.30-1.47 (m, 2H, $NCH_2CH_2CH_3$), 2.42-2.54 (m, 2H, $CHCO_2Et$, $NCH_2CH_2CH_3$), 2.66-2.77 (m, 1H, $NCH_2CH_2CH_3$), 2.86 (dd, *J* = 16.4, 4.2 Hz, 1H, $CHCO_2Et$), 3.10-3.21 [m, 2H, C(2)-H, C(6)-H], 3.24 [t, *J* = 9.6 Hz, 1H, C(3)-H], 3.39 [t, *J* = 9.0 Hz, 1H, C(4)-H], 3.73 (d, *J* = 7.4 Hz, 2H, CH_2OH), 3.82 [dd, *J* = 9.5, 6.2 Hz, 1H, C(5)-H], 4.13 (q, *J* = 7.2 Hz, 2H, OCH_2CH_3) ppm. ^{13}C-NMR: δ = 11.62, 14.50 [$N(CH_2)_2CH_3$, OCH_2CH_3], 24.06 ($NCH_2CH_2CH_3$), 34.98 (CH_2CO_2Et), 49.67, 57.58, 61.75 ($NCH_2CH_2CH_3$, OCH_2CH_3, CH_2OH), 55.76, 62.15, 70.44, 72.66, 77.57 [C(2), C(3), C(4), C(5), C(6)], 174.31 (C=O) ppm. MS-ESI: *m/z* = 292.1756 $[M+H]^+$, calcd. for $C_{13}H_{25}NO_6$ = 291.1682.

Ethyl [(2S,3S,4R,5R,6S)-3,4,5-tris(benzyloxy)-6-[(benzyloxy)methyl]-1-cyclohexylmethylenepiperidin-2-yl]acetate (70): compound **67** (86.5 mg, 0.142 mmol) was dissolved in dry dichloroethane (4 mL), then cyclohexanecarboxyaldehyde (0.051 mL, 0.426 mmol), acetic acid (0.081 mL, 1.42 mmol) were added. The reaction mixture was dried with Na_2SO_4 and was stirred for 0.5 h. Then $Na(OAc)_3BH$ (120.2 mg, 0.567 mmol) was added, stirring overnight. The reaction mixture was neutralized with a satd. solution of $NaHCO_3$, dissolved with CH_2Cl_2 and washed with water. The organic layer was dried with Na_2SO_4, filtered and the solvent was evaporated *in vacuo*. Purification by flash chromatography (petroleum ether/ethyl acetate 9:1) afforded pure compound **70** (72.3 mg, 79.4% yield). $[\alpha]_D^{25}$ = -18.3 (*c* = 1.0, $CHCl_3$). ^{1}H-NMR: δ = 0.63-0.82 [m, 2H, 2 C*H*(Cy)], 1.15 (t, *J* = 7.1 Hz, 3H, OCH_2CH_3), 1.06-1.40 [m, 3H, 3 C*H*(Cy)], 1.58-1.80 [m, 6H, 6 C*H*(Cy)], 2.21-2.32 (m, 1H, NC*H*Cy), 2.35-2.51 (m, 2H, $CHCO_2Et$, NC*H*Cy), 2.69 (dd, *J* = 15.5, 4.7 Hz, 1H, $CHCO_2Et$), 3.22-3.30 [m, 1H, C(6)-H], 3.31-3.38 [m, 1H, C(3)-H], 3.38-3.49 [m, 1H, C(2)-H], 3.67-3.75 [m, 1H, C(4)-H], 3.75-3.82 [m, 2H, C(5)-H, C(7a)-H], 3.85 [dd, *J* = 10.1, 3.4 Hz, 1H, C(7b)-H], 3.91-4.00 (m, 1H, $OCHCH_3$), 4.00-4.09 (m, 1H, $OCHCH_3$), 4.54-4.63 (m, 3H, 3 C*H*Ph), 4.64-4.71 (m, 2H, 2 C*H*Ph), 4.73 (d, *J* = 10.8 Hz, 1H, C*H*Ph), 4.93 (d, *J* = 10.9 Hz, 2H, 2 C*H*Ph), 7.24-7.37 (m, 20H, *H*Ar) ppm. ^{13}C-NMR: δ = 14.27 (OCH_2CH_3), 26.19, 26.26, 27.00, 31.29, 31.39 [5 CH_2(Cy)], 37.00 [CH(Cy)], 36.03

(*C*H_2CO_2Et), 54.51, 60.47, 67.35 (O*C*H_2CH_3, N*C*H_2Cy, *C*H_2OBn), 56.26, 58.69 [C(2), C(6)], 78.41, 80.85, 84.38 [C(3), C(4), C(5)], 72.84, 73.35, 74.89, 75.45 (4 O*C*H_2Ph), 127.4-128.5 (*C*HAr), 138.5, 138.6, 138.9, 138.9 (4 *C*qAr), 172.2 (C=O) ppm. MS-ESI: *m/z* = 705.4029 $[M+H]^+$, calcd. for $C_{45}H_{55}NO_6$ = 706.4107.

Ethyl [(2S,3S,4R,5R,6S)-3,4,5-trihydroxy-6-(hydroxymethyl)-1-cyclohexyl methylenepiperidin-2-yl]acetate (51): compound **70** (72.3 mg, 0.113 mmol) was submitted to catalytic hydrogenation by the same procedure used for the synthesis of compound **49**, affording pure compound **51** (40,0 mg, 100% yield). $[\alpha]_D^{25}$ = -38.0 (*c* = 4.1, MeOH). ^{1}H-NMR: δ = 0.66-0.79 [m, 1H, C*H*(Cy)], 0.80-0.92 [m, 1H, C*H*(Cy)], 1.11-1.24 [m, 2H, 2 C*H*(Cy)], 1.26 (t, *J* = 7.1 Hz, 3H, OCH_2CH_3), 1.28-1.43 [m, 2H, 2 C*H*(Cy)], 1.62-1.78 [m, 6H, 6 C*H*(Cy)], 2.36 (dd, *J* = 13.5, 6.1 Hz, 1H, NC*H*Cy), 2.49 (dd, *J* = 17.1, 10.5 Hz, 1H, C*H*CO_2Et), 2.57 (dd, *J* = 13.5, 8.1 Hz, 1H, NC*H*Cy), 2.87 (dd, *J* = 17.1, 3.7 Hz, 1H, C*H*CO_2Et), 3.14-3.23 [m, 2H, C(2)-H, C(6)-H], 3.27 [dd, *J* = 10.5, 8.5 Hz, 1H, C(3)-H], 3.41 [t, *J* = 9.0 Hz, 1H, C(4)-H], 3.74-3.80 (m, 2H, CH_2OH), 3.85 [dd, *J* = 9.5, 6.1 Hz, 1H, C(5)-H], 4.14 (q, *J* = 7.1 Hz, 2H, OCH_2CH_3) ppm. ^{13}C-NMR: δ = 17.31 (OCH_2CH_3), 29.84, 30.04, 30.58, 34.81, 35.24, 37.09 [5 *C*H_2(Cy), *C*H_2CO_2Et], 41.51 [*C*H(Cy)], 57.69, 60.62, 64.59 (*C*H_2OH, N*C*H_2Cy, O*C*H_2CH_3), 58.26, 65.78, 72.96, 74.88, 80.31 [C(2), C(3), C(4), C(5), C(6)], 177.12 (C=O). MS-ESI: *m/z* = 346.2165 $[M+H]^+$, calcd. for $C_{17}H_{31}NO_6$ = 345.2151.

Ethyl [(2S,3S,4R,5R,6S)-3,4,5-trihydroxy-6-(hydroxymethyl)-1-benzyloxy carbonylpiperidin-2-yl]acetate (68): to a solution of compound **49** (27.3 mg, 0.109 mmol) in methanol (2 mL), benzyl chloroformate (0.047 mL, 0.329 mmol) and $NaHCO_3$ (18.4 mg, 0.219 mmol) were added. After stirring overnight, the solvent was evaporated *in vacuo*. Purification by flash chromatography (ethyl acetate) afforded pure compound **68** (10.5 mg, 25.1% yield). $[\alpha]_D^{25}$ = +83.3 (*c* = 0.1). ^{1}H-NMR: δ = 1.19 (t, *J* = 7.1 Hz, 3H, OCH_2CH_3), 2.88 (dd, *J* = 16.8, 5.9 Hz, 1H, C*H*CO_2Et), 3.12 (dd, *J* = 16.4, 8.5 Hz, 1H, C*H*CO_2Et), 3.39 [dd, *J* = 7.8, 6.7 Hz, 1H, C(3)-H], 3.56 [dd, *J* = 8.2, 6.7 Hz, 1H, C(4)-H], 3.67 [dd, *J* = 8.3, 6.1 Hz, 1H, C(5)-H], 3.86-4.00 [m, 3H, C(2)-H, CH_2OH], 4.01-4.11 (m, 2H, OCH_2CH_3), 4.35-4.46 [m, 1H, C(6)-H], 5.03-5.13 (m, 2H, CH_2Ph), 7.26-7.45 (m, 5H, *H*Ar) ppm. ^{13}C-NMR: δ = 14.43 (OCH_2CH_3), 36.15 (*C*H_2CO_2Et), 54.88, 59.46, 72.48, 74.17,

76.81 [C(2), C(3), C(4), C(5), C(6)], 58.94, 61.76, 68.31 (CH_2OH, OCH_2CH_3, OCH_2Ph), 128.96-129.53 (*C*HAr), 137.86 (*C*qAr), 157.88 (CO_2Bn), 174.09 (CO_2Et) ppm. MS-ESI: *m/z* = 384.1674 $[M+H]^+$, calcd. for $C_{18}H_{25}NO_8$ = 383.1580.

Ethyl [(2S,3S,4R,5R,6S)-3,4,5-trihydroxy-6-(carboxyl)-1-benzyloxycarbonyl piperidin-2-yl]acetate (55): to a solution of compound **68** (10.5 mg, 0.027 mmol) in water (1.5 mL), TEMPO (0.27 mg, 0.00175 mmol) and KBr (9.8 mg, 0.0822 mmol) were added. The reaction mixture was cooled to 0ºC and NaOCl 5% (0.54 mL, 0.363 mmol) was added. After 4 h stirring, methanol (1 mL) was added, the reaction mixture was acidified with HCl 5% and the solvent was removed *in vacuo*. Then the white solid was suspended in ethanol, the suspension was filtered and the solvent was evaporated *in vacuo*. Purification by flash chromatography (ethyl acetate/methanol 8:2) afforded pure compound **55** (9.7 mg, 84.4% yield). $[\alpha]_D^{25}$ = +83.3 (*c* = 0.1). ^{1}H-NMR δ = 1.20 (t, *J* = 7.1 Hz, 3H, OCH_2CH_3), 2.66-2.87 (m, 2H, CH_2CO_2Et), 3.52-3.65 [m, 2H, C(3)-H, C(4)-H], 3.75-3.87 [m, 1H, C(5)-H], 4.06 (dd, *J* = 13.6, 6.6 Hz, 2H, OCH_2CH_3), 4.19-4.39 [m, 1H, C(2)-H], 4.56 [d, *J* = 5.8 Hz, 1H, C(6)-H], 5.10 (m, 2H, OCH_2Ph), 7.23-7.41 (m, 5H, *H*Ar) ppm. ^{13}C-NMR: δ = 14.45 (OCH_2CH_3), 38.33 (CH_2CO_2Et), 56.73, 61.13, 72.50, 75.49, 78.26 [C(2), C(3), C(4), C(5), C(6)], 61.69, 68.50 (OCH_2CH_3, OCH_2Ph), 128.8-129.5 (*C*HAr), 135.8 (*C*qAr), 149.8 (CO_2Bn), 164.9 (CO_2H), 181.8 (CO_2Et) ppm. MS-ESI: *m/z* = 420.1281 $[M+H]^+$, calcd. for $C_{18}H_{22}NO_9Na$ = 419.1192.

5.3. Biological tests

Intracellular calcium mobilization assay: PC-3 cells were maintained as monolayer cultures in F-12 medium supplemented with 10% non heat-inactivated FBS, L-glutamine, penicillin and streptomycin. Cells were grown in 75 cm^2 culture flasks, at 37°C in 5% CO_2 and 95% air, and harvested with trypsin-EDTA when they were in exponential growth. PC-3 cells were plated at 10,000 cells/well into black-walled, clear-bottomed 96-well plates. 24 hours later cells were serum starved for 36 hours. Before assay, cells were incubated in dark conditions with 100 µL of Hanks' balanced salt solution containing HEPES 20 mM, probenecid 2.5 mM, and FLUO-4 NW 4.5 µM at 37°C and 5% CO_2 for 45 minutes following the

Fluo-4 NW calcium assay kit Invitrogen manual's instruction. Fluorescence emissions from 96 were measured with the multilabel spectrophotometer Victor^3 (Perkin Elmer) available at the Faculty of Medicine of the University of Milan-Bicocca at 485/535 nm (excitation/emission filters) for the 60 sec after injection of the stimuli. The tested analogues were diluted, at the different concentration tested, in Hanks' balanced salt solution and injected into the well by an automated injector system. As positive control for our experimental settings, we tested the ability of bombesin 100 nM to stimulate intracellular calcium in PC-3 cells. All the experiments were performed at 37°C.

Elk-1 activation assay: PC-3 cells were plated at 250,000 cells/dish into 35 mm diameter dishes. 24 hours later cells were serum starved for 36 hours. At the end of the incubation cells were treated with the different analogues diluted in cell culture medium alone or in combination with bombesin in order to verify the effect of the analogue as agonist or antagonist of GRP receptor. Untreated cells were used as control. As positive control for our experimental settings, we tested the ability of bombesin 100 nM to stimulate Elk-1 activtion in PC-3 cells. Total protein extract was performed at different time points and Elk-1 activation was tested by western blot analysis using a primary antibody that specifically recognize active (phosphorilated) Elk-1 (Santa Cruz).

Akt activity assay: This test was performed using the Akt/PKB Kinase Activity Assay Kit of Assay Designs Inc. Standard procedure: wells of the PKB Substrate Microtiter Plate were soaked with Kinase Assay Dilution Buffer (50µL) at room temperature for 10 minutes. The liquid was carefully aspirated from each well. Samples were added to appropriate wells of the PKB Substrate Microtiter Plate. Reaction was initiated by adding diluted ATP (10µL) to each well, except the blank, followed by incubation for up to 90 minutes at 30°C. Reaction was stopped by emptying contents of each well. Phosphospecific Substrate Antibody (40µL) was added to each well, except the blank, followed by incubation at room temperature for 60 minutes. Wells were washed 4 times with 1X Wash Buffer (100µL), then diluted Anti-Rabbit IgG: HRP Conjugate (40µL) was added to each well, except the blank, followed by incubation at room temperature for 30 minutes. Wells were washed 4 times with 1X Wash Buffer (100µL). TMB Substrate (60µL)

was added to each well, followed by incubation at room temperature for 30-60 minutes. Stop Solution 2 (20µL) was added to each well. Absorbance was measured at 450 nm.

Bibliography

(1) Gay, P. *Freud: A Life for Our Time*; W. W. Norton & Company: New York, 1988.

(2) WHO 2009; Vol. 2010.

(3) Alberts, B.; Johnson, A.; Lewis, J.; Raff, M.; Roberts, K.; Walter, P. In *Molecular Biology of the Cell*; Garland Science: New York, 2002; Vol. 4.

(4) Meyers, R. A. *Cancer: From Mechanisms to Therapeutic Approaches*; Wiley-VCH: Weinheim, 2007.

(5) David, A. R.; Zimmerman, M. R. *Nature Reviews Cancer* **2010**, *10*, 728.

(6) Ferlay, J.; Shin, H. R.; Bray, F.; Froman, D.; Mathers, C.; Parkin, D. M.; International Agency for Research on Cancer: Lyon, France, 2010; Vol. 2010.

(7) Garcia M, J. A., Ward EM, Center MM, Hao Y, Siegel RL, Thun MJ. *Global Cancer Facts & Figures 2007*, American Cancer Society, 2007.

(8) *Anticancer Drug Development*; Baguley, B. C.; Kerr, D. J., Eds.; Academic Press: San Diego, USA, 2002.

(9) Schally, A. V.; Nagy, A. *European Journal of Endocrinology* **1999**, *141*, 1.

(10) *Tumor Targeting in Cancer Therapy*; Pagé, M., Ed.; Humana Press: Totowa, USA, 2002.

(11) *Drug Targeting: Organ-Specific Strategies*; Molema, G.; Meijer, D. K. F., Eds.; Wiley-VCH: Weinheim, Germany, 2001; Vol. 12.

(12) Reubi, J. C. *Endocrine Reviews* **2003**, *24*, 389.

(13) Aina, O. H.; Liu, R. W.; Sutcliffe, J. L.; Marik, J.; Pan, C. X.; Lam, K. S. *Molecular Pharmaceutics* **2007**, *4*, 631.

(14) Lee, S.; Xie, J.; Chen, X. Y. *Chemical Reviews* **2010**, *110*, 3087.

(15) Okarvi, S. M. *Cancer Treatment Reviews* **2008**, *34*, 13.

(16) Varga, J. M. *Methods in Enzymology* **1985**, *112*, 259.

(17) Krenning, E. P.; Kwekkeboom, D. J.; Bakker, W. H.; Breeman, W. A. P.; Kooij, P. P. M.; Oei, H. Y.; Vanhagen, M.; Postema, P. T. E.; Dejong, M.; Reubi, J. C.; Visser, T. J.; Reijs, A. E. M.; Hofland, L. J.; Koper, J. W.; Lamberts, S. W. J. *European Journal of Nuclear Medicine* **1993**, *20*, 716.

(18) Tai, W. Y.; Mahato, R.; Cheng, K. *Journal of Controlled Release* **2010**, *146*, 264.

(19) Halmos, G.; Nagy, A.; Lamharzi, N.; Schally, A. V. *Cancer Letters* **1999**, *136*, 129.

(20) Engel, J. B.; Schallly, A. V.; Dietl, J.; Rieger, L.; Honig, A. *Molecular Pharmaceutics* **2007**, *4*, 652.

(21) Vol. 2010.

(22) Erspamer, V.; Erspamer, G. F.; Inselvin.M *Journal of Pharmacy and Pharmacology* **1970**, *22*, 875.

(23) McDonald, T. J.; Jornvall, H.; Nilsson, G.; Vagne, M.; Ghatei, M.; Bloom, S. R.; Mutt, V. *Biochemical and Biophysical Research Communications* **1979**, *90*, 227.

(24) Cuttitta, F.; Carney, D. N.; Mulshine, J.; Moody, T. W.; Fedorko, J.; Fischler, A.; Minna, J. D. *Nature* **1985**, *316*, 823.

(25) Jensen, R. T.; Battey, J. F.; Spindel, E. R.; Benya, R. V. *Pharmacological Reviews* **2008**, *60*, 1.

(26) Patel, O.; Shulkes, A.; Baldwin, G. S. *Biochimica Et Biophysica Acta-Reviews on Cancer* **2006**, *1766*, 23.

(27) Rozengurt, E. *Journal of Cellular Physiology* **1998**, *177*, 507.

(28) ToiScott, M.; Jones, C. L. A.; Kane, M. A. *Lung Cancer* **1996**, *15*, 341.

(29) Markwalder, R.; Reubi, J. C. *Cancer Research* **1999**, *59*, 1152.

(30) Gugger, M.; Reubi, J. C. *American Journal of Pathology* **1999**, *155*, 2067.

(31) Reubi, J. C.; Wenger, S.; Schmuckli-Maurer, J.; Schaer, J. C.; Gugger, M. *Clinical Cancer Research* **2002**, *8*, 1139.

(32) Cornelio, D. B.; Roesler, R.; Schwartsmann, G. *Annals of Oncology* **2007**, *18*, 1457.

(33) Hohla, F.; Schally, A. V. *Cell Cycle* **2010**, *9*, 1738.

(34) Grady, E. F.; Slice, L. W.; Brant, W. O.; Walsh, J. H.; Payan, D. G.; Bunnett, N. W. *Journal of Biological Chemistry* **1995**, *270*, 4603.

(35) Heimbrook, D. C.; Saari, W. S.; Balishin, N. L.; Friedman, A.; Moore, K. S.; Riemen, M. W.; Kiefer, D. M.; Rotberg, N. S.; Wallen, J. W.; Oliff, A. *Journal of Biological Chemistry* **1989**, *264*, 11258.

(36) Coy, D. H.; Taylor, J. E.; Jiang, N. Y.; Kim, S. H.; Wang, L. H.; Huang, S. C.; Moreau, J. P.; Gardner, J. D.; Jensen, R. T. *Journal of Biological Chemistry* **1989**, *264*, 14691.

(37) Radulovic, S.; Miller, G.; Schally, A. V. *Cancer Research* **1991**, *51*, 6006.

(38) Qin, Y. F.; Halmos, G.; Cai, R. Z.; Szoke, B.; Ertl, T.; Schally, A. V. *Journal of Cancer Research and Clinical Oncology* **1994**, *120*, 519.

(39) Broccardo, M.; Falconieriespamer, G.; Melchiorri, P.; Negri, L.; Decastiglione, R. *British Journal of Pharmacology* **1975**, *55*, 221.

(40) Marki, W.; Brown, M.; Rivier, J. E. *Peptides* **1981**, *2*, 169.

(41) Coy, D. H.; Heinzerian, P.; Jiang, N. Y.; Sasaki, Y.; Taylor, J.; Moreau, J. P.; Wolfrey, W. T.; Gardner, J. D.; Jensen, R. T. *Journal of Biological Chemistry* **1988**, *263*, 5056.

(42) Coy, D. H.; Jiang, N. Y.; Kim, S. H.; Moreau, J. P.; Lin, J. T.; Frucht, H.; Qian, J. M.; Wang, L. W.; Jensen, R. T. *Journal of Biological Chemistry* **1991**, *266*, 16441.

(43) Wang, L. H.; Coy, D. H.; Taylor, J. E.; Jiang, N. Y.; Moreau, J. P.; Huang, S. C.; Frucht, H.; Haffar, B. M.; Jensen, R. T. *Journal of Biological Chemistry* **1990**, *265*, 15695.

(44) Mokotoff, M.; Ren, K.; Wong, L. K.; Lefever, A. V.; Lee, P. C. *Journal of Medicinal Chemistry* **1992**, *35*, 4696.

(45) Leban, J. J.; Kull, F. C.; Landavazo, A.; Stockstill, B.; McDermed, J. D. *Proc. Natl. Acad. Sci. U. S. A.* **1993**, *90*, 1922.

(46) Pradhan, T. K.; Katsuno, T.; Taylor, J. E.; Kim, S. H.; Ryan, R. R.; Mantey, S. A.; Donohue, P. J.; Weber, H. C.; Sainz, E.; Battey, J. F.; Coy, D. H.; Jensen, R. T. *European Journal of Pharmacology* **1998**, *343*, 275.

(47) Darker, J. G.; Brough, S. J.; Heath, J.; Smart, D. *Journal of Peptide Science* **2001**, *7*, 598.

(48) Guard, S.; Watling, K. J.; Howson, W. *European Journal of Pharmacology* **1993**, *240*, 177.

(49) Fleischmann, A.; Laderach, U.; Friess, H.; Buechler, M. W.; Reubi, J. C. *Laboratory Investigation* **2000**, *80*, 1807.

(50) Mantey, S. A.; Gonzalez, N.; Schumann, M.; Pradhan, T. K.; Shen, L.; Coy, D. H.; Jensen, R. T. *Journal of Pharmacology and Experimental Therapeutics* **2006**, *319*, 980.

(51) Miyazaki, M.; Lamharzi, N.; Schally, A. V.; Halmos, G.; Szepeshazi, K.; Groot, K.; Cai, R. Z. *European Journal of Cancer* **1998**, *34*, 710.

(52) Koppan, M.; Halmos, G.; Arencibia, J. M.; Lamharzi, N.; Schally, A. V. *Cancer* **1998**, *83*, 1335.

(53) Schwartsmann, G.; DiLeone, L. P.; Horowitz, M.; Schunemann, D.; Cancella, A.; Pereira, A. S.; Richter, M.; Souza, F.; da Rocha, A. B.; Souza, F. H.; Pohlmann, P.; de Nucci, G. *Investigational New Drugs* **2006**, *24*, 403.

(54) Nagy, A.; Armatis, P.; Cai, R. Z.; Szepeshazi, K.; Halmos, G.; Schally, A. V. *Proc. Natl. Acad. Sci. U. S. A.* **1997**, *94*, 652.

(55) Engel, J. B.; Schally, A. V.; Halmos, G.; Baker, B.; Nagy, A.; Keller, G. *European Journal of Cancer* **2005**, *41*, 1824.

(56) Moody, T. W.; Mantey, S. A.; Pradhan, T. K.; Schumann, M.; Nakagawa, T.; Martinez, A.; Fuselier, J.; Coy, D. H.; Jensen, R. T. *Journal of Biological Chemistry* **2004**, *279*, 23580.

(57) Moody, T. W.; Sun, L. C.; Mantey, S. A.; Pradhan, T.; Mackey, L. V.; Gonzales, N.; Fuselier, J. A.; Coy, D. H.; Jensen, R. T. *Journal of Pharmacology and Experimental Therapeutics* **2006**, *318*, 1265.

(58) Jaracz, S.; Chen, J.; Kuznetsova, L. V.; Ojima, L. *Bioorganic & Medicinal Chemistry* **2005**, *13*, 5043.

(59) Safavy, A.; Raisch, K. P.; Khazaeli, M. B.; Buchsbaum, D. J.; Bonner, J. A. *Journal of Medicinal Chemistry* **1999**, *42*, 4919.

(60) Lantry, L. E.; Cappelletti, E.; Maddalena, M. E.; Fox, J. S.; Feng, W. W.; Chen, J. Q.; Thomas, R.; Eaton, S. M.; Bogdan, N. J.; Arunachalam, T.; Reubi, J. C.; Raju, N.; Metcalfe, E. C.; Lattuada, L.; Linder, K. E.; Swenson, R. E.; Tweedle, M. F.; Nunn, A. D. *Journal of Nuclear Medicine* **2006**, *47*, 1144.

(61) Schroeder, R. P. J.; Muller, C.; Reneman, S.; Melis, M. L.; Breeman, W. A. P.; de Blois, E.; Bangma, C. H.; Krenning, E. P.; van Weerden, W. M.; de Jong, M. *European Journal of Nuclear Medicine and Molecular Imaging* **2010**, *37*, 1386.

(62) Nock, B.; Nikolopoulou, A.; Chiotellis, E.; Loudos, G.; Maintas, D.; Reubi, J. C.; Maina, T. *European Journal of Nuclear Medicine and Molecular Imaging* **2003**, *30*, 247.

(63) Abd-Elgaliel, W. R.; Gallazzi, F.; Garrison, J. C.; Rold, T. L.; Sieckman, G. L.; Figueroa, S. D.; Hoffman, T. J.; Lever, S. Z. *Bioconjugate Chemistry* **2008**, *19*, 2040.

(64) de Wiele, C. V.; Phonteyne, P.; Pauwels, P.; Goethals, I.; Van den Broecke, R.; Cocquyt, V.; Dierckx, R. A. *Journal of Nuclear Medicine* **2008**, *49*, 260.

(65) Van de Wiele, C.; Dumont, F.; Vanden Broecke, R.; Oosterlinck, W.; Cocquyt, V.; Serreyn, R.; Peers, S.; Thornback, J.; Slegers, G.; Dierckx, R. A. *European Journal of Nuclear Medicine* **2000**, *27*, 1694.

(66) Dimitrakopoulou-Strauss, A.; Hohenberger, P.; Haberkorn, U.; Macke, H. R.; Eisenhut, M.; Strauss, L. G. *Journal of Nuclear Medicine* **2007**, *48*, 1245.

(67) Zhang, H. W.; Schuhmacher, J.; Waser, B.; Wild, D.; Eisenhut, M.; Reubi, J. C.; Maecke, H. R. *European Journal of Nuclear Medicine and Molecular Imaging* **2007**, *34*, 1198.

(68) Zhang, X. Z.; Cai, W. B.; Cao, F.; Schreibmann, E.; Wu, Y.; Wu, J. C.; Xing, L.; Chen, X. Y. *Journal of Nuclear Medicine* **2006**, *47*, 492.

(69) Breeman, W. A. P.; Hofland, L. J.; de Jong, M.; Bernard, B. F.; Srinivasan, A.; Kwekkeboom, D. J.; Visser, T. J.; Krenning, E. P. *International Journal of Cancer* **1999**, *81*, 658.

(70) Breeman, W. A. P.; de Jong, M.; Erion, J. L.; Bugaj, J. E.; Srinivasan, A.; Bernard, B. F.; Kwekkeboom, D. J.; Visser, T. J.; Krenning, E. P. *Journal of Nuclear Medicine* **2002**, *43*, 1650.

(71) Mantey, S.; Frucht, H.; Coy, D. H.; Jensen, R. T. *Molecular Pharmacology* **1993**, *43*, 762.

(72) Zhang, H. W.; Chen, J. H.; Waldherr, C.; Hinni, K.; Waser, B.; Reubi, J. C.; Maecke, H. R. *Cancer Research* **2004**, *64*, 6707.

(73) Ashwood, V.; Brownhill, V.; Higginbottom, M.; Horwell, D. C.; Hughes, J.; Lewthwaite, R. A.; McKnight, A. T.; Pinnock, R. D.; Pritchard, M. C.; Suman-Chauhan, N.; Webb, C.; Williams, S. C. *Bioorganic & Medicinal Chemistry Letters* **1998**, *8*, 2589.

(74) Hirschmann, R.; Nicolaou, K. C.; Pietranico, S.; Salvino, J.; Leahy, E. M.; Sprengeler, P. A.; Furst, G.; Smith, A. B.; Strader, C. D.; Cascieri, M. A.; Candelore, M. R.; Donaldson, C.; Vale, W.; Maechler, L. *Journal of the American Chemical Society* **1992**, *114*, 9217.

(75) Hirschmann, R.; Nicolaou, K. C.; Pietranico, S.; Leahy, E. M.; Salvino, J.; Arison, B.; Cichy, M. A.; Spoors, P. G.; Shakespeare, W. C.; Sprengeler, P. A.; Hamley, P.; Smith, A. B.; Reisine, T.; Raynor, K.; Maechler, L.; Donaldson, C.; Vale, W.; Freidinger, R. M.; Cascieri, M. R.; Strader, C. D. *Journal of the American Chemical Society* **1993**, *115*, 12550.

(76) Hirschmann, R. F.; Nicolaou, K. C.; Angeles, A. R.; Chen, J. S.; Smith, A. B. *Accounts of Chemical Research* **2009**, *42*, 1511.

(77) Schneider, G.; Neidhart, W.; Giller, T.; Schmid, G. *Angewandte Chemie-International Edition* **1999**, *38*, 2894.

(78) Jenkins, J. L.; Glick, M.; Davies, J. W. *Journal of Medicinal Chemistry* **2004**, *47*, 6144.

(79) Schneider, G.; Schneider, P.; Renner, S. *Qsar & Combinatorial Science* **2006**, *25*, 1162.

(80) Tsuchida, K.; Chaki, H.; Takakura, T.; Kotsubo, H.; Tanaka, T.; Aikawa, Y.; Shiozawa, S.; Hirono, S. *Journal of Medicinal Chemistry* **2006**, *49*, 80.

(81) Abbenante, G.; Becker, B.; Blanc, S.; Clark, C.; Condie, G.; Fraser, G.; Grathwohl, M.; Halliday, J.; Henderson, S.; Lam, A.; Liu, L. G.; Mann, M.; Muldoon, C.; Pearson, A.; Premraj, R.; Ramsdale, T.; Rossetti, T.; Schafer, K.; Le Thanh, G.; Tometzki, G.; Vari, F.; Verquin, G.; Waanders, J.; West, M.; Wimmer, N.; Yau, A.; Zuegg, J.; Meutermans, W. *Journal of Medicinal Chemistry* **2010**, *53*, 5576.

(82) Carver, J. A. *Biochemical and Biophysical Research Communications* **1988**, *150*, 552.

(83) Cavatorta, P.; Sartor, G.; Neyroz, P.; Farruggia, G.; Franzoni, L.; Szabo, A. G.; Spisni, A. *Biopolymers* **1991**, *31*, 653.

(84) Condamine, E.; Chapdeleine, G.; Demarcy, L.; Duclos, J. F.; Davoust, D.; Llinares, M.; Azay, J.; Martinez, J.; Chapelle, S. *Journal of Peptide Research* **1998**, *51*, 55.

(85) Diaz, M. D.; Fioroni, M.; Burger, K.; Berger, S. *Chemistry-a European Journal* **2002**, *8*, 1663.

(86) Shin, C.; Mok, K. H.; Han, J. H.; Ahn, J. H.; Lim, Y. *Biochemical and Biophysical Research Communications* **2006**, *350*, 120.

(87) Prakash, P.; Sankararamakrishnan, R. *Protein and Peptide Letters* **2007**, *14*, 590.

(88) Erne, D.; Schwyzer, R. *Biochemistry* **1987**, *26*, 6316.

(89) Schwyzer, R. *Biopolymers* **1995**, *37*, 5.

(90) Sankararamakrishnan, R. *Bioscience Reports* **2006**, *26*, 131.

(91) Cavatorta, P.; Farruggia, G.; Masotti, L.; Sartor, G.; Szabo, A. G. *Biochemical and Biophysical Research Communications* **1986**, *141*, 99.

(92) Malikayil, J. A.; Edwards, J. V.; McLean, L. R. *Biochemistry* **1992**, *31*, 7043.

(93) Polverini, E.; Neyroz, P.; Fariselli, P.; Casadio, R.; Masotti, L. *Biochemical and Biophysical Research Communications* **1995**, *214*, 663.

(94) Vivanco, I.; Sawyers, C. L. *Nature Reviews Cancer* **2002**, *2*, 489.

(95) Coffer, P. J.; Jin, J.; Woodgett, J. R. *Biochemical Journal* **1998**, *335*, 1.

(96) Staal, S. P. *Proc. Natl. Acad. Sci. U. S. A.* **1987**, *84*, 5034.

(97) Bellacosa, A.; Defeo, D.; Godwin, A. K.; Bell, D. W.; Cheng, J. Q.; Altomare, D. A.; Wan, M. H.; Dubeau, L.; Scambia, G.; Masciullo, V.; Ferrandina, G.; Panici, P. B.; Mancuso, S.; Neri, G.; Testa, J. R. *International Journal of Cancer* **1995**, *64*, 280.

(98) Thompson, F. H.; Nelson, M. A.; Trent, J. M.; Guan, X. Y.; Liu, Y.; Yang, J. M.; Emerson, J.; Adair, L.; Wymer, J.; Balfour, C.; Massey, K.; Weinstein, R.; Alberts, D. S.; Taetle, R. *Cancer Genetics and Cytogenetics* **1996**, *87*, 55.

(99) Cheng, J. Q.; Ruggeri, B.; Klein, W. M.; Sonoda, G.; Altomare, D. A.; Watson, D. K.; Testa, J. R. *Proc. Natl. Acad. Sci. U. S. A.* **1996**, *93*, 3636.

(100) Castillo, S. S.; Brognard, J.; Petukhov, P. A.; Zhang, C. Y.; Tsurutani, J.; Granville, C. A.; Li, M.; Jung, M.; West, K. A.; Gills, J. G.; Kozikowski, A. P.; Dennis, P. A. *Cancer Research* **2004**, *64*, 2782.

(101) Lemmon, M. A.; Ferguson, K. M.; Schlessinger, J. *Cell* **1996**, *85*, 621.

(102) Frech, M.; Andjelkovic, M.; Ingley, E.; Reddy, K. K.; Falck, J. R.; Hemmings, B. A. *Journal of Biological Chemistry* **1997**, *272*, 8474.

(103) Stokoe, D.; Stephens, L. R.; Copeland, T.; Gaffney, P. R. J.; Reese, C. B.; Painter, G. F.; Holmes, A. B.; McCormick, F.; Hawkins, P. T. *Science* **1997**, *277*, 567.

(104) Grishin, N. V. *Journal of Molecular Biology* **1999**, *291*, 239.

(105) Cross, D. A. E.; Alessi, D. R.; Cohen, P.; Andjelkovich, M.; Hemmings, B. A. *Nature* **1995**, *378*, 785.

(106) KauffmanZeh, A.; RodriguezViciana, P.; Ulrich, E.; Gilbert, C.; Coffer, P.; Downward, J.; Evan, G. *Nature* **1997**, *385*, 544.

(107) Kulik, G.; Klippel, A.; Weber, M. J. *Molecular and Cellular Biology* **1997**, *17*, 1595.

(108) Paradis, S.; Ailion, M.; Toker, A.; Thomas, J. H.; Ruvkun, G. *Genes & Development* **1999**, *13*, 1438.

(109) Sun, H. Y.; Reddy, G. B.; George, C.; Meuillet, E. J.; Berggren, M.; Powis, G.; Kozikowski, A. P. *Tetrahedron Letters* **2002**, *43*, 2835.

(110) Kozikowski, A. P.; Sun, H. Y.; Brognard, J.; Dennis, P. A. *Journal of the American Chemical Society* **2003**, *125*, 1144.

(111) Hu, Y. H.; Qiao, L. X.; Wang, S. M.; Rong, S. B.; Meuillet, E. J.; Berggren, M.; Gallegos, A.; Powis, G.; Kozikowski, A. P. *Journal of Medicinal Chemistry* **2000**, *43*, 3045.

(112) Thomas, C. C.; Deak, M.; Alessi, D. R.; van Aalten, D. M. F. *Current Biology* **2002**, *12*, 1256.

(113) Allinger, N. L. *Journal of the American Chemical Society* **1977**, *99*, 8127.

(114) Le, G. T.; Abbenante, G.; Becker, B.; Grathwohl, M.; Halliday, J.; Tometzki, G.; Zuegg, J.; Meutermans, W. *Drug Discovery Today* **2003**, *8*, 701.

(115) Capozzi, G.; Dios, A.; Franck, R. W.; Geer, A.; Marzabadi, C.; Menichetti, S.; Nativi, C.; Tamarez, M. *Angew. Chem.-Int. Edit. Engl.* **1996**, *35*, 777.

(116) Mari, S.; Canada, F. J.; Jimenez-Barbero, J.; Bernardi, A.; Marcou, G.; Motto, I.; Velter, I.; Nicotra, F.; La Ferla, B. *European Journal of Organic Chemistry* **2006**, 2925.

(117) Schollkopf, U.; Lonsky, R.; Lehr, P. *Liebigs Annalen Der Chemie* **1985**, 413.

(118) Baussanne, I.; Schwardt, O.; Royer, J.; Pichon, M.; Figadère, B.; Cavé, A. *Tetrahedron Letters* **1997**, *38*, 2259.

(119) Masschelein, K. G. R.; Stevens, C. V.; Dieltiens, N.; Claeys, D. D. *Tetrahedron* **2007**, *63*, 4712.

(120) Wasilenko, W. J.; Cooper, J.; Palad, A. J.; Somers, K. D.; Blackmore, P. F.; Rhim, J. S.; Wright, G. L.; Schellhammer, P. F. *Prostate* **1997**, *30*, 167.

(121) Xiao, D. M.; Qu, X. P.; Weber, H. C. *Regulatory Peptides* **2002**, *109*, 141.

(122) Lehmann, F.; Pettersen, A.; Currier, E. A.; Sherbukhin, V.; Olsson, R.; Hacksell, U.; Luthman, K. *Journal of Medicinal Chemistry* **2006**, *49*, 2232.

(123) Lee, J.-Y.; Yu, J.; Cho, W. J.; Ko, H.; Kim, Y.-C. *Bioorganic & Medicinal Chemistry Letters* **2009**, *19*, 6053.

(124) Lindsay, K. B.; Ferrando, F.; Christensen, K. L.; Overgaard, J.; Roca, T.; Bennasar, M. L.; Skrydstrup, T. *Journal of Organic Chemistry* **2007**, *72*, 4181.

(125) Kozikowski, A. P.; Ma, D.; Pang, Y. P.; Shum, P.; Likic, V.; Mishra, P. K.; Macura, S.; Basu, A.; Lazo, J. S.; Ball, R. G. *Journal of the American Chemical Society* **1993**, *115*, 3957.

(126) Hibbs, R. E.; Sulzenbacher, G.; Shi, J. X.; Talley, T. T.; Conrod, S.; Kem, W. R.; Taylor, P.; Marchot, P.; Bourne, Y. *Embo Journal* **2009**, *28*, 3040.

(127) Yang, J.; Song, H.; Xiao, X.; Wang, J.; Qin, Y. *Organic Letters* **2006**, *8*, 2187.

(128) Battaglia, S.; Boldrini, E.; Da Settimo, F.; Dondio, G.; La Motta, C.; Marini, A. M.; Primofiore, G. *European Journal of Medicinal Chemistry* **1999**, *34*, 93.

(129) Tanaka, R.; Rubio, A.; Harn, N. K.; Gernert, D.; Grese, T. A.; Eishima, J.; Hara, M.; Yoda, N.; Ohashi, R.; Kuwabara, T.; Soga, S.; Akinaga, S.; Nara, S.; Kanda, Y. *Bioorganic & Medicinal Chemistry* **2007**, *15*, 1363.

(130) Peng, H.; Carrico, D.; Van, T.; Blaskovich, M.; Bucher, C.; Pusateri, E. E.; Sebti, S. M.; Hamilton, A. D. *Organic & Biomolecular Chemistry* **2006**, *4*, 1768.

(131) Abecassis, K.; Gibson, S. E.; Martin-Fontecha, M. *European Journal of Organic Chemistry* **2009**, 1606.